BioMed Research International

Advanced User Interfaces for Neurorehabilitation

Guest Editors: Alessandro De Mauro, Belinda Lange, and Andreas Dünser

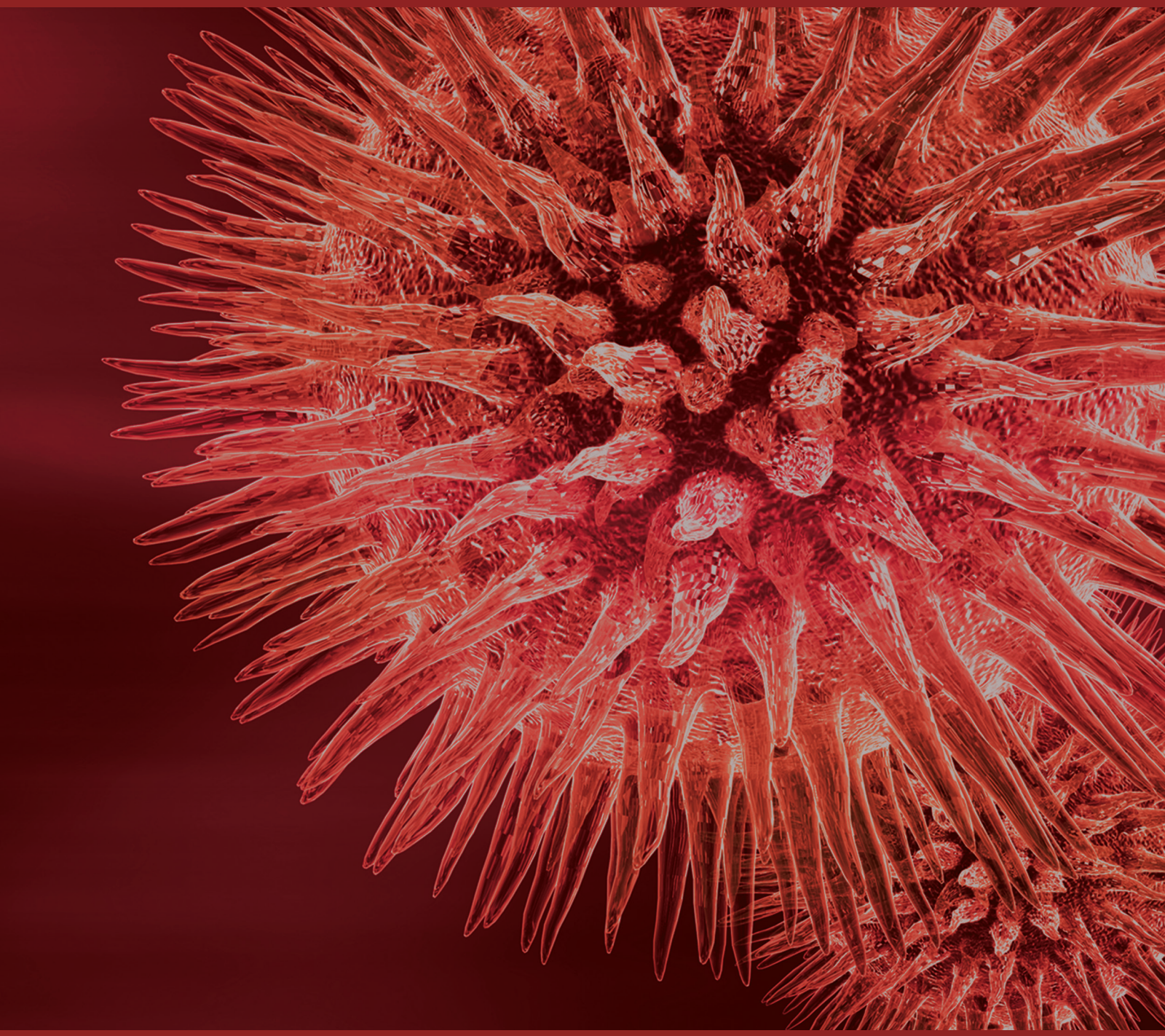

Advanced User Interfaces for Neurorehabilitation

BioMed Research International

Advanced User Interfaces for Neurorehabilitation

Guest Editors: Alessandro De Mauro, Belinda Lange, and Andreas Dünser

Contents

Editorial

Advanced User Interfaces for Neurorehabilitation

Alessandro De Mauro,[1] Belinda Lange,[2] and Andreas Dünser[3]

[1] *eHealth and Biomedical Applications, Vicomtech-IK4, Paseo Mikeletegi 57, 20009 San Sebastian, Spain*
[2] *Institute for Creative Technologies, University of Southern California, 12015 Waterfront Drive, Playa Vista, CA, USA*
[3] *CSIRO, Computational Informatics, 15 College Road, Sandy Bay, Hobart, TAS 7005, Australia*

Correspondence should be addressed to Alessandro De Mauro; ademauro@vicomtech.org

Received 18 May 2014; Accepted 18 May 2014; Published 10 July 2014

A range of new user interfaces and systems have been developed as novel and relevant tools in neurorehabilitation, allowing the implementation and exploration of new rehabilitation approaches and protocols to be complemented and to improve upon traditional methods.

In this special issue both medical and engineering aspects of these tools as well as state-of-the-art research trends have been addressed in order to explore these types of solutions and how they can support and/or extend current clinical or home-based rehabilitation practices. The issue provides six original research articles by some of the leading experts in the field, covering development studies and studies investigating evidence of the effectiveness of new technologies, devices, specific applications, and treatment methodologies.

The paper of F. Trincado-Alonso et al. presents a study on the development of new strategies based on virtual reality (VR) that can provide additional information to clinicians regarding rehabilitation assessment. It includes the definition of set of metrics combining kinematic data in order to obtain parameters of reaching amplitude, joint amplitude, agility, accuracy, and repeatability during the evaluation sessions.

W. Chinthammit et al. report a pilot study that employs a prototype telerehabilitation system called "Ghostman". It is a visual augmentation system designed to allow a physical therapist and patient to inhabit each other's viewpoint in an augmented real-world environment. The presented initial results look promising and suitable to be used in the field of stroke rehabilitation.

J. R. Octavia and K. Coninx focus on integrating adaptivity and personalization in rehabilitation training for multiple sclerosis patients. Their findings showed that adaptive personalized training trajectories have been successfully provided. Furthermore, they report on the development of positive social interaction during the collaborative rehabilitation training.

A. M. Fenuta and A. L. Hicks present a detailed comparison of two commercial rehabilitation treadmills in terms of oxygen demand and muscle activation during therapy. Important and clear indications on the use of both devices have been stated in the paper's conclusions.

C. Cortes et al. provide a mathematical formulation and implementation of a method to estimate the limb posture in VR and robotic assisted rehabilitation systems. Additionally, they present the details of a VR game platform for stroke rehabilitation and the quantitative assessment of the method during the analytic training of the elbow and wrist.

Finally, the paper of D. A. G. Galeano et al. proposes a novel balance training platform which combines postural analysis with synergistic electrical muscle stimulation and is based on low-cost gaming interfaces. Results include the technical validation of the platform using mediolateral and anteroposterior sways as basic balance training therapies.

As the editors of this special issue, we hope that readers will find these articles representative of the state-of-the-art in novel user interfaces for neurorehabilitation. This special issue highlights the latest research and developments in this

important research field and the contributions it has made to improve treatment outcomes for patients, clinical research methodology, and the development of many practical applications.

Acknowledgments

We thank the authors for their very much valued contributions. We would also like to express our special thanks to the expert reviewers for their professional input.

Alessandro De Mauro
Belinda Lange
Andreas Dünser

Hindawi Publishing Corporation
BioMed Research International
Volume 2014, Article ID 821908, 18 pages
http://dx.doi.org/10.1155/2014/821908

Research Article

Upper Limb Posture Estimation in Robotic and Virtual Reality-Based Rehabilitation

Camilo Cortés,[1,2] Aitor Ardanza,[1] F. Molina-Rueda,[3] A. Cuesta-Gómez,[3] Luis Unzueta,[1] Gorka Epelde,[1] Oscar E. Ruiz,[2] Alessandro De Mauro,[1] and Julian Florez[1]

[1] *eHealth and Biomedical Applications, Vicomtech-IK4, Mikeletegi Pasealekua 57, 20009 San Sebastián, Spain*
[2] *Laboratorio de CAD CAM CAE, Universidad EAFIT, Carrera 49 No. 7 Sur-50, 050022 Medellín, Colombia*
[3] *Biomechanics, Ergonomy and Motor Control Laboratory (LAMBECOM), Physical Therapy, Occupational Therapy, Rehabilitation and Physical Medicine Department, Rey Juan Carlos University, 28922 Madrid, Spain*

Correspondence should be addressed to Julian Florez; jflorez@vicomtech.org

Received 25 January 2014; Revised 14 April 2014; Accepted 28 April 2014; Published 8 July 2014

Academic Editor: Andreas Dünser

New motor rehabilitation therapies include virtual reality (VR) and robotic technologies. In limb rehabilitation, limb posture is required to (1) provide a limb realistic representation in VR games and (2) assess the patient improvement. When exoskeleton devices are used in the therapy, the measurements of their joint angles cannot be directly used to represent the posture of the patient limb, since the human and exoskeleton kinematic models differ. In response to this shortcoming, we propose a method to estimate the posture of the human limb attached to the exoskeleton. We use the exoskeleton joint angles measurements and the constraints of the exoskeleton on the limb to estimate the human limb joints angles. This paper presents (a) the mathematical formulation and solution to the problem, (b) the implementation of the proposed solution on a commercial exoskeleton system for the upper limb rehabilitation, (c) its integration into a rehabilitation VR game platform, and (d) the quantitative assessment of the method during elbow and wrist analytic training. Results show that this method properly estimates the limb posture to (i) animate avatars that represent the patient in VR games and (ii) obtain kinematic data for the patient assessment during elbow and wrist analytic rehabilitation.

1. Introduction

Robotic and VR technologies are important components of the modern neurorehabilitation systems for pathologies such as stroke or spinal cord injury [1–3]. In this field, our general research has two main goals:

(a) to improve the assessment of the rehabilitation progress through precise estimation of the patient kinematics. This is the focus of this paper;

(b) to optimize the rehabilitation processes by using the kinematic (and other) patient models. This optimization includes hybrid technologies (e.g., robotics, virtual reality, functional electrical stimulation [4], etc.). Even though this domain is very important for rehabilitation, we see it as a natural consequence of (a) and we concentrate on (a) at this time.

In the mentioned scenario, the proper estimation of the patient limb posture is a fundamental prerequisite for the following:

(1) design and control of the advanced robotic exoskeletons which provide assistance to the patient during motor rehabilitation [5, 6],

(2) animation of realistic avatars representing the patient in virtual reality (VR) scenarios (e.g., games, bionics), and

(3) acquisition of kinematic data of the patient during the training exercises to assess improvement along the therapy.

This paper presents a method for estimation of limb posture from the exoskeleton posture. Notice that such an estimation is not trivial, since the limb is not rigid, is not

standard, and has kinematic topology different from the exoskeleton topology.

Our method delivers limb postures estimates to strengthen and to enable downstream applications in robotic rehabilitation (among others, using VR [4]).

1.1. Robotic-Based Motor Rehabilitation Therapy. The inclusion of robotic devices in motor rehabilitation therapies has been increasing over the last decade. The robot-assisted therapies complement conventional rehabilitation by providing intensive, repetitive, task-specific, and interactive treatment. All these factors contribute to a more effective rehabilitation [7–9].

Robotic-assisted therapy has been shown to improve active movement, strengthening, and coordination in stroke patients [10]. The majority of clinical studies have reported that robot-assisted therapy can ease impairments and lower disabilities of the affected patient [11]. Moreover, evidence suggests that task-oriented exercises using robotic devices produce significant improvements in recovering lost abilities [12].

Combining these exercises with VR games makes the therapy more attractive to the patient, increasing motivation and treatment effects [4, 13]. It is important that these games are designed to be consistent with the principles of physical therapy and adjustable to the level of impairment [14].

A central element in designing a therapy is the feedback that patients receive. To achieve relatively permanent changes in the capability of producing skilled action, it is crucial to provide the patient with proper feedback in order to produce a positive impact on the neural mechanism promoting motor learning [15].

Feedback includes all the sensory information as the result of a movement and it is divided into two classes: (1) intrinsic or inherent feedback, which is information captured by human sensory systems as a result of the normal production of the movement, and (2) extrinsic or augmented feedback, which is information that supplements intrinsic feedback [15, 16]. Robotic-assisted therapy with VR games including animated realistic avatars may improve the quality and specificity of extrinsic feedback that the patient receives.

From the perspective of the therapist, robotic devices can be used to obtain quantitative metrics for the assessment of the improvement of the patient. The kinematic information of the affected limb during the exercises is required to compute several evaluation metrics, such as joint amplitudes, speeds, movement smoothness, and directional control.

1.2. Case Study Armeo Exoskeleton. Our proposed therapy uses the Armeo Spring exoskeleton for the upper limb intervention (Figure 1). We find the following limitations of this system.

(1) Currently, the gaming platform provides an elementary assessment of the patient performance with metrics such as Hand Path Ratio [17] and joint range of motion, which are only available in certain games of the Armeo proprietary platform. We propose a continuous quantification of the patient performance along the treatment therapies, involving metrics that are highly correlated with the functional recovery of the patient.

(2) Currently, the games only provide the patient with feedback of his hand position. We propose to provide a 3-dimensional representation of the arm, which would help the patient to immerse in the VR environment.

Figure 1: Armeo Spring orthosis.

The kinematic data provided by the exoskeleton samples the angular position of its joints. Such information cannot be used directly to represent the human arm, since the patient limb and the exoskeleton kinematic models differ significantly.

This paper presents a method to estimate the posture of the limb by using the kinematic data provided by the exoskeleton. We propose to solve the limb's inverse kinematics (IK) problem extended with the kinematic constraints of the exoskeleton fixations on the limb. This extended problem is solved in real time with standard robotic libraries. In this manner, we aim to overcome the limitations of the Armeo system regarding to the feedback and assessment of the patient.

This paper is organized as follows: Section 2 presents a brief literature review. Section 3 addresses the formal statement of the problem and the proposed method to solve it. Section 4 discusses the implementation of our approach and its use in VR games. Section 5 presents the evaluation methodology of our approach in the realm of motor rehabilitation. Section 6 informs and discusses the results of the experiments conducted using our solution strategy. Section 7 concludes the paper and identifies future developments.

2. Literature Review

Several estimation methods and human models have been proposed in the literature to solve the problem of limb posture estimation. Next, we present a brief review of developments in these areas.

2.1. Limb Posture Estimation

2.1.1. Free Movement Scenario. Most of the existing work on limb posture estimation focuses on free movement scenarios. We define a free movement scenario as a situation in which the patient limb does not wear an exoskeleton or interact with any other robotic interface. Under the mentioned conditions, the literature that addresses upper limb posture estimation considers tasks in which the human subject has to reach a desired object. Therefore, these approaches are designed to estimate the posture of the upper limb based on a given target position and orientation of the hand.

Statistical [18, 19], IK [20–22], and direct optimization [23–28] methods are the most used approaches to estimate the limb posture [29].

Statistical or data-based approaches model the human kinematics with regressive models from empirical data [30]. Factors such as the size of the database of captured motions [31] and the characteristics of the population involved in the experiments impact the accuracy and usefulness of these models.

Kinematic approaches model the human limbs with links, joints of different degrees of freedom, and end-effectors [27]. The IK problem is then solved with either closed-form or numerical methods. The quality of the kinematic model and the convergence speed and robustness of the approach used to solve the IK problem directly affect the accuracy of the estimations.

Optimization approaches require a nontrivial function to minimize, which actually leads to the desired configuration (typically, a minimal energy one [31]). When optimization is used to solve an IK problem, additional constraints can be easily included in the formulation [26–28].

Approaches combining optimization-based and statistical models have been also proposed to overcome the individual limitations of optimization and statistical methods [31, 32]. Naturally, the composed method requires a high-quality dataset of motions and the formulation of proper objective and constraints functions.

2.1.2. Robotic-Assisted Scenario. There is a shortage in the literature addressing posture estimation of the human limb while interacting with an exoskeleton. Although exoskeletons are designed with the ultimate goal of minimizing their kinematic differences with human limbs and interact seamlessly with them, the following factors influence the human motion patterns and therefore the posture of the limb:

(1) the mechanic design of the exoskeleton (inertia, back drivability, friction, joint motion limits, etc.).

(2) the type of assistance that the exoskeleton provides (passive, active, and assist-when-needed).

(3) the performance of the exoskeleton motion controller. Here, using a naive one-to-one mapping between the joint angles of the human limb and exoskeleton leads to poor positioning results [33].

References [6, 21] propose the computation of the arm's IK by using a disambiguation criteria for its redundancy which chooses a swivel angle such that the palm points to the head region. This methodology is suitable for real-time implementation and it is used in the control strategy of the active 7-DOF exoskeleton developed by the authors' research team [34]. The authors report that the mean error in the estimation of the swivel angle is less than 5 degrees. The magnitude of the errors in the estimation of the wrist, elbow, and GH-joint angles is not reported.

References [6, 21] do not consider the motions of the clavicle and scapula (which affect the position of the GH-joint center) in the estimation of the posture of the arm, as they assume the position of the GH-joint center to be known. Therefore, this approach should not be used in cases in which the position of the GH-joint center cannot be determined from data provided by the exoskeleton (e.g., Armeo Spring) or by any additional motion capture system.

Other common methods to estimate the posture of human limbs cannot be used or are impractical in robotic-assisted scenarios. For example, inertial and magnetic measurement systems (IMMSs) presented in [35, 36] are unusable because the magnetic disturbances produced by the metallic components of the exoskeleton corrupt the magnetic sensor measurements.

If optical tracking systems are used, arrays of markers need to be attached to the patient in order to measure the limb joint angles. Occlusions of such markers are frequently produced by the mechanic structure of the exoskeleton when performing the rehabilitation exercises. To overcome the occlusions of the markers, a redundant setup is necessary [29]. This limitation makes the use of optical tracking systems cumbersome for frequent use in the rehabilitation therapy.

2.2. Human Model.

A central element in human posture estimation is the human kinematic model itself. Simple models based on hierarchies of links and lower kinematic pairs can be found in [27, 37–40]. These approaches results are convenient for real-time tasks and for implementation. However, more elaborated models should be used to describe complex kinematic relationships [41], such as the shoulder rhythm [42]. On the other hand, musculoskeletal models reported in [43–45] offer better accuracy for dynamics computations, since they include forces from muscles and ligaments.

The selection of the human kinematics model rests not only on the kinematic statement of the problem, but also on the compromise between accuracy and speed required in a particular application.

2.3. Conclusions of Literature Review.

Although the methods designed to estimate the posture of the upper limb (in absence of a robotic interface) reviewed in Section 2.1.1 could be used in robotic-assisted rehabilitation, we have not found any actual implementation of them in this context. Usage of these methods without any change in their design parameters in robotic-assisted applications may lead to erroneous posture estimations, given the influence of the exoskeleton on human motion patterns. Therefore, the validity of these methods in the robotic-assisted scenario remains to be proven. An

additional limitation of these methods is that only few of them have been validated quantitatively by determining the errors in their estimations.

On the other hand, the few posture estimation approaches that address limb interaction with an exoskeleton (Section 2.1.2) have been designed to specifically solve the arm posture estimation problem, limiting their usability in posture estimation of other human limbs.

In response to the mentioned issues, in this paper we present the following:

(1) a method that can be applied, in a general manner, to solve the limb posture estimation problem using kinematic data provided by the exoskeleton attached to the limb,

(2) the implementation of our proposed method for the upper limb posture estimation using the Armeo Spring exoskeleton, and

(3) the quantitative validation of our proposed method by determining the estimation errors during the training of meaningful upper limb rehabilitation exercises.

3. Materials and Methods

3.1. Problem Description. In this section, we state the problem of estimating the joint angles of the patient limb during robotic-assisted rehabilitation therapy from the kinematic information provided by the robot. The elements that are considered inputs to the problem are the following: (1) the geometry and topology (e.g., the Denavit-Hartenberg parameters [46]) of the exoskeleton and the human limb, (2) a known configuration of the angles of the joints of the exoskeleton, (3) the kinematic constraints imposed by the fixations of the exoskeleton over the patient limb (which result from wearing the exoskeleton), and (4) the constraints that govern the posture of the patient limb while interacting with the exoskeleton, which are related to mechanical and control factors of the exoskeleton that influence the patient movement. The goal of the proposed algorithm is to find the approximate joint angles of the patient limb, such that the mentioned constraints are met.

This problem can be formally stated as follows.

Given

(1) the kinematic model of the exoskeleton $R(L_R, J_R)$, where L_R and J_R are sets of links and joints, respectively,

  (a) $L_R = \{l_{R_0}, \ldots, l_{R_{f+1}}\}$;

  (b) $J_R = \{j_{R_0}, \ldots, j_{R_f}\}$:

    (i) $N(j_{R_i})$ denotes the degrees of freedom (DOF) of j_{R_i};

    (ii) $v_{R_i} = \{\theta_1, \ldots, \theta_{N(j_{R_i})}\}$ is a vector that contains the angles of each DOF of j_{R_i} ($i \in [0, f]$);

  (c) R is an open kinematic chain. Therefore, l_{R_i} and $l_{R_{i+1}}$ are connected by joint j_{R_i}, where $i \in [0, f]$;

  (d) the vector $q_R \in \mathbb{R}^n$, $n = \sum_{i=0}^{f} N(j_{R_i})$, contains the set of independent coordinates that defines a configuration of R uniquely:

    (i) $q_R = \{v_{R_0}, \ldots, v_{R_i}, \ldots, v_{R_f}\}$;

    (ii) q_{R_t} represents the state of q_R in instant t and its value is known;

(2) a human patient with a kinematic model of his limb $H(L_H, J_H)$, where L_H and J_H are sets of links and joints, respectively,

  (a) $L_H = \{l_{H_0}, \ldots, l_{H_{g+1}}\}$;

  (b) $J_H = \{j_{H_0}, \ldots, j_{H_g}\}$:

    (i) $N(j_{H_i})$ denotes the DOF of j_{H_i};

    (ii) $v_{H_i} = \{\theta_1, \ldots, \theta_{N(j_{H_i})}\}$ is a vector that contains the angles of each DOF of j_{H_i} ($i \in [0, g]$);

  (c) H is an open kinematic chain. Therefore, (l_{H_i}) and $(l_{H_{i+1}})$ are connected by joint (j_{H_i}), where $i \in [0, g]$;

  (d) the vector $q_H \in \mathbb{R}^k$, $k = \sum_{i=0}^{g} N(j_{H_i})$, contains the set of independent coordinates that defines a configuration of H uniquely:

    (i) $q_H = \{v_{H_0}, \ldots, v_{H_i}, \ldots, v_{H_g}\}$;

    (ii) the ith element of q_H, θ_i, is subject to $h_i(\theta_i) = \theta_{\min_i} \leq \theta_i \leq \theta_{\max_i}$ ($i \in [0, k-1]$);

    (iii) q_{H_t} represents the state of q_H in instant t and its real value is unknown;

(3) a set of passive mechanisms $M = \{m_0, \ldots, m_p\}$ that connect R and H:

  (a) m_i ($i \in [0, p]$) connects l_{R_a} ($a \in [0, f+1]$) and l_{H_b} ($b \in [0, g+1]$);

  (b) m_i imposes a movement constraint of $N(m_i)$-DOF to l_{H_b} with respect to l_{R_a};

  (c) the set $C(M) = \{c_0, \ldots, c_p\}$ contains vector-valued functions $c_i(q_{H_t}, q_{R_t}) \in \mathbb{R}^{N(m_i)}$ ($i \in [0, p]$) that model the kinematic constraint imposed by m_i;

  (d) each $c_i(q_{H_t}, q_{R_t})$ is an equality constraint of the form $c_i(q_{H_t}, q_{R_t}) = 0$;

(4) a set of vector-valued constraint functions $D = \{d_0, \ldots, d_s\}$ that intend to represent the performance measures that govern the posture of the limb in a specific situation:

  (a) each $d_i(q_{H_t})$ ($i \in [0, s]$) is an equality constraint of the form $d_i(q_{H_t}) = 0$;

  (b) the dimension of the d_i vector is denoted by $\dim(d_i)$.

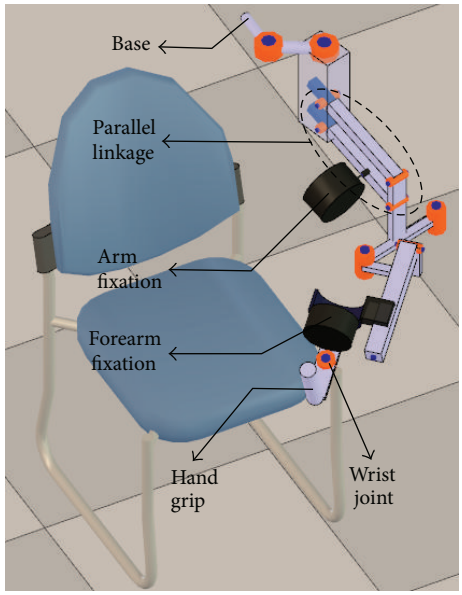

Figure 2: Exoskeleton kinematic model.

Goal is as follows

(1) to find the vector $\tilde{q}_{H_t} \in \mathbb{R}^k$, which approximates q_{H_t} such that

(a) $c_i(q_{H_t}, q_{R_t}) = 0 \ \forall i \in [0, p]$;
(b) $h_j(\theta_j) = \theta_{\min_j} \leq \theta_j \leq \theta_{\max_j} \ \forall j \in [0, k-1]$;
(c) $d_u(q_{H_t}) = 0 \ \forall u \in [0, s]$.

To solve this problem, a method based on IK of the limb has been developed. The following sections describe the methodology implemented.

3.2. Kinematic Modeling of the Exoskeleton. The Armeo Spring (Figure 1) is a passive exoskeleton (orthosis) that supports the weight of the arm of the patient. The level of support provided by the system springs can be adjusted, regulating the effort of the patient arm to overcome gravity. The exoskeleton has a total of seven angle sensors to measure the position of its rotational joints and one pressure sensor to measure the gripping force at the hand [47].

We built a kinematic model of the Armeo Spring (Figure 2), which contains both prismatic and revolute joints. The prismatic joints of the exoskeleton allow adjusting it to the different sizes of the patients, and they remain fixed during the training.

Our implementation models the links and joints of the Armeo exoskeleton and creates a hierarchical structure of them.

Although the Armeo exoskeleton presents a parallelogram mechanism in its kinematic chain, the exoskeleton can be modeled with a serial chain extended with a dependency equation among the joints used to represent the parallel mechanism.

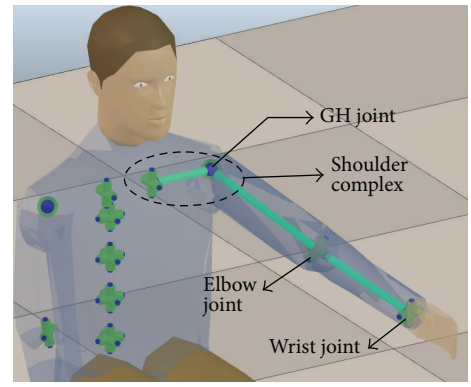

Figure 3: Human upper body kinematic model.

3.3. Kinematic Modeling of the Human Upper Body. Figure 3 shows the kinematic model of the human upper body that we created for this application. The joints of the model are represented with green color. The upper limb is highlighted using links in light green color.

Our upper body model (33-DOF) includes joints of the spine, shoulder complex, elbow, and wrist. It is based on the ones presented in [27–29, 38, 39, 48], which have been widely used in the area of human posture estimation. The main advantages of those models are their easy implementation and their suitability for solving the posture estimation problem in real time, which is one of the main requirements of our application. A weakness of those kinematic models is that the glenohumeral (GH) joint is modeled with a kinematic chain of three concurrent revolute joints, orthogonal to each other. In this way, the rotation of the GH joint is parameterized with Euler angles and suffers from gimbal lock [49]. In order to avoid this limitation, the GH joint is represented in our model with a spherical joint, such that other rotation parameterizations (e.g., quaternion or exponential map) can be used.

Although there are more complex and accurate kinematic models of the upper body, the results obtained in [39], in a scenario where the subject does not interact with an exoskeleton in an application that is not related to motor rehabilitation, show that posture estimations for the upper limb can be obtained with a reasonable accuracy by using their original model.

The neutral or rest posture of the arm is defined with the arm fully extended along the body as in [50]. The range of motion of the joints of the arm obtained in [34] (derived from a motion study during the execution of activities of daily living) is used as reference to establish the joint limits of our model, which correspond to constraint 2(d)(ii) in the list presented in Section 3.1.

3.4. Modeling the Kinematic Constraints of Interaction of the Upper Limb and the Exoskeleton. The Armeo provides fixations for the human limb. These fixations introduce constraints on the position and orientation of the coordinate systems attached to the arm, forearm, and hand.

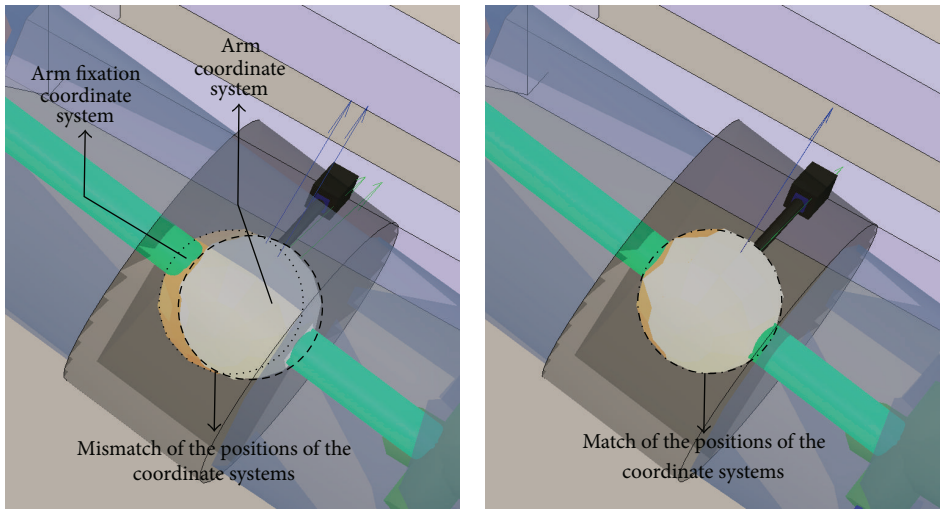

(a) Small error while meeting the arm fixation constraint

(b) Negligible error while meeting the arm fixation constraint

Figure 4: Constraint modeling the interaction of the Armeo's arm fixation.

There are several factors that affect the satisfaction of the constraints during the execution of the exercises. This set includes (1) deformation of the coupling mechanisms and (2) uncertainty or errors in the modeling of the human upper limb. Therefore, these constraints are exactly met only under ideal conditions and in practice they do not capture all the details of the real interaction. However, as we prove, they suffice to obtain a reasonable accuracy in the estimation of the limb posture.

3.4.1. Arm Constraint. The arm fixation imposes a position (3-DOF) constraint on the human arm. The point on the arm that follows the position of the fixation is determined by an initialization process between the R and H kinematic chains (see Section 3.6).

In our model, the fixations are modeled as rigid bodies. However, the exoskeleton fixations are made of flexible materials, such that their geometry is deformed when large forces are applied on them.

The arm fixation suffers significant deformation when the arm is moved towards a horizontal configuration (e.g., when performing a complete stretching of the arm along the sagittal or frontal plane). In those cases, the coordinate system at the exoskeleton arm fixation center undergoes a translation, resulting from the deformation of the fixation mechanism that is not reproduced by our model.

To deal with this kind of situations, the weights of constraints representing fixations that suffer less deformation than other ones are adjusted such that they receive more importance when solving the IK problem. In this way, the limb posture is estimated meeting the constraints that model with more fidelity the observed behavior. In this case, the weight of the arm constraint is lower than the ones belonging to the forearm and arm restrictions.

Figure 4 shows the human arm (blue transparent cylinder) with the fixation of the exoskeleton for the arm (black transparent ring) around it. The constraint imposed by this fixation to the arm is represented by the matching of (a) human arm (white disk) versus (b) fixation (yellow disk) coordinate systems. Figures 4(a) and 4(b) correspond to unsatisfied and satisfied constraints, respectively.

3.4.2. Forearm Constraint. The forearm fixation imposes a 3-DOF position constraint on the human forearm. The point on the human forearm that moves together with the fixation is determined in the initializing stage. Additionally, the fixation is able to rotate around its longitudinal axis, according to the forearm pronation/supination movement (1-DOF orientation constraint). The rotation angle is measured with an encoder. The forearm constraint forces the human wrist flexion/extension axis to be approximately aligned with the exoskeleton's wrist joint axis.

3.4.3. Hand Constraint. The hand constraint forces the human hand to follow the position and orientation (6-DOF) of the Armeo hand grip. The patient exercises while grabbing the handle of the exoskeleton. The mechanic design of the Armeo avoids the slippage of the hand with respect to the axis of the handle during the execution of the exercises. As with the previous fixations, the point on the hand where the coordinate system of the hand is located is calculated in the initialization stage.

3.4.4. Shoulder Constraint. The shoulder constraint does not belong to the set of movement restrictions imposed by the coupling mechanisms of the Armeo. Instead, it is related to the restrictions intended to produce a natural posture of the upper limb considering also the influence of the exoskeleton on the patient movements. This constraint helps to choose one of the multiple configurations of the human kinematic chain that comply with the other categories of constraints.

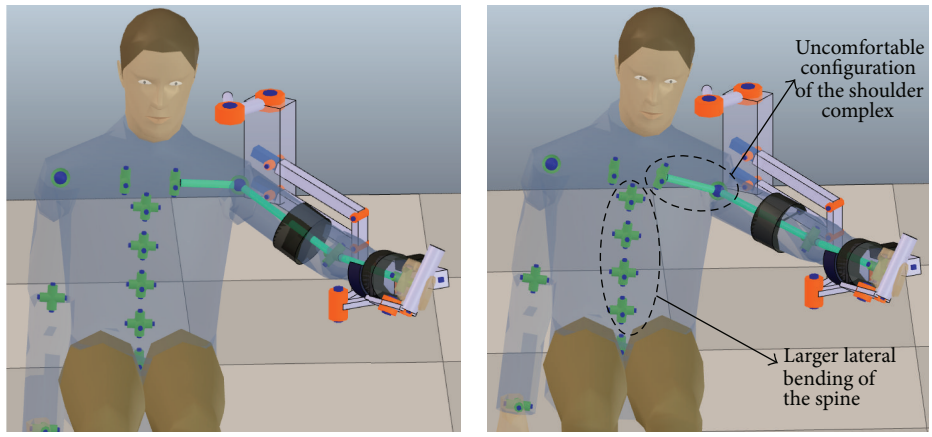

(a) Estimation using the shoulder constraint (b) Estimation without using the shoulder constraint

FIGURE 5: Effect of the shoulder constraint in the upper limb posture estimation.

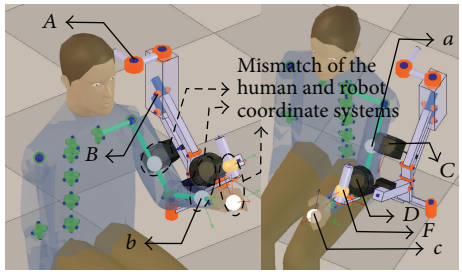

FIGURE 6: State of the kinematic chains before the initialization process (notation in Table 1).

TABLE 1: Glossary related to the Figure 6.

Symbol	Description
A	j_{R_0}
B	j_{R_2}
C	Arm fixation coordinate system
D	Forearm fixation coordinate system
F	Armeo hand grip coordinate system
a	Human arm end-effector coordinate system
b	Human forearm end-effector coordinate system
c	Human hand end-effector coordinate system

Currently, it is implemented to attract the GH joint to a position (3-DOF position constraint) below the first joint of the Armeo (j_{R_0} joint represented with symbol A in Figure 6), which does not suffer any translation during the training of the patient. By keeping the GH joint near j_{R_0} comfortable postures for the spine and arm can be achieved.

Figure 5 shows that the shoulder constraint prevents the excessive motion of the joints of the spine, which is a compensatory movement that should be also avoided during the rehabilitation therapy. The shoulder constraint is central to proper posture estimation during shoulder abduction.

3.5. Inverse Kinematics. Given a desired pose (position and orientation) vector $T_r \in \mathbb{R}^6$ for the end-effector of an open kinematic chain r, the IK problem is to find the vector of angles of the robot's joints $q_r \in \mathbb{R}^N$ (where N corresponds to the DOFs of r), such that the difference $e = T_r - X_r$ between T_r and the actual pose of the end-effector of r, $X_r \in \mathbb{R}^6$, approaches zero.

There are several approaches to solve this problem, including analytic [51] and numerical methods [52, 53]. The iterative strategy used to solve the IK problem is based on the Jacobian matrix of the manipulator $Z(q_r)$, which linearly relates the velocity of the end-effector and the joints by

$$\dot{X}_r = Z(q_r)\,\dot{q}_r. \tag{1}$$

By replacing ΔX_r for e in (2), which is obtained by discretizing (1), the necessary Δq_r to approximate T_r is obtained:

$$\Delta q_r = Z(q_r)^{-1}\Delta X_r. \tag{2}$$

Notice that $Z(q_r)$ may not be square (consider, e.g., a kinematic chain with more than 6-DOF) or invertible. In those cases, the pseudoinverse and damped least squares (DLS) methods (among others) can be used to obtain Δq_r, such that $\|e\|$ is minimized. The pseudoinverse method is computationally faster than the DLS but tends to be unstable when the robot approaches a singular configuration. The DLS method offers more robustness (specially when T_r is out of reach) at the cost of a slower convergence [52].

3.5.1. Relation among End-Effectors and Targets. The aforementioned strategy to solve the IK problem can also be used in situations in which the manipulator has more than one end-effector. In this case, the error vector e is given by $e = \{T_{r_1} - X_{r_1}, \ldots, T_{r_i} - X_{r_i}, \ldots, T_{r_{\text{Nee}}} - X_{r_{\text{Nee}}}\}$ where Nee is the number of end-effectors of the robot. Notice that vector $e_i = T_{r_i} - X_{r_i}$ is not necessarily a point $\in \mathbb{R}^6$. For example, if only the position (and not the orientation) of the ith end-effector is specified, $e_i \in \mathbb{R}^3$.

In our application, the formulation of the IK problem with multiple end-effectors and targets can be used to

represent the constraints discussed in Section 3.4. In this way, each constraint can be represented by a target and end-effector pair. The coordinate frames of the end-effectors $X_{H_i}(q_{H_t})$ ($i \in [1, \ldots, \text{Nee}]$) are attached to the human limb, so their position and orientation depend on the current configuration of the limb, q_{H_t}. The coordinate frames of the targets of the limb $T_{H_i}(q_{R_t})$ ($i \in [1, \ldots, \text{Nee}]$) are attached to the exoskeleton such that they are transformed according to its current configuration q_{R_t}. Then, the IK problem is solved for the limb, finding q_{H_t} such that $e_i = \|T_{H_i}(q_{R_t}) - X_{H_i}(q_{H_t})\| \approx 0$ ($i \in [1, \ldots, \text{Nee}]$). Notice that if e_i represents a kinematic constraint, $e_i \in \mathbb{R}^{N(m_i)}$ where $i \in [0, p]$. Otherwise, e_i represents a restriction related to the natural posture of the limb, and therefore $e_i \in \mathbb{R}^{\dim(d_i)}$, where $i \in [0, s]$, and $\text{Nee} = p + s + 2$.

Notice that, due to modeling inaccuracies of the kinematic chains or the constraints, it is possible that for a configuration q_{R_t} some constraints cannot be satisfied within the desired tolerance. That situation can be interpreted as if some targets $T_{H_i}(q_{R_t})$ are not reachable. It is important that the method used to solve the IK problem handles this situation robustly, avoiding oscillations. For this reason the DLS method was used.

3.5.2. Joints and Constraint Weights. References [38, 39] state that giving more importance to some of the model joints over others, by assigning weights to the joints, allows estimating more accurately the posture of the human limb.

Let us assume that w_{J_i} is the weight of joint J_{H_i} and that joints J_c and J_d can contribute to the movement of end-effector i to diminish e_i. Then, if $w_{J_c} > w_{J_d}$, the displacement that J_c performs is larger than the one done by J_d. This means that J_c is preferred to be moved over J_d to reach a desired target.

In our model, the weights of the joints of the upper body were adjusted such that the joints on the spine of the model perform small displacements in comparison with the movement performed by the shoulder, elbow, and wrist joints.

On the other hand, applying weights to the error vector e gives more importance to reach a specific target over others. In our approach, this translates into giving some constraints more importance than others. Let us define with w_{c_i} ($i \in [0, p]$) the weight of the c_i constraint and with w_{d_u} ($u \in [0, s]$) the weight of d_u constraint.

In our model, high weights were adjusted for the kinematic constraints imposed by the exoskeleton fixations ($w_{c_i} \approx 1.0$). Otherwise, low weights ($w_{d_i} \approx 0.2$) were assigned to the other type of constraints.

There are different formulations of the DLS method that incorporate weights for the joints and error vector (e.g., [54]). In V-REP, the following DLS formulation is used to solve IK problems. The angles of the joints of the human model are given by $q_{H_t} = \sqrt{W_q} q_{H_{t_w}}$, where $q_{H_{t_w}} = Z_w^* e_w$ and $Z_w^* = Z_w^t (Z_w Z_w^t + \alpha I)^{-1}$. The weighted Jacobian matrix is given by $Z_w = Z\sqrt{W_q}$, where $W_q = \text{diag}\{w_0, \ldots, w_{k-1}\}$. Here, if w_a and w_b are related to J_{H_i} (e.g., a joint with DOFs > 1), $w_a = w_b = w_{J_i}$. The weighted error vector is given by $e_w = W_e e$, where $W_e = \text{diag}\{w_0, \ldots, w_{\nu-1}\}$ and $\nu = \sum_{i=0}^{p} N(m_i) + \sum_{j=0}^{s} \dim(d_j)$. If w_a and w_b are related to the same c_i constraint, $w_a = w_b = w_{c_i}$. This also applies for weights related to constraints d_u. However, independent weights can be assigned for the position and orientation components of a constraint.

3.6. Initialization of the Kinematic Chains. To accurately estimate the limb posture, it is required to properly couple the human and exoskeleton kinematic models. To do so, we require to correctly position the end-effectors of the human kinematic model with respect to the arm, forearm, and hand coordinate systems. These end-effectors must be positioned such that they are able to move together with the coordinate systems of the fixations of the exoskeleton model (targets). Notice that the position of the end-effectors with respect to the links of the human model changes according to the actual patient and exoskeleton dimensions.

Figure 6 depicts a state in which the human and exoskeleton models are decoupled. The correct position and orientation of the coordinate systems of the end-effectors of the human model have not been calculated, and, therefore, they do not match the position and orientation of the exoskeleton's fixations coordinate systems.

The initialization of the kinematic chains requires a reference pose of the exoskeleton in which (a) the human joints angles can be determined accurately and (b) the exoskeleton's fixations undergo negligible deformation, reducing the uncertainty about the position of the human model end-effectors.

The pose of the exoskeleton that meets the mentioned requirements is the one in which the flexion/extension of the shoulder and elbow take place in the sagittal plane (Figure 6). In this pose, the position of the human GH joint with respect to the exoskeleton base can be easily determined because the joints of the spine and shoulder complex are in their rest position.

The coupling process involves the following steps.

(1) Position the exoskeleton model such that the joint j_{R_0} lies above the human GH joint. Adjust the height of the exoskeleton model such that j_{R_2} is at the level of the human GH joint. These instructions are prescribed by the manufacturer of exoskeleton to use it with the actual patient.

(2) Compute the arm flexion and abduction angles such that the arm passes through the origin of the arm fixation coordinate system. Adjust the origin of the arm end-effector coordinate system to match the origin of the arm fixation.

(3) With the position of the elbow joint defined, compute the elbow flexion and the GH internal rotation angles such that the forearm passes through the origin of the exoskeleton forearm fixation. Adjust the origin of the forearm end-effector coordinate system to match the origin of the forearm fixation.

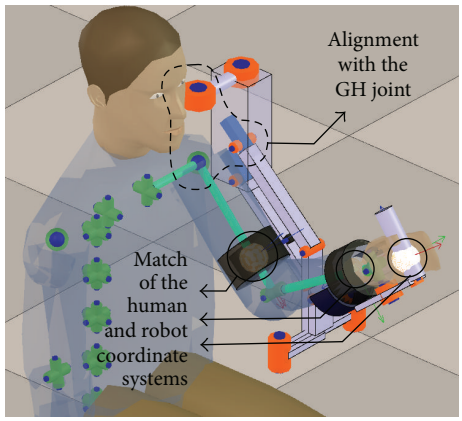

Figure 7: Result of the initialization procedure.

(4) Compute the wrist extension angle such that the human hand is able to grasp the exoskeleton's hand grip. Adjust the hand end-effector to match the position of the Armeo's end-effector at the hand grip.

(5) Calculate the forearm pronation/supination angle such that the wrist's extension/flexion axis matches the orientation of the Armeo's hand grip longitudinal axis with respect to the human forearm pronation/supination axis.

(6) Adjust the human forearm and hand end-effector coordinate systems to match the orientation of the forearm and Armeo's end-effector coordinate systems, respectively.

The result of the initialization process is depicted in Figure 7.

4. Implementation

To implement the proposed method the virtual robot experimentation platform (V-REP) was used [55], which is an open source robotics simulator. V-REP provides tools to easily and efficiently create kinematic models of rigid multibody systems and to solve IK problems. Using the simulator, a scene was created, which contains both the human upper body and Armeo kinematic models (Figures 2 and 3). The weights of the human kinematic model were adjusted (Section 3.5.2) and the simulator's IK module was configured to include the kinematic constraints (Section 3.4).

The source code of the simulator was compiled, modified, and integrated into our rehabilitation platform. Custom classes and functions were programmed to allow easy data exchange among the Armeo, the rehabilitation game platform, and the IK module of the simulator.

The limb posture estimation process consists of the following steps.

(1) Obtain the angles of the Armeo's joints by using hardware and software interfaces provided by HOCOMA AG [47].

(2) Use the obtained angles to update the joints angles of the Armeo's kinematic model in the simulator.

(3) Retrieve the angles of the joints of the human model computed by the simulator's IK module.

Computing the inverse kinematics of our upper limb kinematic model, once the Armeo model is updated in the simulator with the real joint measurements of the exoskeleton, takes less than 4 ms on a 2.13 Ghz dual-core CPU. Therefore, the implemented method is suitable for real-time posture estimation without using high-performance hardware.

After the joint estimates are produced, we use them to update the patient avatar in VR games. We also store them in a database for a posterior patient assessment.

Figure 8 presents a user test of the limb posture estimation algorithm feeding the Armeo kinematic model in the simulator (in real time) with the Armeo Spring joint positions measured by its encoders. This figure presents the posture of the test subject and Armeo Spring in parallel with estimations of the user posture in the simulator. The test subject performed

(a) reaching exercises, in which the subject recreated the postures of his arm to reach and grab objects that are close to his body (Figure 8(a)). These exercises are frequently practiced during the arm rehabilitation;

(b) extreme region exercises, in which the subject positioned his hand in the boundaries of his arm workspace (Figure 8(b)). These exercises are challenging for the subject and are less likely to occur during the therapies due to the exercises difficulty.

4.1. VR Games. Currently, we have implemented two types of games for the robotic-assisted upper limb rehabilitation therapy. The first type of games focuses on the rehabilitation of reaching movements. The second type of games addresses the rehabilitation of analytic movements of the GH, elbow, and wrist joints.

4.1.1. Reaching Rehabilitation. Reaching rehabilitation is performed by training the movements that are required to reach and grasp objects with the hand. These exercises involve several joints of the upper limb, and, therefore, they are considered complex.

To train these exercises, we have programmed a game in which the patient controls the movement of a virtual human arm by moving his own arm (Figure 9(a)). The target of the patient is to reach a specific object (e.g., cube) in the scene, grab it, and bring it to a releasing area (e.g., green circle).

4.1.2. Analytic Movements Rehabilitation. According to motor learning theories, the training of analytic movements constitutes the first step into learning complex motor tasks. In such a step, simple movements involving few DOFs of the limb are practiced [56–58].

For this scenario, we have programmed a game (Figure 9(b)) in which the patient controls the position

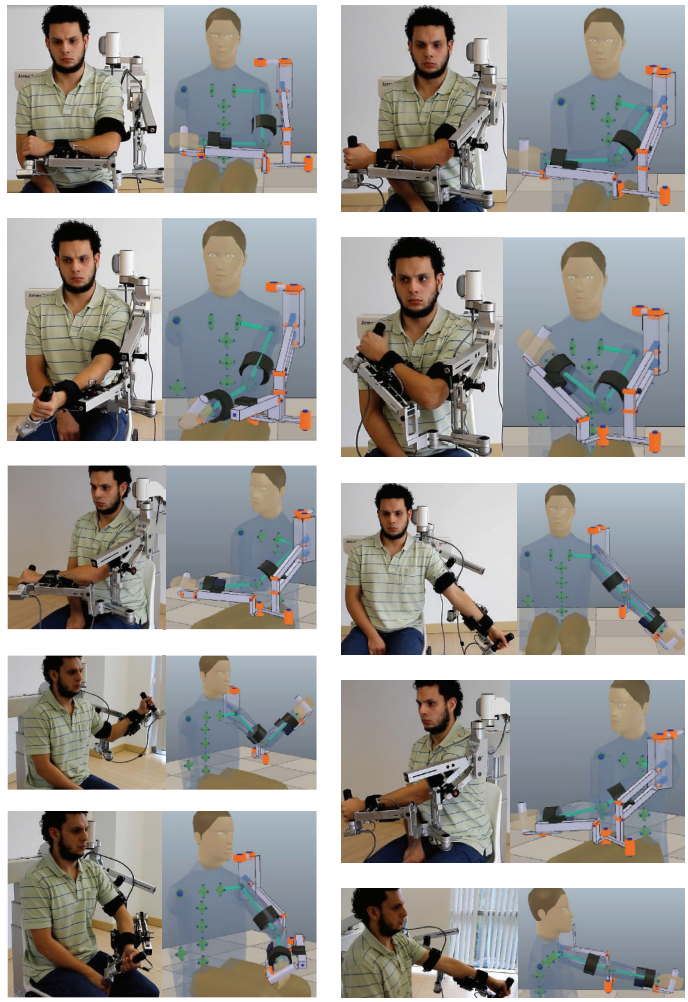

(a) (b)

Figure 8: Test subject in parallel with estimations of his posture in the simulator. (a) shows reaching exercises and (b) shows extreme region exercises.

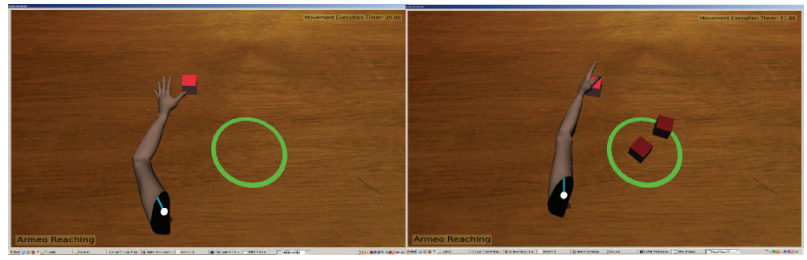

(a) Reaching game

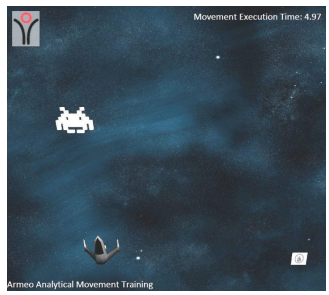

(b) Analytic game

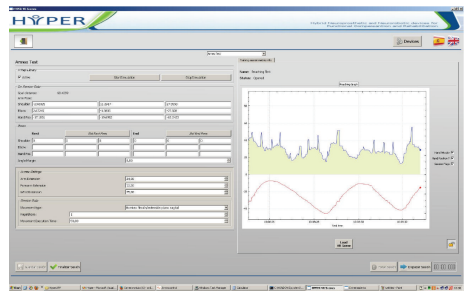

(c) Medical interface

Figure 9: Games and medical interface.

of a spaceship, along the horizontal axis of the screen, by performing 1-DOF movements with the wrist, elbow, or GH joint. The target of the game is that the patient positions the spaceship under an alien that moves along a vertical path from the top to the bottom of the screen. When the position of the spaceship is correct, it fires a gun and destroys the alien.

For both games, the limitations of the mobility of the patient are identified in a calibration phase, guarantying that the target of the games is properly located. Other game parameters (number of executions, max execution time per task, target size, etc.) are adjusted through the medical interface (Figure 9(c)). The medical interface allows the physician to select the games for the training, configure its parameters, and review metrics related to the performance of the patient during a game.

The VR games were programed with the OpenSceneGraph API [59], which allows animating deformable virtual objects and creating scenes with dynamic simulations using the Bullet Physics package. The graphic rendering of the VR game runs at 30 frames per second using a ATI Radeon HD 4600 GPU, which is a midrange graphic card.

During the therapy, the patient sees the VR scene. The kinematic models are used for IK computations and they are not displayed.

5. Evaluation

In order to determine the accuracy of our developed method, the joint angles of 4 voluntary healthy male test subjects (average age 34 years) were measured by using an optical tracking system and compared with the angles obtained from our posture estimation algorithm during the execution of typical (in this case, analytic movements) robotic-assisted rehabilitation exercises. As discussed in Section 4.1.2, the rehabilitation of analytic movements is a necessary step before addressing the rehabilitation of complex motor tasks.

The specific exercises performed by the test subjects were

(1) wrist flexion/extension (WFE),

(2) elbow flexion/extension (EFE),

(3) forearm pronation/supination (FPS),

(4) simultaneous elbow flexion/extension and forearm pronation/supination (SEFEFPS).

The evaluation of our method has been conducted without performing any previous setting or automatic adjustment of the weights or other parameters of the approach in order to reduce the estimation errors. However, algorithm training might be used in the future to improve the method's performance.

5.1. Measurement of the Upper Limb Joint Angles. A detailed explanation of the method that was used to measure the human joint angles would merit an additional manuscript. Nevertheless, a basic description of this method is provided next.

In order to measure the limb joint angles of the test subject, we use a Polaris Spectra optical tracking system (OTS) [60]. In order to track the limb movements, it is necessary to install on test subject limb a set of rigid bodies with passive markers. By detecting these passive markers (reflective spheres), the OTS is able to compute the position and orientation of each rigid body.

Table 2: Installation of the reference and mobile rigid bodies in the evaluation.

Angle to measure	Reference rigid body installed on	Mobile rigid body installed on
WFE	Forearm	Hand
EFE	Upper arm	Forearm
FPS	Upper arm	Forearm

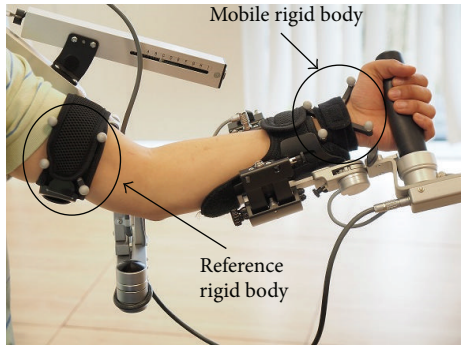

Figure 10: Setup for the quantitative assessment of the estimation errors in elbow flexion/extension exercise.

One rigid body (reference rigid body) is used as the coordinate system of reference for the measurements of the OTS. The position and orientation of the other rigid bodies (mobile rigid bodies) are computed with respect to the reference rigid body.

The reference and mobile rigid bodies are installed on different arm segments (i.e., upper arm, forearm, and hand) according to the joint angle to be measured. Table 2 shows the installation of the reference and mobile rigid bodies for each of the joint angles that we measured. Figure 10 shows the configuration of the rigid bodies to measure the elbow flexion/extension angle.

In order to measure the human joint angles, we have adapted the method presented in [61], which is originally proposed to be used with IMMSs, to implement it by using an OTS. In [61] it is proposed to measure the joint angles by following the next steps.

(1) Compute a reference coordinate system for the joint of interest. A subset of the axes of the resulting coordinate system match the axes of rotation of the joint. The position and orientation of the joint coordinate system are defined with respect to the reference rigid body.

(2) Compute the orientation of the mobile rigid body with respect to the joint coordinate system.

(3) Compute the joint angles that result from rotations of the mobile rigid body by using Euler-angles decomposition. The rotations of the mobile rigid body are caused by the exercising of the subject joint.

To build an orthogonal right-handed coordinate system of reference for the joint, we identify each axis of rotation of the joint, as proposed in [61].

To identify each rotation axis of the joint, we use the instant helical axis method described in [62]. A rotational axis of the joint is computed from the kinematic data of the mobile rigid body while the subject performs 1-DOF movements of the joint.

In contrast to the proposal presented in [61] to compute the wrist joint coordinate system, we build this coordinate system by identifying only the flexion/extension axis, given that the ulnar/radial deviation cannot be trained with the Armeo Spring.

Accuracy of the Limb Joint Angles Measurement Method. In motor rehabilitation, *goniometry* is the standard method to measure the angle at the patient joints. This is a manual method, and, therefore, its efficacy depends on the examiner experience [63]. One of the limitations of this method is that it provides a resolution (minimal detectable change) in measuring limb joint angles of about 8 degrees [64]. In other words, this method should not be used to measure angles smaller than 8 degrees because in those cases measurements present large uncertainty.

Alternative approaches to measure the patient limb joint angles are IMMS-based methods. One of the methods that provide better accuracy than goniometry is presented in [35]. This method provides a measurement accuracy characterized by a RMSE of less than 3.6 degrees. The authors of the mentioned work conclude that this accuracy is proper for measuring elbow and shoulder angles of clinical relevance in ambulatory settings.

In tests with an artificial 1-DOF joint, the method to measure the limb joint angles that we have adapted from [61] allowed us to estimate the joint angle with a RMSE smaller than 1 degree. According to a comparison with the accuracy provided by the reviewed methods, we conclude that the method proposed by [61] to measure the limb posture is valid to determine the accuracy of our proposed limb posture estimation method.

5.2. Protocol. Table 3 summarizes the main features of the evaluation that we have conducted.

For each trial of the evaluation exercises we performed the following steps.

(1) Compute the joint coordinate system corresponding to the evaluation exercise (Section 5.1).

(2) Instruct the subject to perform the corresponding evaluation exercise until the number of desired joint angle measurements is taken.

(3) Compute the RMSE in the estimation of each joint angle by comparing the measured angle with the estimation provided by our algorithm.

(4) Compute the ROM of the subject movements from the measured angles.

During the execution of the evaluation exercises the amplitude, speed and the number of cycles of the movements in each trial were left to the discretion of each test subject. In the evaluation, the VR games were not executed, given that they are not necessary to assess the accuracy of the posture estimation algorithm. Furthermore, in this way the influence of the VR games on the subject movement amplitude, speed, and repetitions is avoided, which derives a richer variety of movement features in the evaluation exercises.

However, it is worth mentioning that the joint limits of the exoskeleton, the need to avoid occlusions of the passive markers on the rigid bodies attached to the test subject, and the limited detection volume of the OTS do constrain the subject's movements.

Table 3: Summary of main features of the evaluation tests.

Number of test subjects	Number of exercises performed by each test subject	Number of trials per exercise	Joint angles measurements per trial
4	4 (WFE, EFE, FPS, and SEFEFPS)	4	2960 at 66.6 Hz

Table 4: Estimation errors in wrist flexion/extension exercise (units in degrees).

Subject	Average WFE RMSE	Average WFE ROM
1	1.137	53.389
2	1.432	54.824
3	3.282	63.869
4	3.555	53.977
Average	2.351	56.265

Table 5: Motion features for subjects 1 and 3 in WFE exercise.

Aspect	Subject 1	Subject 3
Average angular speed (deg/s)	26	82
Time delay (ms)	15	60

6. Results and Discussion

In this section, we present the results of the experiments described in Section 5. Tables 4, 6, 7, and 8 (angles expressed in degrees) present the average RMSE obtained in the estimation of the angle of interest by using our proposed algorithm. Each table presents the average ROM of the movement performed by each test subject. The average RMSE and ROM metrics mentioned previously are obtained from the 4 trials that each subject performed for each exercise. The last row in the tables presents the average values of each of the computed metrics for all subjects.

N.B.: in this section we compare our results against freely moving subject cases reported in the literature. We resort to such free movement cases since we found no reports concerning estimations errors of the wrist or elbow angles in limbs constrained with exoskeletons.

Table 6: Estimation errors in elbow flexion/extension exercise (units in degrees).

Subject	Av. EFE RMSE	Av. EFE ROM	Av. FPS RMSE	Av. FPS ROM
1	1.636	36.948	0.980	4.148
2	1.553	33.897	1.408	4.921
3	2.815	49.333	2.187	5.216
4	4.381	36.442	1.128	7.160
Average	2.596	39.150	1.426	5.361

Table 7: Estimation errors in forearm pronation/supination exercise (units in degrees).

Subject	Av. EFE RMSE	Av. EFE ROM	Av. FPS RMSE	Av. FPS ROM
1	1.221	5.799	1.965	70.453
2	1.799	7.395	2.639	48.500
3	1.627	9.691	4.147	90.527
4	1.132	2.459	4.568	37.717
Average	1.445	6.336	3.330	61.799

Table 8: Estimation errors in simultaneous elbow flexion/extension and forearm pronation/supination exercise (units in degrees).

Subject	Av. EFE RMSE	Av. EFE ROM	Av. FPS RMSE	Av. FPS ROM
1	2.224	35.762	2.707	59.878
2	2.773	40.837	3.037	58.441
3	5.212	47.850	4.429	55.228
4	2.679	36.654	2.158	59.673
Average	3.222	40.276	3.083	58.305

6.1. Wrist Flexion/Extension. Table 4 presents angle estimation statistics for wrist flexion and extension. The ROM exercised by the subjects presents small variability and seems not to correlate with RSME. However, we did observe that subjects 1 and 2 performed slow movements while subjects 3 and 4 moved fast. Such a difference reflects on the RMSE values.

To elaborate this point, we present in Figure 11 the history of the measured versus estimated angle, for subjects 1 and 3. The sampling span is 250 (approx. 3.75 seconds). The motion features of the movements shown in Figure 11 are summarized in Table 5. In such table, the time delay aspect refers to the time delay that the estimations provided by our algorithm present with respect to the measured angles. The time delay is larger when the subject moves fast. This causes the increment in the RMSE estimation values.

These results suggest that the response speed of our algorithm, given a change in the Armeo joint angles caused by the movement of the human subject, allows providing better estimates when the subject moves slowly (as in rehabilitation therapy). In our algorithm, the response speed largely depends on the damping constant used in the DLS method to solve the limb's IK. By using a smaller damping constant in the DLS method, the response speed can be improved, sacrificing some stability.

Nevertheless, the average RMSE obtained for all subjects shows a better performance of our method with respect to [39], an optimization-based approach which presents errors around 3.5 degrees. Compared to [36], which presents a IMMS-based method to estimate the wrist angles with a RMSE of less than 3 degrees, our results are slightly better.

6.2. Elbow Flexion/Extension. In flexion and extension of elbow (Figure 12, Table 6), involuntary movement along the pronation/supination axis is not avoided. Therefore, small excursions in this DOF were observed.

For all subjects, our method overestimates the amplitude of rotational movements about the flexion/extension axis, when compared against the measured values (see Figure 12(a) for subject 2).

Our method performs better than the one in [39], in which the reported mean error in estimating the flexion/extension angle is approximately 14 degrees. Compared to the approach in [35], which uses a IMMS-based method and presents a RMSE of 3.6 degrees in estimating elbow and shoulder angles, our method also presents better performance.

We include in Table 6 the estimation statistics for pronation/supination angle in order to illustrate the performance of our method with small angular displacements. Figure 12(b) displays the estimation and measurement of pronation/supination angle for a trial of subject 2. In this figure, we observe that there is an underestimation of the angle. However, it must be taken into account that estimation errors for small ROMs are in the same order of the measurement method accuracy (RMSE 1 degree).

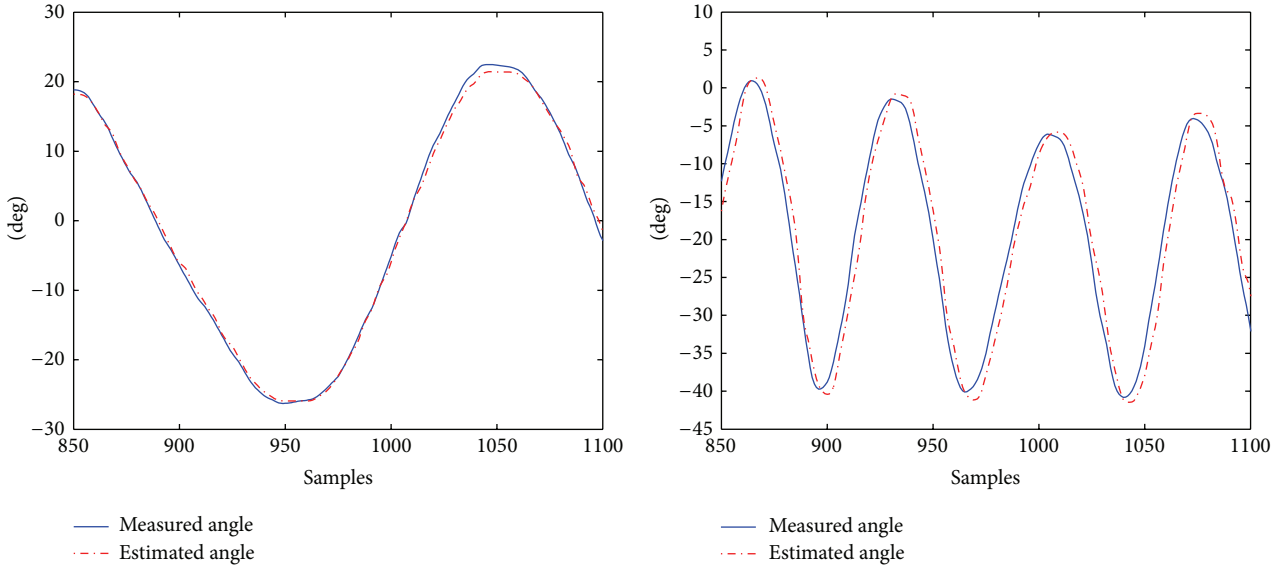

(a) Motion of subject 1

(b) Motion of subject 3

Figure 11: Motion patterns of subjects 1 and 3 during a trial of wrist flexion/extension.

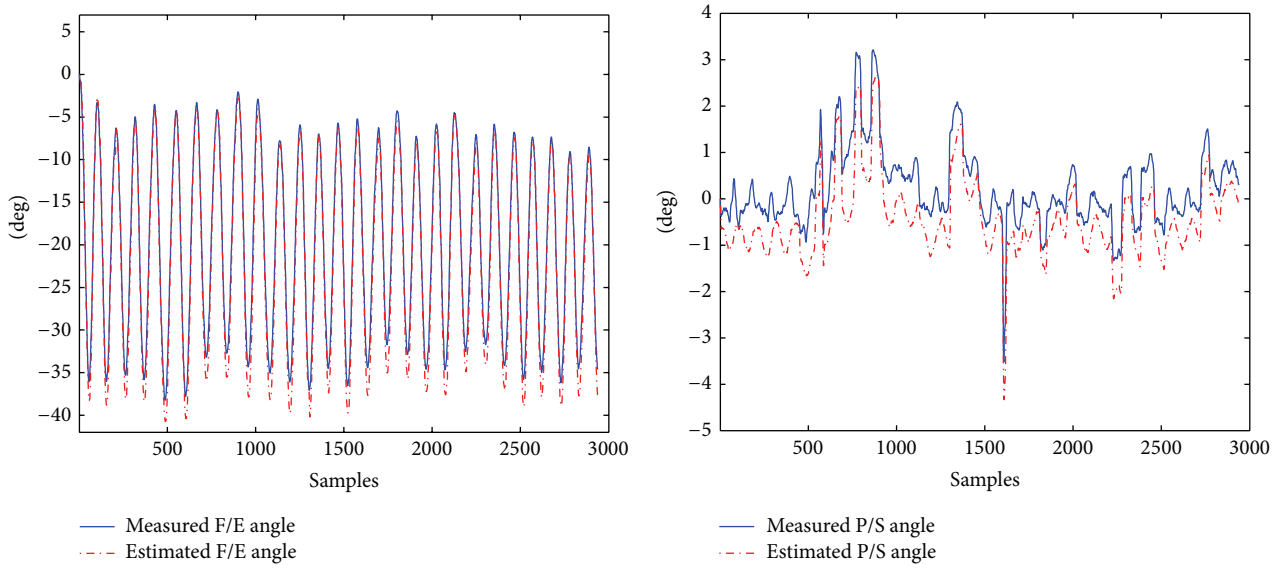

(a) Estimation results of the flexion/extension angle

(b) Estimation results of the pronation/supination angle

Figure 12: Estimation results of the elbow angles during flexion/extension for trial of subject 2.

6.3. Forearm Pronation/Supination. Table 7 and Figure 13 show the statistics of our method for forearm pronation/supination angle estimation. We remark that motion in the elbow flexion/extension axis may occur during the forearm pronation/supination exercise. Therefore, we also report (in Table 7 and Figure 13) the estimation results for the small angular movements around the flexion/extension axis.

The average RMSE in the estimation of the pronation/supination DOF of our method presents an accuracy similar to the one of [35] (RMSE 3.6 degrees).

Figure 13 shows the elbow angles estimation results for a trial of the FPS exercise of subject 1. Figure 13(a) shows that estimations in the flexion/extension DOF, in which small movements were performed, do not present the oscillations of the measured angle (RMSE 1.175 degrees). On the other hand, Figure 13(b) shows that estimations of the pronation/supination angle are very close to the measured values.

For the pronation/supination angle, the worse estimations were obtained for subject 4, who performed short but

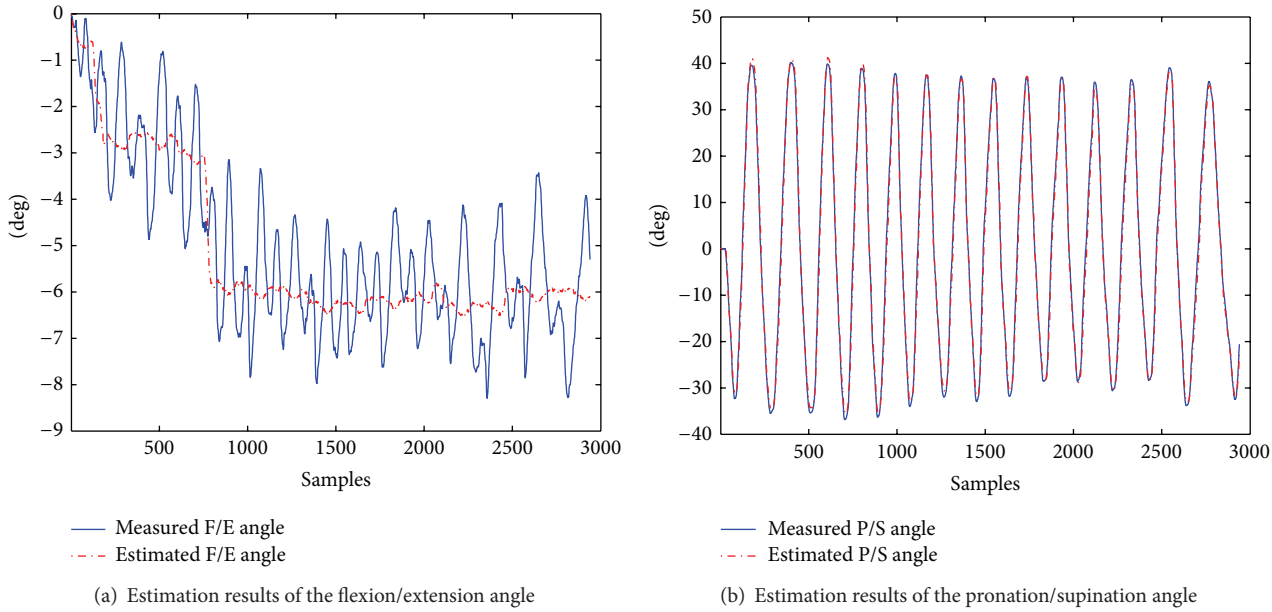

(a) Estimation results of the flexion/extension angle

(b) Estimation results of the pronation/supination angle

Figure 13: Estimation results of the elbow angles during pronation/supination for a trial of subject 1.

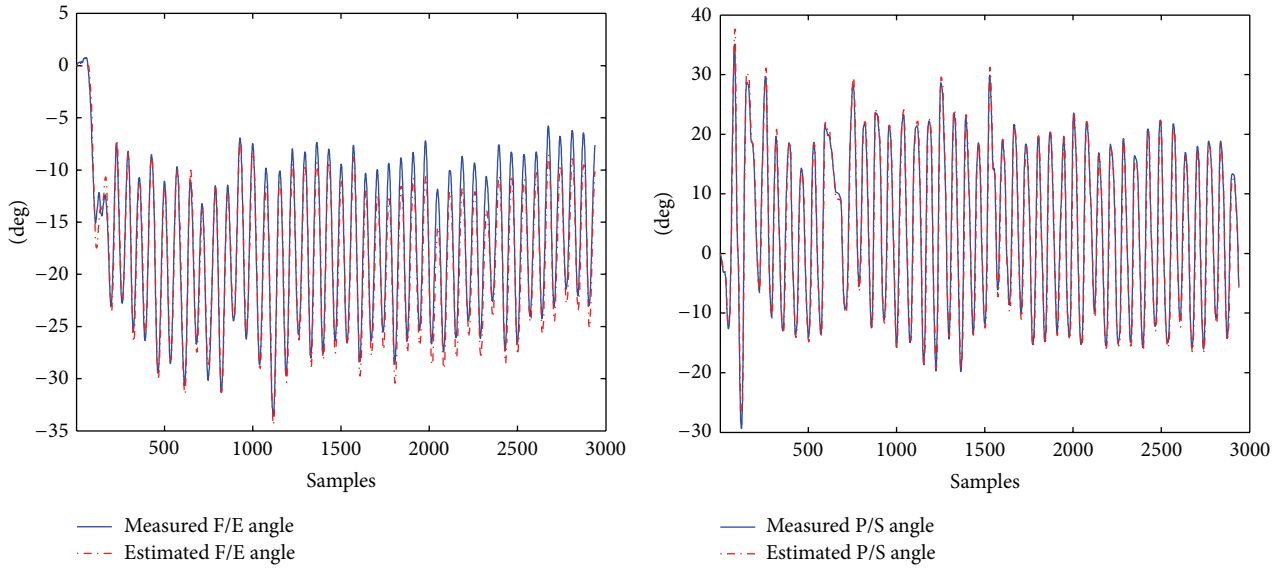

(a) Estimation results of the flexion/extension angle

(b) Estimation results of the pronation/supination angle

Figure 14: Estimation results of the elbow angles during simultaneous flexion/extension and pronation/supination for a trial of subject 4.

very fast movements, affecting the estimation accuracy as described in Section 6.1.

According to results presented here and in Section 6.2, it seems that for small movements the estimation approach is slightly more sensitive to movements in the pronation/supination DOF than on the flexion/extension DOF.

6.4. Simultaneous Elbow Flexion/Extension and Forearm Pronation/Supination. The objective of this exercise is to evaluate how simultaneous movements of both DOFs of the elbow affect the angle estimations for this joint. The results are presented in Table 8. In this table, it is shown that, for both elbow DOFs, the average of the RMSE for all the subjects is similar to the one presented in [35] (RMSE 3.6 degrees).

This result also suggests that, during the performance of a functional rehabilitation exercise, such as reaching, in which simultaneous flexion/extension and pronation/supination movement are necessary, the accuracy of the estimations would remain in an adequate range.

Figure 14 presents the estimation results of a trial of this exercise of subject 4. In this figure, it can be observed that estimations follow closely the measured angles.

7. Conclusions and Future Work

This paper presents a method that can be applied to estimate the posture of the human limbs during the interaction with exoskeletons by solving the limb IK problem extended with the kinematic constraints of the exoskeleton fixations on the limb. The few approaches in the literature that deal with limb posture estimation in a robotic-assisted scenario are specifically designed to estimate the arm posture. In contrast, the method that we propose provides a general formulation, which is not specific to any human limb or exoskeleton. Our method is based on inverse kinematics and it can be implemented using standard robotics libraries.

In this paper, we have also shown the implementation of the method to provide upper limb posture estimations, in real time, using the Armeo Spring. We have also presented the use of the resulting limb postures estimations in the animation of avatars in VR rehabilitation games.

We have evaluated the accuracy of the estimations of our method during the performance of analytic rehabilitation exercises of the wrist and elbow. The obtained results show that our approach presents an accuracy that is better than the one provided by goniometry, which is the traditional method to measure the patient angles in motor rehabilitation. Compared to the accuracy provided by IMMSs-based methods, which are considered enough accurate to measure clinical relevant limb joint angles in nonrobotic-assisted scenarios, we have obtained very similar results.

Based on the mentioned results, we conclude that our approach can be used to (a) provide an estimation of the pose of the human upper limb with enough accuracy to be used for avatar animation in VR games and (b) obtain the kinematic data for the patient assessment during analytic training of the elbow and wrist.

Future work includes (a) the exploration of other approaches to model the flexible fixations of the exoskeleton, (b) the definition of a set of weights for the human model joints that represent the movement features of a set of human subjects, and (c) a quantitative assessment of the performance of our method in a functional rehabilitation scenario.

Nomenclature

Clavicle: One of the bones of the shoulder girdle. It is located at the root of the neck
DLS: Damped least squares
DOF: Degree of freedom
EFE: Elbow flexion/extension
FPS: Forearm pronation/supination
GH: Glenohumeral
Humerus: Upper arm bone
IK: Inverse kinematics
IMMSs: Inertial and magnetic measurement systems
OTS: Optical tracking system
RMSE: Root mean square error
ROM: Range of motion
Scapula: One of the bones of the shoulder girdle. It connects the humerus with the clavicle
SEFEFPS: Simultaneous EFE and FPS
VR: Virtual reality
V-REP: Virtual robot experimentation platform
WFE: Wrist flexion/extension
v: Total number of constraints of the IK problem ($v \in \mathbb{N}$)
e: IK error vector ($e \in \mathbb{R}^v$)
k: Total DOFs of the human kinematic model ($k \in \mathbb{N}$)
n: Total DOFs of the exoskeleton kinematic model ($n \in \mathbb{N}$)
Z: Jacobian matrix of the IK problem ($Z \in \mathbb{R}^{v \times k}$)
I: $v \times v$ identity matrix
W_q: Diagonal matrix of joints weights ($W_q \in \mathbb{R}^{+k \times k}$)
W_e: Diagonal matrix of constraints weights ($W_e \in \mathbb{R}^{+v \times v}$)
q_{H_t}: Vector of joint angles of the human kinematic model in instant t ($q_{H_t} \in \mathbb{R}^k$)
q_{R_t}: Vector of joint angles of the exoskeleton kinematic model in instant t ($q_{R_t} \in \mathbb{R}^n$)
α: Damping factor of DLS method ($\alpha \in \mathbb{R}^+$).

Conflict of Interests

The authors declare that there is no conflict of interests regarding the publication of this paper.

Acknowledgment

This research is a part of the HYPER Project funded by CONSOLIDER-INGENIO 2010, Spanish Ministry for Science and Innovation.

References

[1] J. W. Krakauer, "Motor learning: its relevance to stroke recovery and neurorehabilitation," *Current Opinion in Neurology*, vol. 19, no. 1, pp. 84–90, 2006.

[2] S. V. Adamevich, A. S. Merians, R. Boian et al., "A virtual reality-based exercise system for hand rehabilitation post-stroke," *Presence: Teleoperators and Virtual Environments*, vol. 14, no. 2, pp. 161–174, 2005.

[3] R. Riener, T. Nef, and G. Colombo, "Robot-aided neurorehabilitation of the upper extremities," *Medical & Biological Engineering & Computing*, vol. 43, no. 1, pp. 2–10, 2005.

[4] A. De Mauro, E. Carrasco, D. Oyarzun et al., "Advanced hybrid technology for neurorehabilitation: the HYPER project," in *Advances in Robotics and Virtual Reality*, T. Gulrez and A. Hassanien, Eds., vol. 26 of *Intelligent Systems Reference Library*, pp. 89–108, Springer, Berlin, Germany, 2012.

[5] N. Jarrassé and G. Morel, "On the kinematic design of exoskeletons and their fixations with a human member," in *Robotics: Science and Systems*, Citeseer, 2010.

[6] H. Kim, L. M. Miller, Z. Li, J. R. Roldan, and J. Rosen, "Admittance control of an upper limb exoskeleton—reduction of energy exchange," in *Proceedings of the 34th Annual International Conference of the IEEE Engineering in Medicine and*

Biology Society (EMBS '12), pp. 6467–6470, San Diego, Calif, USA, September 2012.

[7] M. Guidali, A. Duschau-Wicke, S. Broggi, V. Klamroth-Marganska, T. Nef, and R. Riener, "A robotic system to train activities of daily living in a virtual environment.," *Medical & biological engineering & computing*, vol. 49, no. 10, pp. 1213–1223, 2011.

[8] A. Frisoli, C. Procopio, C. Chisari et al., "Positive effects of robotic exoskeleton training of upper limb reaching movements after stroke," *Journal of NeuroEngineering and Rehabilitation*, vol. 9, no. 1, article 36, 2012.

[9] M. Gilliaux, T. Lejeune, C. Detrembleur, J. Sapin, B. Dehez, and G. Stoquart, "A robotic device as a sensitive quantitative tool to assess upper limb impairments in stroke patients: a preliminary prospective cohort study," *Journal of Rehabilitation Medicine*, vol. 44, no. 3, pp. 210–217, 2012.

[10] S. E. Fasoli, H. I. Krebs, J. Stein, W. R. Frontera, and N. Hogan, "Effects of robotic therapy on motor impairment and recovery in chronic stroke," *Archives of Physical Medicine and Rehabilitation*, vol. 84, no. 4, pp. 477–482, 2003.

[11] B. R. Brewer, S. K. McDowell, and L. C. Worthen-Chaudhari, "Poststroke upper extremity rehabilitation: a review of robotic systems and clinical results," *Topics in Stroke Rehabilitation*, vol. 14, no. 6, pp. 22–44, 2007.

[12] R. W. Teasell and L. Kalra, "Whats new in stroke rehabilitation," *Stroke*, vol. 35, no. 2, pp. 383–385, 2004.

[13] G. Epelde, X. Valencia, A. Ardanza et al., "Virtual arm representation an d multimodal monitoring for the upper limb robot assisted teletherapy," in *Proceedings of the International Congress on Neurotechnology, Electronics and Informatics (NEUROTECHNIX '13)*, vol. 43, pp. 69–80, ScitePress, 2013.

[14] H. S. Lo and S. Q. Xie, "Exoskeleton robots for upper-limb rehabilitation: state of the art and future prospects," *Medical Engineering and Physics*, vol. 34, no. 3, pp. 261–268, 2012.

[15] A. Shumway-Cook and M. H. Woollacott, *Motor Control: Translating Research into Clinical Practice*, Wolters Kluwer Health, 2007.

[16] R. A. Schmidt and T. Lee, "Motor Control and Learning, 5E," Human kinetics, 1988.

[17] J. Broeren, K. S. Sunnerhagen, and M. Rydmark, "A kinematic analysis of a haptic handheld stylus in a virtual environment: a study in healthy subjects," *Journal of NeuroEngineering and Rehabilitation*, vol. 4, no. 1, article 13, 2007.

[18] D. B. Chaffin, "Human motion simulation for vehicle and workplace design," *Human Factors and Ergonomics in Manufacturing & Service Industries*, vol. 17, no. 5, pp. 475–484, 2007.

[19] J. Faraway and M. P. Reed, "Statistics for digital human motion modeling in ergonomics," *Technometrics A: Journal of Statistics for the Physical, Chemical and Engineering Sciences*, vol. 49, no. 3, 2007.

[20] P. Baerlocher and R. Boulic, "An inverse kinematics architecture enforcing an arbitrary number of strict priority levels," *Visual Computer*, vol. 20, no. 6, pp. 402–417, 2004.

[21] H. Kim, L. M. Miller, N. Byl, G. M. Abrams, and J. Rosen, "Redundancy resolution of the human arm and an upper limb exoskeleton," *IEEE Transactions on Biomedical Engineering*, vol. 59, no. 6, pp. 1770–1779, 2012.

[22] E. S. Jung and Y. Shin, "Two-handed human reach prediction models for ergonomic evaluation," *Human Factors and Ergonomics in Manufacturing & Service Industries*, vol. 20, no. 3, pp. 192–201, 2010.

[23] Y. Xiang, J. S. Arora, and K. Abdel-Malek, "3D human lifting motion prediction with different performance measures," *International Journal of Humanoid Robotics*, vol. 9, no. 2, Article ID 1250012, 2012.

[24] L. Ma, W. Zhang, D. Chablat, F. Bennis, and F. Guillaume, "Multi-objective optimisation method for posture prediction and analysis with consideration of fatigue effect and its application case," *Computers & Industrial Engineering*, vol. 57, no. 4, pp. 1235–1246, 2009.

[25] Z. Mi, J. Yang, and K. Abdel-Malek, "Optimization-based posture prediction for human upper body," *Robotica*, vol. 27, no. 4, pp. 607–620, 2009.

[26] Z. Li, H. Kim, D. Milutinović, and J. Rosen, "Synthesizing redundancy resolution criteria of the human arm posture in reaching movements," in *Redundancy in Robot Manipulators and Multi-Robot Systems*, vol. 57 of *Lecture Notes in Electrical Engineering*, pp. 201–240, Springer, Berlin, Germany, 2013.

[27] J. Yang, R. T. Marler, S. Beck, K. Abdel-Malek, and J. Kim, "Real-time optimal reach-posture prediction in a new interactive virtual environment," *Journal of Computer Science and Technology*, vol. 21, no. 2, pp. 189–198, 2006.

[28] J. Gragg and J. Yang, "Posture reconstruction-some insights," in *Proceedings of the 1st International Symposium on Digital Human Modeling-IEA-DHM*, pp. 14–16, 2011.

[29] J. Yang, S. Rahmatalla, T. Marler, K. Abdel-Malek, and C. Harrison, "Validation of predicted posture for the virtual human santos," in *Proceedings of the 1st International Conference on Digital Human Modeling*, pp. 500–510, Springer, Beijing, China, July 2007.

[30] J. Yang, R. T. Marler, H. Kim, J. S. Arora, and K. Abdel-Malek, "Multi-objective optimization for upper body posture prediction," in *Proceedings of the 10th AIAA/ISSMO Multidisciplinary Analysis and Optimization Conference*, vol. 30, pp. 2288–2305, September 2004.

[31] I. Pasciuto, S. Ausejo, J. T. Celigüeta, Á. Suescun, and A. Cazón, "A comparison between optimization-based human motion prediction methods: data-based, knowledge-based and hybrid approaches," *Structural and Multidisciplinary Optimization*, vol. 49, no. 1, pp. 169–183, 2014.

[32] Y. Xiang, J. S. Arora, and K. Abdel-Malek, "Hybrid predictive dynamics: a new approach to simulate human motion," *Multibody System Dynamics*, vol. 28, no. 3, pp. 199–224, 2012.

[33] N. Jarrasse, V. Crocher, and M. Guillaume, "A method for measuring the upper limb motion and com puting a compatible exoskeleton trajectory," in *Proceedings of the IEEE/RSJ International Conference on Intelligent Robots and Systems (IROS '12)*, pp. 3461–3466, 2012.

[34] J. C. Perry, J. Rosen, and S. Burns, "Upper-limb powered exoskeleton design," *IEEE/ASME Transactions on Mechatronics*, vol. 12, no. 4, pp. 408–417, 2007.

[35] A. G. Cutti, A. Giovanardi, L. Rocchi, A. Davalli, and R. Sacchetti, "Ambulatory measurement of shoulder and elbow kinematics through inertial and magnetic sensors," *Medical and Biological Engineering and Computing*, vol. 46, no. 2, pp. 169–178, 2008.

[36] H. Zhou and H. Hu, "Reducing drifts in the inertial measurements of wrist and elbow positions," *IEEE Transactions on Instrumentation and Measurement*, vol. 59, no. 3, pp. 575–585, 2010.

[37] J. Yang, K. Abdel-Malek, and K. Nebel, "Reach envelope of a 9-degree-of-freedom model of the upper extremity," *International*

Journal of Robotics and Automation, vol. 20, no. 4, pp. 240–259, 2005.

[38] Q. Zou, Q. Zhang, J. Yang et al., "Determining weights of joint displacement objective function for standing reach tasks," in *Proceedings of the 1st International Symposium on Digital Human Modeling*, Lyon, France, 2011.

[39] Q. Zou, Q. Zhang, J. Yang et al., "An alternative formulation for determining weights of joint displacement objective function in seated posture prediction," in *Proceedings of the 3rd International Conference on Digital Human Modeling*, pp. 231–242, Springer, 2011.

[40] J. Gragg, J. Yang, and B. Howard, "Hybrid method for driver accommodation using optimization-based digital human models," *Computer Aided Design*, vol. 44, no. 1, pp. 29–39, 2012.

[41] A. M. Hill, A. M. J. Bull, A. L. Wallace, and G. R. Johnson, "Qualitative and quantitative descriptions of glenohumeral motion," *Gait & Posture*, vol. 27, no. 2, pp. 177–188, 2008.

[42] W. Maurel and D. Thalmann, "Human shoulder modeling including scapulo-thoracic constraint and joint sinus cones," *Computers & Graphics*, vol. 24, no. 2, pp. 203–218, 2000.

[43] K. R. S. Holzbaur, W. M. Murray, and S. L. Delp, "A model of the upper extremity for simulating musculoskeletal surgery and analyzing neuromuscular control," *Annals of Biomedical Engineering*, vol. 33, no. 6, pp. 829–840, 2005.

[44] J. Ambrósioa, C. Quental, B. Pilarczyk, J. Folgado, and J. Monteiro, "Multibody biomechanical models of the upper limb," in *Proceedings of the IUTAM Symposium on Human Body Dynamics: From Multibody Systems to Biomechanics*, pp. 4–17, June 2011.

[45] S. Kim, D. Kim, and S. Chae, "Musculoskeletal upper limb modeling with muscle activation for flexible body simulation," *International Journal of Precision Engineering and Manufacturing*, vol. 10, no. 4, pp. 123–129, 2009.

[46] J. Denavit and R. S. Hartenberg, "A kinematic notation for lower-pair mechanisms based on matrices," *Transactions of the ASME, Journal of Applied Mechanics*, vol. 22, Article ID 215221, pp. 215–221, 1955.

[47] HOCOMA AG, *Armeo Spring—Functional Arm and Hand Therapy for Children*, 2013, http://www.hocoma.com/products/armeo/armeospring/.

[48] A. Cloutier, R. Boothby, and J. Yang, "Motion capture experiments for validating optimization-based human models," in *Proceedings of the 3rd International Conference on Digital Human Modeling*, pp. 59–68, Springer, 2011.

[49] F. S. Grassia, "Practical parameterization of rotations using the exponential map," *Journal of Graphics Tools*, vol. 3, no. 3, pp. 29–48, 1998.

[50] J. Rosen, J. C. Perry, N. Manning, S. Burns, and B. Hannaford, "The human arm kinematics and dynamics during daily activities-toward a 7 DOF upper limb powered exoskeleton," in *Proceedings of the 12th International Conference on Advanced Robotics (ICAR '05)*, pp. 532–539, Seattle, Wash, USA, July 2005.

[51] P. H. Chang, "Closed-form solution for inverse kinematics of robot manipulators with redundancy," *IEEE Journal of Robotics and Automation*, vol. 3, no. 5, pp. 393–403, 1987.

[52] S. R. Buss, Introduction to inverse kinematics with jacobian transpose, pseudoinverse and damped least squares methods, 2009, http://math.ucsd.edu/~sbuss/ResearchWeb/ikmethods/iksurvey.pdf.

[53] S. R. Buss and J.-S. Kim, "Selectively damped least squares for inverse kinematics," *Journal of Graphics, GPU, and Game Tools*, vol. 10, no. 3, pp. 37–49, 2005.

[54] D. E. Schinstock, T. N. Faddis, and R. B. Greenway, "Robust inverse kinematics using damped least squares with dynamic weighting," in *Proceedings of the Conference on Intelligent Robotics in Field, Factory, Service and Space (CIRFFSS '94)*, vol. 2, NASA, Johnson Space Center, 1994.

[55] Coppelia Robotics, V-rep, 2013, http://www.coppeliarobotics.com/.

[56] A. Shumway-Cook and M. H. Woollacott, *Motor Control: Translating Research into Clinical Practice*, Lippincott Williams & Wilkins, Philadelphia, Pa, USA, 4th edition, 2012.

[57] B. Vereijken, E. A. Richard van Emmerik, H. T. A. Whiting, and M. Karl Newell, "Freezing degrees of freedom in skill acquisition," *Journal of Motor Behavior*, vol. 24, no. 1, pp. 133–142, 1992.

[58] R. Cano-de-la Cuerda, A. Molero-Sanchez, M. Carratala-Tejada et al., *Teoriasy Modelos de Control y Aprendizaje Motor. Aplicaciones Clinicas en Neurorrehabilitaci on Neurologia*, 2012.

[59] OpenSceneGraph, "Openscenegraph," April 2014, http://trac.openscenegraph.org/projects/osg/.

[60] NDI, *Polaris Family of Optical Tracking Systems*, January 2014, http://www.ndigital.com/medical/polarisfamily.php.

[61] W. H. K. de Vries, H. E. J. Veeger, A. G. Cutti, C. Baten, and F. C. T. van der Helm, "Functionally interpretable local coordinate systems for the upper extremity using inertial & magnetic measurement systems," *Journal of Biomechanics*, vol. 43, no. 10, pp. 1983–1988, 2010.

[62] H. E. J. Veeger and B. Yu, "Orientation of axes in the elbow and forearm for biomechanical modelling," in *Proceedings of the 15th Southern Biomedical Engineering Conference*, pp. 377–380, March 1996.

[63] R. M. F. de Carvalho, N. Mazzer, and C. H. Barbieri, "Analysis of the reliability and reproducibility of goniometry compared to hand photogrammetry," *Acta Ortopedica Brasileira*, vol. 20, no. 3, pp. 139–149, 2012.

[64] M. J. Kolber, C. Fuller, J. Marshall, A. Wright, and W. J. Hanney, "The reliability and concurrent validity of scapular plane shoulder elevation measurements using a digital inclinometer and goniometer," *Physiotherapy Theory and Practice*, vol. 28, no. 2, pp. 161–168, 2012.

Hindawi Publishing Corporation
BioMed Research International
Volume 2014, Article ID 565370, 13 pages
http://dx.doi.org/10.1155/2014/565370

Research Article

A Tool for Balance Control Training Using Muscle Synergies and Multimodal Interfaces

D. Galeano,[1] F. Brunetti,[1,2] D. Torricelli,[2] S. Piazza,[2] and J. L. Pons[2]

[1] *Catholic University of Asunción, 1394 Asunción, Paraguay*
[2] *Bioenginering Group, Spanish Research Council (CSIC), 28500 Madrid, Spain*

Correspondence should be addressed to D. Galeano; diegogaleano05@gmail.com

Received 27 January 2014; Accepted 5 March 2014; Published 29 May 2014

Academic Editor: Alessandro De Mauro

Balance control plays a key role in neuromotor rehabilitation after stroke or spinal cord injuries. Computerized dynamic posturography (CDP) is a classic technological tool to assess the status of balance control and to identify potential disorders. Despite the more accurate diagnosis generated by these tools, the current strategies to promote rehabilitation are still limited and do not take full advantage of the technologies available. This paper presents a novel balance training platform which combines a CDP device made from low-cost interfaces, such as the Nintendo Wii Balance Board and the Microsoft Kinect. In addition, it integrates a custom electrical stimulator that uses the concept of muscle synergies to promote natural interaction. The aim of the platform is to support the exploration of innovative multimodal therapies. Results include the technical validation of the platform using mediolateral and anteroposterior sways as basic balance training therapies.

1. Introduction

Balance control is a critcal aspect for the growing elderly population and one of the first rehabilitation goals after spinal cord injury (SCI) and stroke [1].

Generally, balance control rehabilitation consists of the execution of specific movements (sway, inclination) or the adoption of static postures. In some therapeutic scenarios, electrical stimulation is also used to promote the recruitment of the muscles that take part in balance control. Recently the use of robotics devices has been also proposed, without yet generating a significant impact on the clinical practice. In this scenario, computerized dynamic posturography (CDP) is a valuable tool to measure balance control and to assess neuromotor recovery through a rehabilitation process.

In this paper, we present a novel multimodal tool for balance control training of elderly and neurologically injured people. The system makes use of the concept of muscle synergies, in the attempt to achieve a closer and more natural interaction with the central nervous system (CNS) of the patient, possibly resulting in better rehabilitation outcomes.

The document is structured as follows. A detailed introduction on the motivations behind the development of the platform is given in Sections 1.1, 1.2, and 1.3. Section 2 describes how the paradigm of muscle synergies is applied to postural control rehabilitation. In Sections 3 and 4, the technical details of the system are presented, with special attention to the importance of timing and synchronization between the multiple interfaces and devices used. In Section 5, the results of the technical validation are presented. In Section 6, we discuss the concepts and features of our platform and present our conclusions.

1.1. Evaluation of Postural and Balance Control. CDP can be considered as an objective assessment tool of postural control. It allows us to know a subject's ability to integrate information from the visual, vestibular, and somatosensory systems or possible alterations of these systems. It enables the assessment of multiple pathologies that can manifest as loss of balance control, vestibular diseases (Meniere's disease, positional vertigo, and vestibular neuritis among others), or neurological diseases (multiple sclerosis, brain

trauma, etc.) [2]. Posturography is usually used to design and implement tailored retraining program balance using visual feedback techniques based on diagnosed sensory deficits and functional capacity of the patient. Besides all these advantages and applications, posturographic systems enable the physician to monitor the evolution of subject treatment and help to evaluate the effectiveness of the prescribed therapy [1, 3].

CDP is based on the idea that the oscillations of the center of pressure (CoP) reflect the postural instability [4]. In line with this hypothesis, the American Medical Association (AMA) has included the monitoring and assessment of CoP trajectories as one of the methods that allows us to objectify deficits or disabilities of postural control. The American Academy of Neurology affirms that CoP monitoring is a useful clinical tool for the analysis of human balance [5]. The CoP is measured by means of force platforms [6], which record forces and moments in the three orthogonal axes. The information is collected by a computer application and used to calculate parameters and indexes from the displacement of the CoP trajectory.

The main drawback of CDP systems is the cost of the equipment. The second major drawback is that there is no agreement in the literature regarding the validity, importance, and relevance of certain postural parameters and indexes obtained by these posturography tools and their relationship with neuromotor disorders.

In the framework of the project HYPER, which is aimed at developing new therapies based on novel neuroprosthetic and neurorobotic solutions, we developed a low-cost posturography and balance training system, composed of inexpensive components like the Wii Balance Board, the Microsoft Kinect, and an electrostimulator. The Wii Balance Board is responsible for obtaining registration of the CoP during testing, whereas the Microsoft Kinect provides online and offline posturography measurements (skeletal tracking). The electrostimulator, called TEREFES [7], provides appropriate muscle stimulation by means of electrical current. All details of the designed posturography system can be found in [8]. Latest changes to this posturography system that are not included in [8] are simplified architecture of the skeleton tracking in 3D with Kinect using `SkeletonPainter3D` [9] (see Figures 1 and 2) and user interface changes in posturography software.

1.2. Rehabilitation of Postural Control. Current efforts in rehabilitation research are increasingly focused on the integration of neuroscientific knowledge in order to develop new effective means of neurorehabilitation based on a deeper understanding of the human control system. At the same time, the recent advances in low-cost technology permit us to complement the basic rehabilitation protocols with new techniques, such as the Rhythmic Weight Shift (RWS) Test [10], the use of functional electrostimulation (FES) [11], robotic devices according to the assisted as needed (AAN) paradigm [12], and virtual reality systems [13].

The RWS Test consists to follow a target reference that moves sinusoidally in the medial-lateral or anterior-posterior axis. This test is included in most commercial posturography

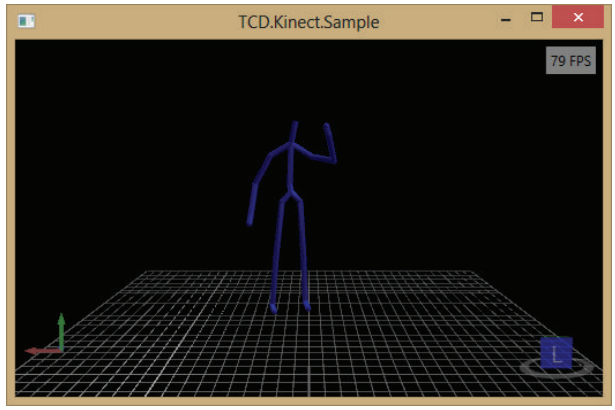

Figure 1: 3D skeleton tracking with Kinect.

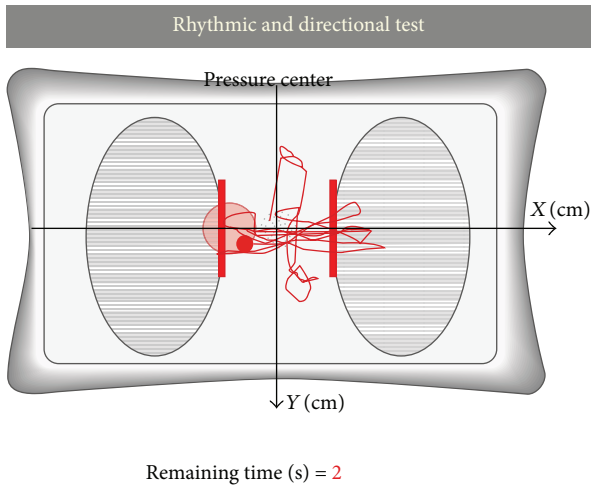

Figure 2: Patient's reference during the rhythmic and directional test.

platforms [14–16]. Used as a training, RWS exercises can generate several benefits as improved balance and reduced risk of falls. Positive effects can extend to other tasks as improved gait kinematics and walking and appears to indirectly contribute to the social insertion of the patient in the community [17].

Functional electrical stimulation (FES) therapy consists in the application of electrical pulses of current used transcutaneous or surface electrodes, in order to promote the execution of functional movements. In recent years, advances in microelectronics and electrode manufacturing led to the development of more powerful, flexible, and smart electrostimulators [7, 18–20]. New FES systems are capable of handling electrode arrays and enable the implementation of more complex control algorithms to generate dynamic stimulation patterns [21]. Despite these advances, very few solutions reached the clinical practice. The main unresolved problems of FES-based interventions are related to muscle fatigue, coordination of multiple muscular patterns, selectivity of muscles, and functional stability of human-machine interfaces. The controlled application of electrical currents

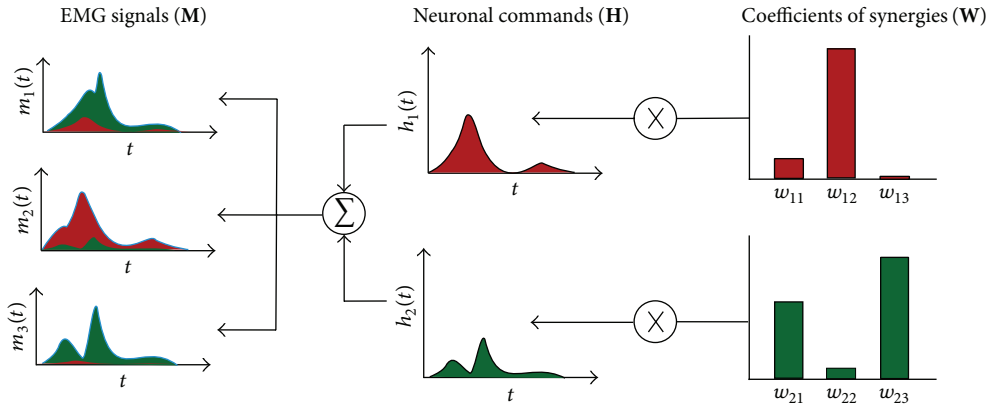

FIGURE 3: Muscle synergy concept. Each neural command activates a specific synergy with a factor $h_j(t)$, which may be a function of time or the type of movement. Therefore, muscle activations are a weighted average of the activations of each synergy [27].

into the body provides both therapeutic and functional benefits. FES can help to avoid atrophy of affected muscles and upper motor neurons and in conjunction with a dynamic activity can improve cardiopulmonary health. There is also growing evidence that FES can improve functional movements, such as running or jumping. Electrical stimulation also has influence on the central nervous system (CNS), probably due to multimodal afferent signals occurring during stimulation. This fact can promote the reorganization of the primary motor cortex [22–24] and change the recruitment techniques of spinal motor neuron pools, [25, 26]. These evidences encouraged the scientific community to use FES as a tool to guide and promote plasticity and adaptation of motor skills to new conditions after stroke or SCI [7].

Assisted as needed (AAN) is one of the emerging rehabilitation paradigms currently proposed in rehabilitation robotics [27]. According to this paradigm, the machine is intended to simulate the operation of a therapist during the execution of a motor task, providing assistance only if the patient is not able to execute the movement correctly by him or herself. Most implementations follow fixed profiles in terms of kinematic or dynamic patterns; that is, the patient is asked to follow a fixed path which is assumed to be the correct one. According to [21], this fixed-trajectory approach has two main drawbacks: (i) it does not take into account the specificity of the patient, since the reference trajectory is fixed for all users, and (ii) it ignores the implications of muscle activity within the therapy, by acting only at a kinematic level.

1.3. Muscle Synergies and Rehabilitation. The rehabilitation paradigm of the presented platform is based on the recent theory of muscle synergies [28]. From a biomechanical point of view, the human body is a redundant system of many degrees of freedom. The efficient and robust control generated by the CNS is still not sufficiently understood [29]. Recent neurological research hypothesizes that the CNS incorporates a library of motor activation modules in order to exert specific and common motor tasks by contributing to the synchronized activation of different muscles. These modules are called muscle synergies, and their combination can lead to more complex and functional muscle activation patterns at the spinal level, while maintaining a relatively simple control at higher centers.

Mathematically, muscle synergies can be expressed by the following equation, which describes the activation of a muscle $m_i(t)$:

$$m_i(t) = \sum_{j}^{K} h_j(t)\, w_{ji}, \tag{1}$$

where $m_i(t)$ is the time function of muscle activation (EMG signal) for muscle i, w_{ji} is the coefficient of jth synergy to the ith muscle, $h_j(t)$ is the temporal function of the neuronal command j, and K is the number of synergies. This concept is shown diagrammatically in Figure 3.

In its complete form, $\mathbf{M} = \mathbf{H} \times \mathbf{W}$, where $\mathbf{M}$ is a matrix of $1 \times N$ (N muscles), $\mathbf{H}$ is a matrix of $1 \times K$ (K neural modules), and $\mathbf{W}$ is an array of $K \times N$.

This process of decomposition and distribution of muscle activation reduces the computational requirements of motor control and possibly influences the learning of new motor tasks [30]. According to this hypothesis, the brain recruits muscle groups (synergies) in spite of controlling individual muscles independently. It has been demonstrated that the composition of muscle synergies depends on the motor task and can be affected by neuromotor pathologies [5]. According to [27], taking a set of synergies as a reference for a rehabilitation task may have two innovative potential effects:

(i) improving neural plasticity, since the therapeutic action is located at the level of muscle activation, which is closer to the CNS with respect to kinematics;

(ii) adapting to subject-specific kinematics constraints, since synergies mainly depend on the functional goal and not on biomechanical constraints.

These potential effects are motivated by three key properties of muscle synergies. First, muscle synergies have been found to be consistent among subjects despite the precise kinematic trajectory [31, 32]. Second, they can be trained and are prone to change if task conditions change [33–35]. Finally,

they somehow codify functional movements, so they can be used to train specific rehabilitation targets [36].

2. Synergies and Balance Control Training Based on Sway Movements

According to [5], the application of the concept of muscle synergies in clinical settings is twofold. In the *diagnosis* of neuromotor disorders, it may provide access and an overall view of motor control information at a higher level than muscular activity. In the *rehabilitation* field, it can help in the effective design of better training and rehabilitation therapies, for instance, in combination with an FES system. In order to define a reference set of synergies, a series of experiments were conducted to study healthy subjects during RWS in the mediolateral (ML) and anteroposterior (AT) directions [5].

This experiment was designed to measure the trajectory of the CoP of 6 healthy subjects (3 men and 3 women), during the rhythmic postural sway in the ML and AT directions. The CoP was measured using a CDP platform, the Neurocom `Smart Equitest`, which is depicted in Figure 4. The patient's visual reference was replaced by an auditory reference, a digital metronome, indicating the expected frequency of the movements. This change was motivated by the intention of increasing the VAF of the synergies [5]. During the execution of this test, electromyographic signals (EMG) were acquired using a 16-wireless channel electromyograph (ZeroWire). Three sway frequencies were defined (low = 0.167, medium = 0.25, and high = 0.5 Hz). The sway frequencies obtained by the patients are shown in Table 1. The algorithm NNMF (nonnegative matrix factorization) was used to extract the values of **H** and **W**. The EMG signal reconstructed using **H** and **W** (1) has then been compared with the original one. The quality of the reconstruction was expressed with the variance accounted for (VAF) [5].

Results revealed that two synergy modules are responsible for more than 90% of VAF (Figure 5) for all subjects in all conditions. This study showed evidences that support the existence of consistent modular control in healthy volunteers while doing lateral sway movements. Similarities can be seen in terms of number of modules, composition of synergies, and time-varying activations. Two modules represent most of the variability of the EMG for all subjects. Coefficient values are similar for different frequencies. This fact suggests that the muscle coordination and muscle synergies are not much influenced by the movement speed.

The comparison between subjects suggests high similarity in muscle synergies modules. However, a dedicated analysis should be performed to confirm this hypothesis. With the synergies modules found for these tasks, we proceeded with the development of a multimodal tool for balance control training.

3. Training Platform

In this section, we present a low-cost training platform for balance control. The contribution of this tool relies on the use of muscle synergies and multimodal interfaces. The system is based on a previously developed low-cost posturography platform [8]. It includes inexpensive components, such as the Wii Balance Board (WBB), the Microsoft Kinect, the TEREFES electrostimulator [7], and a central PC running a synergistic control algorithm driven by the position of the CoP of the subject. The kinematic information of the CoP is retrieved by means of the Microsoft Kinect and the WBB. This set of interfaces enables the development of close and open loop training tasks, using different type of interaction and information. The system includes a visual feedback (monitor) and an auditory reference (digital metronome). The proposed architecture is shown in Figure 6.

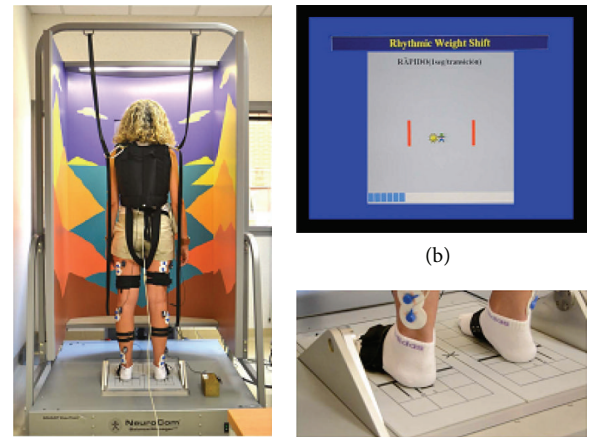

Figure 4: On the left, there is an instrumented subject on the NeuroCom Smart Equitest (Oregon, USA). On the top-right, there is the visual interface of the patient. It represents the current exercise, indicating with a stylized dark man the current position of the CoP of the patient and with a yellow sun the target position of the exercise. On the bottom-right, there is a detail of the dynamometric platform the forces applied by the user to determinate CoP position [5].

Table 1: Target and mean sway frequency of CoP for all subjects. Values are expressed in Hz [5].

Target frequency	0.17 Hz	0.25 Hz	0.5 Hz
Measured frequency (ML)	0.18 ± 0.03	0.26 ± 0.04	0.47 ± 0.11
Measured frequency (AT)	0.18 ± 0.03	0.25 ± 0.04	0.46 ± 0.12

3.1. Wii Balance Board. The WBB is an input device manufactured by Nintendo. It is a wireless device that communicates with the Wii console using the Bluetooth standard. It has a dimension of 45 × 26.5 cm and contains four pressure sensors located in each corner to measure the force in the vertical direction. The performance of WBB has been already studied in the literature [37–40], and the general conclusions are that the WBB can replace conventional force platform in slow range movements (0.01 Hz–10 Hz). These movements do not require a higher resolution. The platform specifications fulfill all requirements for our application and studies.

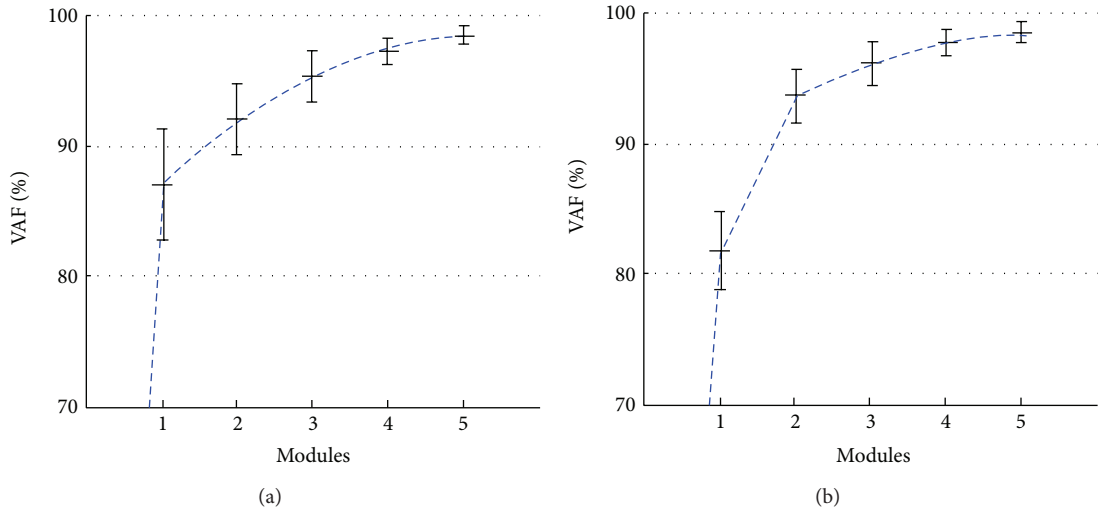

FIGURE 5: Variance accounted for (VAF) as a function of the number of modules during the execution of mediolateral (a) and anteroposterior (b) sway movements [5].

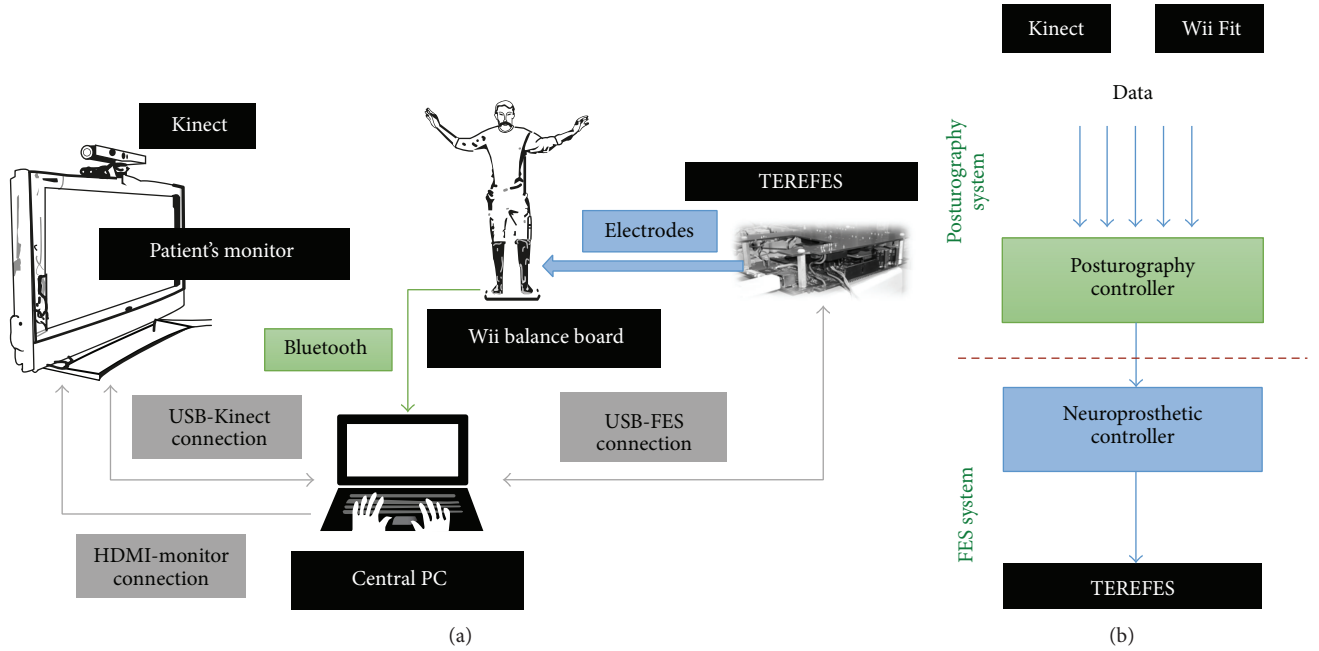

FIGURE 6: (a) Proposed platform architecture and (b) functional description diagram including the different components: the posturography system (balance control assessment) and the FES system (balance control training and rehabilitation).

3.1.1. Connectivity. A specific study to analyze the connection jitter of the received data by the WBB was carried out in the literature [8]. The result shows that the sample frequency responds to a nonparametric probability distribution with a mean value given at 100 Hz. This result matches the sampling period specified by the manufacturer. In the mentioned study [8], it is also shown that the probability that the sample frequency being greater or equal than 50 Hz. is 94.02%. Test condition has been fully described in the paper.

3.1.2. Accuracy and Reliability. Consistent documentation about the force and center of pressure (CoP) accuracy and reliability of the WBB is not available. However, [41] reported that the force measurements total uncertainly was within ±9.1 N and that the CoP location was within ±4.1 mm between different WBBs [41]. They also found that the measurement repeatability of both parameters are ±4.5 N and ±1.5 mm with each WBB. They suggest that the WBB may be useful for low-resolution measurements but should not be considered as a replacement for laboratory-grade force plates.

In golden standard commercials force plates, sensors register forces and moments in 3D. These force plates are accurate and durable and recordings are independent of temperature and stable along time. The disadvantages are low

portability due to mass (10–45 kg) and mounting requirements and their cost (US$ 15000–20000). Commercial low-cost platforms usually have the same quantity of pressure sensor, as WBB does. The difference between these systems is the resolution accuracy and possibility of 3D force measurements. However, for CoP assessment, a pressure platform is enough and there is no need for a 3D dynamometric platform. Typically, commercial platforms have a resolution less than 0.2 mm. According to [42], the CoP resolution of the WBB is approximately 0.5 mm.

The estimation of CoP using WBB has a drawback. The shear forces and moments cannot be taken into account. As a consequence, these additional forces are neglected and problems may arise when trying to assess dynamic movements or static forces applied in the horizontal plane.

3.1.3. Library. A library called Wiimotelib permits us to link the WBB system with other Wii accessories and is programmed in C# language. Using this library we can connect with the device and get all WBB data (CoP displacement, battery status, etc.) as a burst of events that the WBB sends continuously to the PC. There is also a community called Wiibrew [43] that provides support for developers regarding these libraries and the devices.

3.2. FES System. The TEREFES was proposed within the framework of the TERERE and HYPER projects [7]. The TEREFES electrostimulator provides up to 32 stimulation channels driven by controllable, stable, and close loop current sources. In addition, the system is portable and flexible. It is powered by 4 AA batteries and includes a USB communication interface (1 Mbps) that allows its configuration via external software. Monophasic and biphasic stimulation signal can be obtained across the 32 available channels. These channels are divided into two independent groups of 16 channels each that can be stimulated simultaneously. The TEREFES has a current range of 0–150 mA, pulse width of 0–5 ms, high frequency stimulation of 100 Hz, and maximum stimulation voltage of 250 V.

A synergistic FES controller was already proposed in [44]. Following these concepts, an upgrade of firmware of TEREFES has been done in order to meet technical specifications required by the experimental validation. Two parameters could be changed while stimulating muscle synergies: amplitude and pulse-width. All the changes in the parameters can be performed while the stimulation is running. This feature allows us to develop dynamic stimulation algorithms.

4. Timing and Synchronization of the Multimodal Interface

The proposed platform can be a seen as a control system, characterized by a strong human-machine interaction. This interaction, specifically the one related to FES, is control-oriented, meaning that FES is prone to generate motor effects in users. In many cases, a hard real-time system would be the best solution for this type of application. However, in this scenario, where many different and distributed technologies are combined together, the development or use of a real-time architecture may compromise the use of these low-cost components.

The system was developed for training balance control during ML and AP sway movements and works as follows. Prior to the training session, four variables should be defined (i) **H** and **W** (activation and synergy) matrices, as obtained from human experiments; (ii) the mapping between the columns of **W** (muscles) and the TEREFES' channels (0–31); (iii) the maximum current for each channel, $\mathbf{I}_{max}$; and (iv) the frequency of the sway movement. According to the selected frequency, the system computes a reference signal, namely, the CoP reference trajectory, which the subject should follow during the training session. The system uses a digital metronome to help subjects to synchronize with this reference signal during the session. The system continuously calculates the neural command for every point of the CoP reference trajectory and, according to this value, it computes corresponding current pulses to be applied to each muscle at a given time. All this process is illustrated in Figure 7.

The synergistic controller is responsible for calculating the muscle activations as a function of CoP coordinates and for controlling the currents to be applied to muscles through the TEREFES. So far, it works in an open loop manner. This means that the synergistic controller only considers the CoP reference to calculate muscles activations. The measured CoP provided by the WBB is just used to provide visual feedback to the user. The synergistic controller runs in the PC. It is an application developed in C# Visual Studio 2012. In order to calculate the desired muscle activations, the controller uses synergies (**W**) and activation coefficients (**H**) obtained during ML and AT experiments previously described. Because of the cyclical nature of the sinusoidal reference, the neural commands were calculated as a function of the percentage of the sway cycle. Each point of the sine wave corresponds to a certain percentage of the sway period and also to a specific neural command value. Thus, there is a direct mapping between current position value of CoP and neural commands. Specifically, the neural commands were calculated with a variation of 1% of the sway period, getting a total of 100 samples per cycle.

The system assumes that the patient starts at a certain point of the sway cycle, usually where the CoP trajectory is zero, meaning approximately 75% of the sway cycle, as shown in Figure 7. It is further assumed that a therapist or a robotic system ensures that the patient follows the simulated reference. The application allows us to compare online the measured CoP trajectory by the WBB with the one generated by the system. Thus, the therapist and the user can know how synchronized the current movement and the reference signal are.

The synergistic controller has to keep a precise timing in order to control effectively and periodically the TEREFES stimulation parameters. This is achieved by using the Stopwatch class of C#. This class allows us to measure execution times with high precision. Each time this timer expires, the synergisitc controller calculates the percentage of the sway cycle based on the current amplitude of the CoP trajectory. The result is transformed again into the correspodding

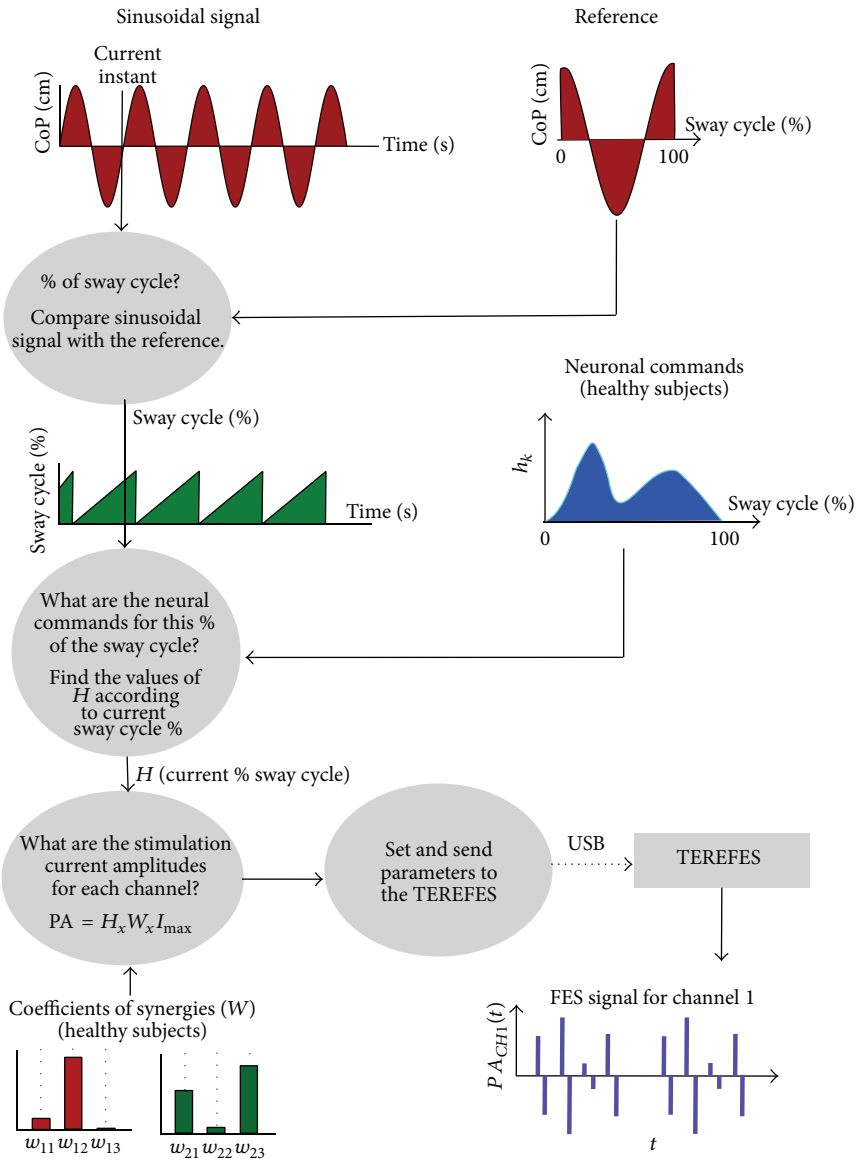

Figure 7: Functional diagram of the synergistic controller implemented in the PC.

stimulation parameters that are afterwards transmitted to the TEREFES. Once the TEREFES receives new modulation parameters, it immediately updates its parameters.

Since the controller is running over non-real-time operating systems and communicates with the TEREFES using also a non-real-time communication technology (USB), the systems take advantage of real-time TEREFES hardware to implement a timing monitor to verify that the stimulation parameters are updated periodically in a precise manner. Thus, the systems know when the timing requirements are and can stop the control/stimulation signals.

The system also includes a second synchronization tool that monitors the differences between the reference local CoP and the real user CoP, so that user and therapist can train prior to the synergistic stimulation.

The synergistic controller has several other functions, as summarized in the following part.

(1) *Capture*. It continuously receives WBB samples at an average frequency of 100 Hz.

(2) *Show*. The program displays the trajectory of CoP, the sampling period of the WBB, the current percentage of sway cycle, and the precise timing of TEREFES configuration.

(3) *Save*. The application saves all the data that has been acquired, calculated, or received, in MAT files that can be later exported to MATLAB for further analysis.

(4) *Debugging*. The application has implemented a serial terminal, allowing the user to send and receive TEREFES commands.

(5) *Configuration*. The application allows the configuration of several parameters, such as the frequency of the stimulation of the TEREFES, the refresh rate of synergies, test duration, the mode of operation of the TEREFES (single burst or continuous mode), and the amplitude and frequency of the sine wave reference.

5. Results

In this section, we present the preliminary results of our platform. We carried out two experiments. The first one was aimed at verifying the performance of the system in terms of timing, focusing in particular on the limitations of the non-real-time architecture running on Windows. The second experiment was designed to validate the proposed system with the ultimate goal of generating correct FES timulation patterns according to the concept of muscle synergies. The following sections detail these two experiments.

5.1. System Performance. There are two fundamental parameters of the system. The first one is the frequency stimulation of the TEREFES (F_t). The device must continuously stimulate at a certain frequency (usually in the range of 40–50 Hz). This frequency is fixed and controlled autonomously within the TEREFES. The second important parameter is the refresh rate of muscle synergies (F_s), which should be lower than F_t but large enough to sample every variation of neural commands during the sway cycle. From previous experiment, we observed that there is high correlation between the frequency of the reference sine wave and the frequency of neural commands [5]. Considering that voluntary postural sway frequency usually lies below 0.5 Hz, a synergy frequency of 5–10 Hz may be enough for these movements.

Different tests of 50 seconds duration were performed. In each test, the TEREFES frequency was set to $F_t = 40$ Hz (implies a period $T_t = 1/F_t = 25$ ms). Four frequencies for synergy modulation have been chosen: $F_s = \{1, 5, 10, 20\}$ Hz meaning that synergy update period was $T_{sE} = \{1000, 200, 100, 50\}$ ms, respectively. The reference sine wave was set at a frequency of 0.1 Hz for all tests.

We defined the period of synergies (T_s) as the period which take to the operating system to refresh the new value to the TEREFES. In fact, $T_s = 1/F_s$, where F_s is the frequency of synergies. Given the random nature of the period of synergies (the controller is running on a nonreal operating system), we analyze the performance of the system in all listed conditions. The values of the random variable T_s were measured in the C# application, using the methods of the class`Stopwatch` and the TEREFES with a 500 μ timer accuracy. The results were analyzed with the`Distribution Fitting Tool` in MATLAB R2011a.

Since $T_{sE} = \{1000, 200, 100, 50\}$ ms are the expected values (configured) of the synergies period, we analyze the probability that the random variable T_s is less than or equal to $T_{sE} \pm T_t$, where $T_t = 25$ ms for all conditions. That is, how likely T_s is below (or postponed to) its expected value during stimulation.

Table 2: Probabilistic analysis of synergy update period measured in the TEREFES. $T_t = 25$ ms and $T_{sE} = 1/F_{sE}$.

Parameters	Frequency F_{sE}			
	20 Hz	10 Hz	5 Hz	1 Hz
$P(T_s \leq T_{sE} + T_t)$	98.87%	99.19%	97.99%	98%
$P(T_s \leq T_{sE} - T_t)$	0.82%	1.41%	0.8%	6%

Table 3: Probabilistic analysis of the synergy period update measured in C# with Stopwatch. $T_t = 25$ ms and $T_{sE} = 1/F_{sE}$.

Parameters	Frequency F_{sE}			
	20 Hz	10 Hz	5 Hz	1 Hz
$P(T_s \leq T_{sE} + T_t)$	98.88%	98.39%	98%	99.99%
$P(T_s \leq T_{sE} - T_t)$	0.71%	2.6%	1.6%	2%

This tolerance window for T_{sE} is acceptable if we analyze the behavior of the FES system. The FES system generates a pulse train for N stimulation channels (1). Stimulation of each channel (current pulse) occurs every T_t. If a new synergy value is obtained, the stimulation parameters of every channel are updated. However, if this update takes place during an on-going stimulation, only those channels, which were not stimulated yet, are affected by these new values. This behavior allows us to establish a tolerance of stimulation period, because it is not possible to establish perfect synchronization between non-real-time systems. Also because the frequency of the TEREFES is much higher than synergies frequency, changes during a period of TEREFES are not relevant in obtaining the envelope of the stimulation signal.

The results are shown in Figure 8. The high probability (>95%) that the update of the synergies occurs before the expiry of a further period of TEREFES and the low probability (<3%) that the update occurs before the stimulation period represent a metric for the good performance of the platform. High similarity between the results obtained with TEREFES and Stopwatch is also observed.

Two random variables affect the accuracy of the measures from TEREFES and Stopwatch: the shipping time of the serial data and the time that elapses until the TEREFES updates its parameters with the new values received.

The results of the experiments are summarized in Tables 2 and 3. For all frequencies, a concentration greater than 95% of the density of the samples around $T_{sE} \pm T_t$ was observed. This implies an uncertainty of a window of stimulation (T_t) around the expected value (right and left). This result is explained graphically in Figure 9.

5.2. Reconstruction of EMG Envelopes. This section shows the next validation step aimed to demonstrate that the stimulation signal provided by the TEREFES produces similar muscle contractions as those obtained by the synergistic neural commands, as observed in human experiments.

The validation experiment can be divided into the following steps.

(1) *Simulation of* **H** *and* **W**. Neuronal commands and synergies have been simulated in MATLAB

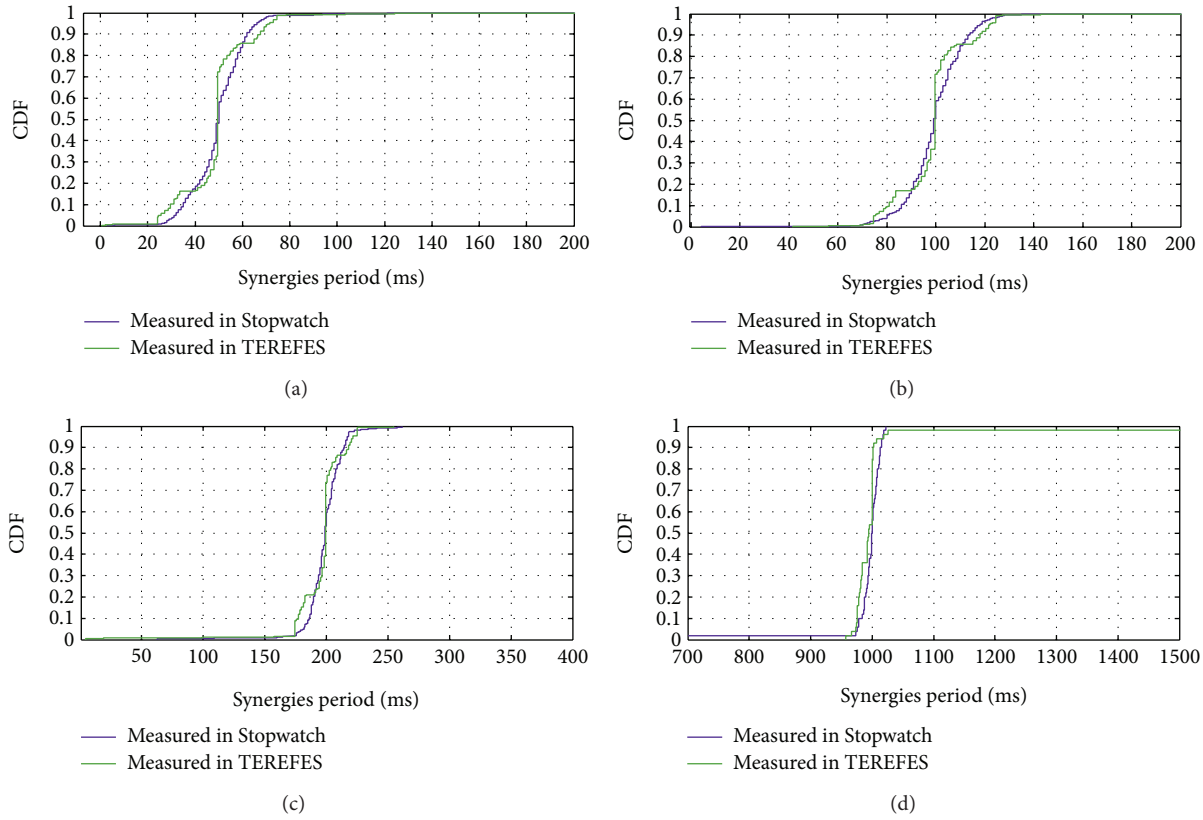

FIGURE 8: Cumulative distribution function of synergies period for (a) T_{sE} = 50 ms (F_{sE} = 20 Hz), (b) T_{sE} = 100 ms (F_{sE} = 10 Hz), (c) T_{sE} = 200 ms (F_{sE} = 5 Hz), and (d) T_{sE} = 1000 ms (F_{sE} = 1 Hz).

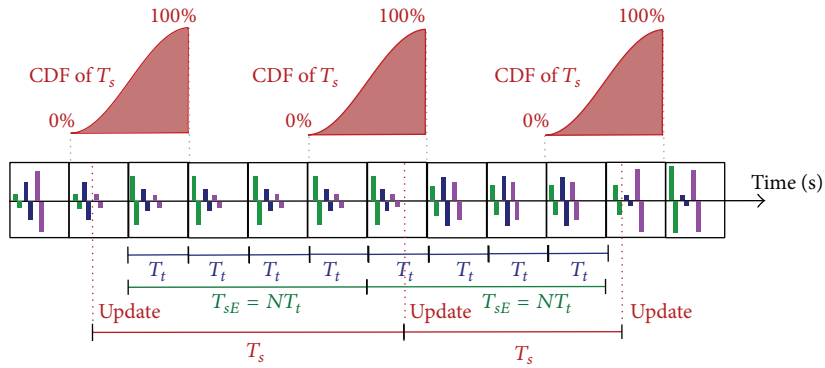

FIGURE 9: Stimulation patterns for three channels. CDFs are displayed around the expected synergies period (T_{sE}).

(Figure 10) and then loaded into the application as MAT files. For this test, three neural modules and 8 stimulation muscles were considered.

(2) *Configuration of Parameters*. A sinusoid reference with an amplitude of 10 cm and 0.1 Hz frequency was used. Stimulation was performed at a frequency of 40 Hz, and the synergy frequency was 20 Hz. Test duration was set to 50 seconds.

(3) *Data Collection*. During stimulation, the TEREFES monitors the timing of the overall system. To do this, the device measures the elapsed time between consecutive reception of new stimulation parameters sent by the synergistic controller. The measured value is sent back to the controller. These values are stored in the application in dynamic lists.

(4) *Data Analysis*. When the test is complete, we can export all the data collected in MAT files. They include synergies period measured by Stopwatch and TEREFES, WBB data arrival periods, values of CoP displacements, and a diferent kind of vector which measures the point in time when events occur in the execution time. For instance, we use Stopwatch class

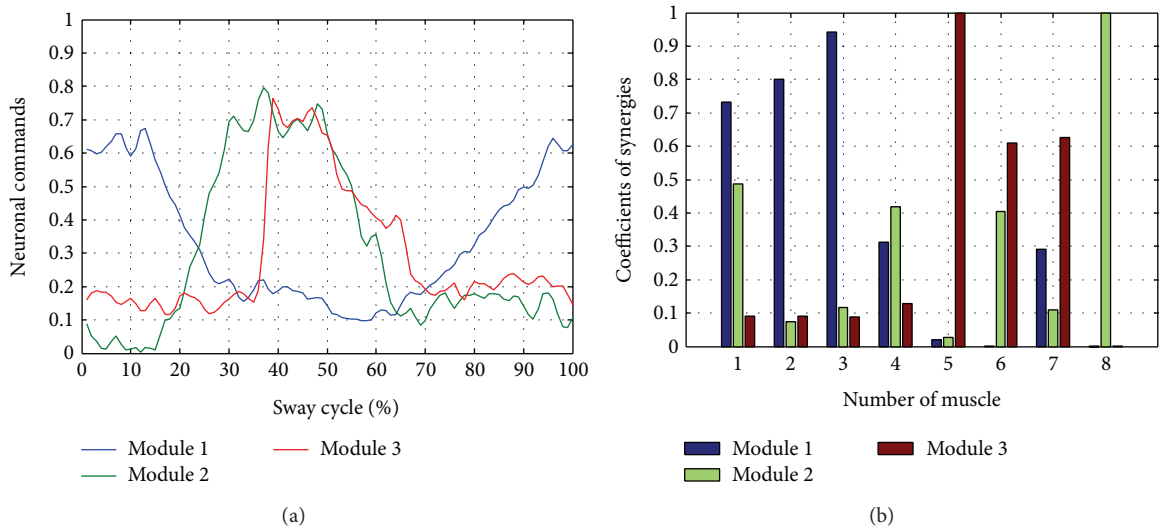

FIGURE 10: (a) Neural Commands. (b) Coefficients synergies simulated in MATLAB.

timers to know (i) when the configured execution time is finished, (ii) when a new data from the WBB arrive, (iii) when a new frame is sent to the TEREFES; and (iv) when the new synergy period value measured by the TEREFES arrives. All of these data were previously recorded in dynamic lists when the test was run.

Using temporary values (when we send a new frame to the TEREFES), it is possible to simulate in MATLAB the outputs obtained with the FES system during the test. In this simulation we considered the resolution of the TEREFES, which means that the TEREFES output simulated is the same as that generated.

In Figure 11, the output generated by the TEREFES for a single channel (corresponding to muscle 1) is shown. The output signals are modulated in amplitude according to the theoretical values of reconstructed EMG envelopes obtained for healthy subjects (according to (1)). To retrieve the EMG envelope signal, a low pass filter is applied to the TEREFES outputs. The butterworth filter was designed in MATLAB, and the filter parameters were set, as shown in Algorithm 1.

The filter represents roughly the low-pass behavior of the skin-muscle system. The resulting signal of the designed filter is shown in Figure 12. The theoretical EMG envelope for muscle 1 (according to the (1)) is plotted in blue, the envelope signal for the TEREFES output (adjusted to resolution of 782.7μA) is in magenta, and the envelope obtained by filtering the TEREFES signal is in red. The similarity between the first and last signals allows us to demonstrate that the stimulation patterns obtained with the synergistic controller represent in a good manner the muscle activation used previously to obtain these stimulation patterns.

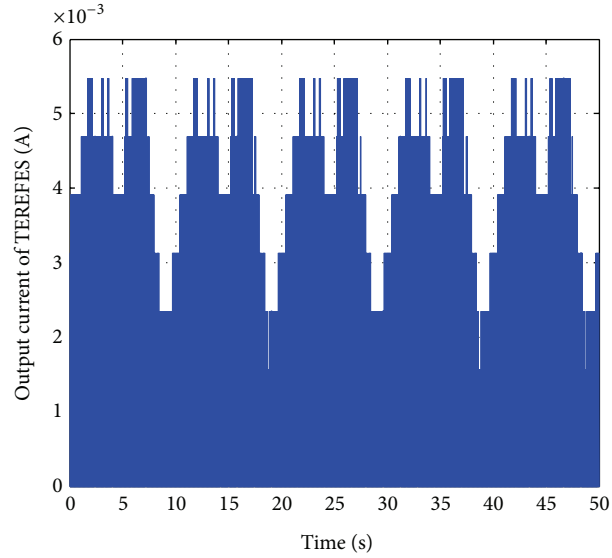

FIGURE 11: TEREFES output current for muscle 1. The signal is modulated in amplitude according to $\mathbf{M} = \mathbf{H} \times \mathbf{W} \times \mathbf{I}_{max}$ during 50 seconds.

6. Discussion

In this work, we presented an innovative balance training system, which combines postural analysis with synergistic electrical muscle stimulation. The experiments presented here were mainly focused on testing the timing and synchronization performance of the system. Timing is a particularly crucial aspect, because the proposed system is made of commercial off-the-shelf technology, which prevents them from having real-time performance. Several efforts were dedicated to get the best timing performance of the system. For instance, two timing and synchronization monitors were implemented in a distributed way, to robustly verify that timing is correct during training sessions. The system succeeded in providing synergistic EMG profiles, but only in an open-loop fashion.

Closed loop control might be needed depending on the rehabilitation task strategy. For example, the system could

```
Fs = 20000;            % Sampling Frequency
Fpass = 3;             % Passband Frequency
Fstop = 10;            % Stopband Frequency
Apass = 10;            % Passband Ripple (dB)
Astop = 100;           % Stopband Attenuation (dB)
match = 'stopband';    % band to match exactly

% construct an FDESIGN object and call its BUTTER method.
h = fdesign.lowpass (Fpass, Fstop, Apass, Astop, Fs);
Hd = design(h, 'butter', 'MatchExactly',match);

y = filter(Hd, IoutTerefes);
```

Algorithm 1

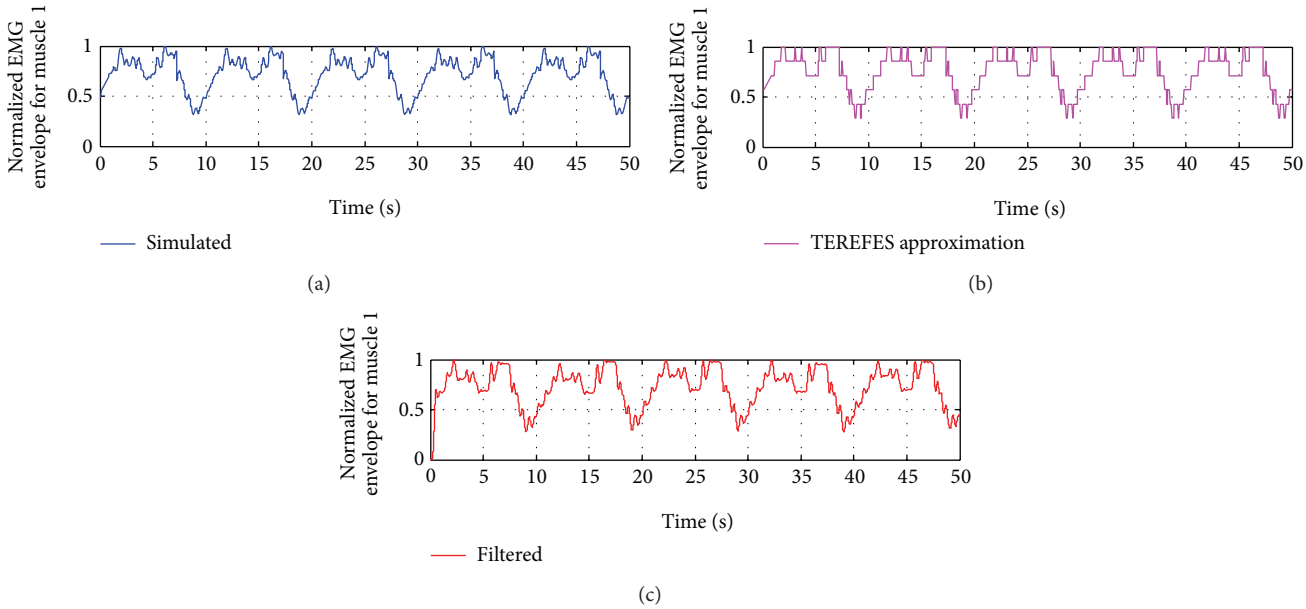

Figure 12: Comparison between normalized EMGs envelopes for muscle 1.

stimulate according to the current user's CoP and not as a function of a predefined reference. In such closed-loop configuration, a better and deeper knowledge regarding the effective sensing-to-actuation time is needed. According to the literature, this time can be approximately 100 ms, which lies in the same order of magnitude of the system control frequency imposed by the different modules (WBB and TEREFES). This immediately shows that a close loop strategy would be very challenging, at least based on a sample to sample feedback.

Regarding the multimodal interfaces, it is worth to mention that the human-machine system communicates through kinematic, CoP, auditory, visual, and electric signals. The potential use and further impact of this multimodal interfaces have not been explored yet. Despite these aspects, an important outcome of this work is the development of a flexible and powerful tool for the assessment and training of balance control using off-the-shelf technologies.

The potential impact of the introduction of novel concepts and platforms for balance training is huge but still not completely defined. The use of muscle synergies paradigm as a basis for the rehabilitation paradigm represents the most scientific innovative aspect behind this work and still needs to be deeply explored. In order to test this approach, new tools are needed, and the one here proposed may be one of them. The objective of this paper is to provide the technological tool to explore this rehabilitation approach, but further trials are needed to define its effectiveness.

The impact of FES on internal neuromotor mechanisms is still far from being understood, and its use in rehabilitation may vary depending on the therapy. There is evidence of cause-effect relationship, but no extensive description is provided in the literature. The therapy based on electrostimulation can be either applied in an efferent way (mostly functional) or afferent. For both types of electrostimulation, devices are the same, and the difference is mainly in the

amplitude of the current signals. In this paper, we always mention the stimulation as a functional one, that is, FES. While the developed system supports both types of stimulations (afferent or efferent), the stimulation profile is another open research variable to be explored.

7. Conclusions

In this paper, we have presented a multimodal low-cost tool for training human balance control following a muscle synergy theory scheme. The system consists of a combination of off-the-shelf technologies such as the Wii Balance Board and the Kinect, an electrostimulator and a software application running in a PC.

In this work, we focused on mediolateral (ML) and anteroposterior (AP) voluntary postural sways. For this purpose, the synergy modules described in [5] were used as an input of the system. Based on this information, the system stimulates the muscle synergistically.

The synergy-based controller architecture is based on three non-real-time elements (a) Wii Balance Board; (b) the operating system; and (c) the TEREFES (FES system). The interaction between these off-the-shelf systems was studied and evaluated in this paper. The performance results showed in this paper are expressed in terms of the probability distribution function of timing and synchronization among components. The outcomes of these studies were as follows.

(i) The system can stimulate with a frequency up to 50 Hz. This frequency range meets the requirement of FES control system available in the scientific literature [7].

(ii) The system can handle and modify while running the stimulation frequency in range of 1–20 Hz. These frequencies are fast enough for balance training since it is a slow movement. The highest frequency of the sinusoidal reference trajectory is 0.5 Hz (sway movement).

(iii) The uncertainty of synergy sampling/update period is approximately ±25 ms (elapsed time between sampled reference trajectory and updated stimulation pulses). It was also demonstrated that the envelope reconstruction is not affected by this uncertainty.

Despite non-real-time performance, the tool showed an acceptable timing and synchronization among modules. These operation ranges are enough for these training scenarios. To get a better online feedback regarding these issues, a monitor of real-time performance was implemented to measure the timing and synchronization between modules.

The system uses multimodal interfaces to get kinematic and CoP information of user and to provide auditory, visual, and electrical signals to the user and the therapist. The interface also includes important features for training purposes, like online graphs of signals, data session storage, and a configuration interface to tailor training for each user.

Future work will be focused on the application of the proposed platform in clinical settings. In particular, preclinical studies in neurologically injured people, for example, spinal cord injured and stroke patients, will be addressed to evaluate the rehabilitation potential of synergistic FES.

Conflict of Interests

The authors declare that there is no conflict of interests regarding the publication of this paper.

Acknowledgment

This project was funded by the Spanish Ministry of Science and Innovation CONSOLIDER-INGENIO, project HYPER (Hybrid NeuroProsthetic and NeuroRobotic Devices for Functional Compensation and Rehabilitation of Motor Disorders, CSD2009-00067).

References

[1] M. P. de Moya, "Assessment and rehabilitation of balance by posturography," *Rehabilitación*, vol. 39, no. 30, Article ID 315323, 2005.

[2] R. B. García, *Valoración de un método de posturografía estática con pruebas dinámicas para evaluar funcionalmente pacientes vestibulares en edad laboral y su relación con el índice de discapacidad (ESP) [Ph.D. thesis]*, Polytechnic University of Valencia, Valencia, Spain , 2012.

[3] B. Schwab, M. Durisin, and G. Kontorinis, "Investigation of balance function using dynamic posturography under electrical-acoustic stimulation in cochlear implant recipients," *International Journal of Otolaryngology*, vol. 2010, Article ID 978594, 7 pages, 2010.

[4] D. Pérennou, P. Decavel, P. Manckoundia et al., "Evaluation of balance in neurologic and geriatric disorders," *Annales de Readaptation et de Medecine Physique*, vol. 128, pp. 372–381, 2005.

[5] S. Piazza, *Muscle synergies in postural sway movements: neurophysiologial evidences and reabilitation potentials [M.S. thesis]*, University Carlos III of Madrid, Madrid, Spain, 2013.

[6] T. Kapteyn, W. Bles, J. Njiokiktjien, L. Kodde, C. Massen, and J. Mol, "Standardization in platform stabilometry being a part of posturography," *Agressologie*, vol. 24, no. 7, pp. 321–326, 1983.

[7] F. Brunetti, Á. Garay, J. C. Moreno, and J. L. Pons, "Enhancing functional electrical stimulation for emerging rehabilitation robotics in the framework of hyper project," in *Proceedings of the IEEE International Conference on Rehabilitation Robotics (ICORR '11)*, pp. 1–6, ETH Zurich Science, IEEE, Zurich, Switzerland, July 2011.

[8] D. Galeano, F. Brunetti, D. Torricelli, S. Piazza, and J. Pons, "A low cost platform based on fes and muscle synergies for postural control research and rehabilitation," in *Proceedings of the International Congress on Neurotechnology, Electronics and Informatics*, p. 11, Vilamoura, Portugal, 2013.

[9] M. Osthege, "Skeleton Painter 3D for Microsoft Kinect," Microsoft Development Network, 2013, http://code.msdn.microsoft.com/windowsdesktop/Implementation-of-f175b025#content.

[10] G.] Vervoort, E. Nackaerts, F. Mohammadi et al., "Which aspects of postural control differentiate between patients with parkinsons disease with and without freezing of gait?" *Parkinson's Disease*, vol. 2013, Article ID 971480, 8 pages, 2013.

[11] K. Kubo, T. Miyoshi, A. Kanai, and K. Terashima, "Gait rehabilitation device in central nervous system disease: a review," *Journal of Robotics*, vol. 2011, Article ID 348207, 14 pages, 2011.

[12] J. L. Emken, R. Benitez, and D. J. Reinkensmeyer, "Human-robot cooperative movement training: learning a novel sensory motor transformation during walking with robotic assistance-as-needed," *Journal of NeuroEngineering and Rehabilitation*, vol. 4, article 8, 2007.

[13] N. G. Kim, C. K. Yoo, and J. J. Im, "A new rehabilitation training system for postural balance control using virtual reality technology," *IEEE Transactions on Rehabilitation Engineering*, vol. 7, no. 4, pp. 482–485, 1999.

[14] J. Baydal A, J. Castelli, I. Garrido et al., *NedSVE/IBV V. 5 a New System for postural Control Assessment in Patients with Visual Conflict*, vol. 40, Instituto de Biomecánica de Valencia (IBV), 2010.

[15] Bertec, "Bertec force plates," 2013, http://bertec.com/products/force-plates.html.

[16] Neurocom, "Equitest," 2013, http://resourcesonbalance.com/default.aspx.

[17] B. Lange, S. Flynn, R. Proffitt, C.-Y. Chang, and A. Rizzo, "Development of an interactive game-based rehabilitation tool for dynamic balance training," *Topics in Stroke Rehabilitation*, vol. 17, no. 5, pp. 345–352, 2010.

[18] T. Keller, M. R. Popovic, I. P. I. Pappas, and P.-Y. Müller, "Transcutaneous functional electrical stimulator 'compex motion'," *Artificial Organs*, vol. 26, no. 3, pp. 219–223, 2002.

[19] B. J. Broderick, P. P. Breen, and G. Laighin, "Electronic stimulators for surface neural prosthesis," *Journal of Automatic Control*, vol. 18, no. 2, pp. 25–33, 2008.

[20] T. Schauer, Negaard, and Behling, "Sciencemode, rehastim stimulation device," HASOMED GmbH, 2009.

[21] S. Piazza, D. Torricelli, F. Brunetti, A. J. del Ama, A. Gil-Agudo, and J. Pons, "A novel fes control paradigm based on muscle synergies for postural rehabilitation therapy with hybrid exoskeletons," in *Proceedings of 34th Annual International Conference of the Engineering in Medicine and Biology Society (EMBC '12).*, IEEE, 2012.

[22] G. Smith, G. Alon, S. Roys, and R. Gullapalli, "Functional MRI determination of a dose-response relationship to lower extremity neuromuscular electrical stimulation in healthy subjects," *Experimental Brain Research*, vol. 150, no. 1, pp. 33–39, 2003.

[23] M. McDonnell and M. Ridding, "Transient motor evoked potential suppression following a complex sensorimotor task," *Clinical Neurophysiology*, vol. 117, no. 6, pp. 1266–1272, 2006.

[24] S. M. Schabrun and M. C. Ridding, "The influence of correlated afferent input on motor cortical representations in humans," *Experimental Brain Research*, vol. 183, no. 1, pp. 41–49, 2007.

[25] D. F. Collins, "Central contributions to contractions evoked by tetanic neuromuscular electrical stimulation," *Exercise and Sport Sciences Reviews*, vol. 35, no. 3, pp. 102–109, 2007.

[26] C. Mang, A. Bergquist, S. Roshko, and D. Collins, "Loss of short-latency afferent inhibition and emergence of afferent facilitation following neuromuscular electrical stimulation," *Neuroscience Letters*, vol. 529, no. 1, pp. 80–85, 2012.

[27] D. Torricelli, J. C. Moreno, and J. L. Pons, "A new paradigm for neurorehabilitation based on muscle synergies," in *Proceeding of The 32nd Jornadas de Automtica*, Sevilla, Spain, January 2011.

[28] A. d'Avella, P. Saltiel, and E. Bizzi, "Combinations of muscle synergies in the construction of a natural motor behavior," *Nature Neuroscience*, vol. 6, no. 3, pp. 300–308, 2003.

[29] E. Bizzi and V. C. Cheung, "The neural origin of muscle synergies," *Frontiers in Computational Neuroscience*, vol. 7, no. 51, 2013.

[30] A. d'Avella, A. Portone, L. Fernandez, and F. Lacquaniti, "Control of fast-reaching movements by muscle synergy combinations," *Journal of Neuroscience*, vol. 26, no. 30, pp. 7791–7810, 2006.

[31] G. Torres-Oviedo, L. H. Ting, S. Kautz, M. Bowden, D. Clark, and R. Neptune, "Muscle synergies characterizing human postural responses," *Journal of Neurophysiology*, vol. 98, no. 4, pp. 2144–2156, 2007.

[32] G. Torres-Oviedo and L. H. Ting, "Subject-specific muscle synergies in human balance control are consistent across different biomechanical contexts," *Journal of Neurophysiology*, vol. 103, no. 6, pp. 3084–3098, 2010.

[33] R. Gentner, S. Gorges, D. Weise, K. Aufm Kampe, M. Buttmann, and J. Classen, "Encoding of motor skill in the corticomuscular system of musicians," *Current Biology*, vol. 20, no. 20, pp. 1869–1874, 2010.

[34] P. G. Gerbino, E. D. Griffin, and D. Zurakowski, "Comparison of standing balance between female collegiate dancers and soccer players," *Gait & Posture*, vol. 26, no. 4, pp. 501–507, 2007.

[35] W. W. Tsang and C. W. Hui-Chan, "Comparison of muscle torque, balance, and confindence in older tai chi and healthy adults," *Medicine and Science in Sports and Exercise*, vol. 37, no. 2, pp. 280–289, 2005.

[36] M. G. Bowden, D. J. Clark, and S. A. Kautz, "Evaluation of abnormal synergy patterns poststroke: relationship of the fuglmeyer assessment to hemiparetic locomotion," *Neurorehabilitation and Neural Repair*, vol. 24, no. 4, pp. 328–337, 2010.

[37] R. A. Clark, A. L. Bryant, Y. Pua, P. McCrory, K. Bennell, and M. Hunt, "Validity and reliability of the nintendo wii balance board for assessment of standing balance," *Gait & Posture*, vol. 31, no. 3, pp. 307–310, 2010.

[38] S. M. Deans, *Determining the validity of the nintendo wii kbalance board as an assessment tool for balance [M.S. thesis]*, University of Nevada, Las Vegas, Nev, USA, 2011.

[39] C. Ma, *The effects of safety flooring on sit-to-stand and quiet stance balance reactions in retirement home-dwellers [M.S. thesis]*, University of Waterloo, Ontario, Canada, 2012.

[40] K. Yamamoto and M. Matsuzawa, "Validity of a jump training apparatus using wii balance board," *Gait & Posture*, vol. 38, no. 1, pp. 132–135, 2012.

[41] H. L. Bartlett, L. H. Ting, and J. T. Bingham, "Accuracy of force and center of pressure measures of the wii balance board," *Gait & Posture*, vol. 39, no. 1, pp. 224–228, 2014.

[42] G. Pagnacco, E. Oggero, and C. H. Wright, "Biomedical instruments versus toys: a preliminary comparison of force platforms and the nintendo wii balance board," *Biomedical Sciences Instrumentation*, vol. 47, pp. 12–17, 2011.

[43] WiiBrew, "A Wiki Dedicated to Homebrew on the Nintendo Wii," 2010, http://www.wiibrew.org/wiki/Main_Page.

[44] W. Denis, F. Brunetti, S. Piazza, D. Torricelli, and J. Pons, "Functional electrical stimulation controller based on muscle synergies," in *Proceedings of the 1st International Conference on Neurorehabiltiation, Converging Clinical and Engineering Research on Neurorehabilitation*, 2012.

Hindawi Publishing Corporation
BioMed Research International
Volume 2014, Article ID 345728, 22 pages
http://dx.doi.org/10.1155/2014/345728

Clinical Study

Adaptive Personalized Training Games for Individual and Collaborative Rehabilitation of People with Multiple Sclerosis

Johanna Renny Octavia[1,2] and Karin Coninx[2]

[1] *Industrial Engineering Department, Parahyangan Catholic University, Ciumbuleuit 94, Bandung 40141, Indonesia*
[2] *Expertise Centre for Digital Media-tUL-iMinds, Hasselt University, Wetenschapspark 2, 3590 Diepenbeek, Belgium*

Correspondence should be addressed to Johanna Renny Octavia; johanna@unpar.ac.id

Received 23 December 2013; Revised 10 March 2014; Accepted 13 March 2014; Published 28 May 2014

Academic Editor: Alessandro De Mauro

Any rehabilitation involves people who are unique individuals with their own characteristics and rehabilitation needs, including patients suffering from Multiple Sclerosis (MS). The prominent variation of MS symptoms and the disease severity elevate a need to accommodate the patient diversity and support adaptive personalized training to meet every patient's rehabilitation needs. In this paper, we focus on integrating adaptivity and personalization in rehabilitation training for MS patients. We introduced the automatic adjustment of difficulty levels as an adaptation that can be provided in individual and collaborative rehabilitation training exercises for MS patients. Two user studies have been carried out with nine MS patients to investigate the outcome of this adaptation. The findings showed that adaptive personalized training trajectories have been successfully provided to MS patients according to their individual training progress, which was appreciated by the patients and the therapist. They considered the automatic adjustment of difficulty levels to provide more variety in the training and to minimize the therapists involvement in setting up the training. With regard to social interaction in the collaborative training exercise, we have observed some social behaviors between the patients and their training partner which indicated the development of social interaction during the training.

1. Introduction

Multiple Sclerosis (MS) is an autoimmune, chronic, and progressive disease of the central nervous systemof humans. People with MS suffer from damaged nerves which lead to the progressive interference with functions that are controlled by the nervous system such as vision, speech, walking, writing, and memory, causing severe limitations of functioning in daily life. To date, no cure has been found for MS yet. Therefore, for MS patients, the aim of rehabilitation training is different compared to any other disease. Rehabilitation training will not completely recover MS patients; however, it may improve their functional mobility and quality of life.

People who are in need of any kind of rehabilitation are individuals with their own characteristics and needs. Although they might be subjected to the same background cause for rehabilitation, the stage of their condition or the severity of their disease may differ which requires different treatments and forms of rehabilitation. In the case of MS, the individual differences among its patients are quite prominent due to the great variation of MS symptoms and the impact levels of the disease. For example, their physical abilities, which are largely influenced by the degree of muscle weakness experienced by the patients, differ a lot. The difference in physical abilities has an impact on the course of the rehabilitation training. Some training tasks may be difficult for some patients because of their limited capabilities due to their high degree of muscle weakness, while other patients experience less problems in performing those tasks.

During rehabilitation, each patient progresses in different ways; thus, the training exercises must be tailored to each individual differently. For example, the difficulty of an exercise should increase faster for those who are progressing well compared to those who are having trouble performing the exercise. The condition of patients may also change over time: it can deteriorate according to the progress of the disease or

it can improve as a result of the treatment and rehabilitation efforts. This change of condition should be taken into account to ensure providing the right level of rehabilitation training to the patient at the right time. Therefore, due to the diversity among MS patients, it would be unwise to offer the same rehabilitation training to every patient. This situation demands a suited, personalized rehabilitation training to meet every patient's needs.

To acquire a good result of rehabilitation, it is necessary to maintain patient motivation. Generally, rehabilitation involves the same training exercises that should be performed repetitively and for a long period of time. Using games as the training platform has been considered to maintain and enhance patients' motivation during rehabilitation, especially collaborative games in which social interaction is incorporated. However, the usage of game-like training exercise is not the ultimate solution. Some patients may feel less motivated when finding the game to be too easy or too difficult or when reaching a certain point in the training where they become bored with the game. Therefore, rehabilitation training should be set at an appropriate level of challenge or difficulty to maintain the motivation of patients. This raises the need of adaptivity in the rehabilitation training to ensure the effectiveness of the rehabilitation.

Our work focuses on the idea of integrating adaptivity and personalization into the rehabilitation training for MS patients and investigating to what extent the adaptive personalized training may contribute to a successful neurological rehabilitation. This paper firstly discusses the survey of related work concerning adaptation in rehabilitation training, followed by a description of our rehabilitation system developed to support personalized rehabilitation training for MS patients. We further elaborate on the investigation of integrating the adaptivity of automatic difficulty level adjustment in the rehabilitation training for MS patients, including the user studies carried out with a group of MS patients to acquire their feedback.

2. Related Work

In this section, we first provide a brief overview of research which has studied adaptation in rehabilitation training. We then discuss several works which have investigated the usage of virtual environments as the platform for rehabilitation training. Lastly, we describe a number of studies which combined both and attempted to integrate adaptation in virtual environments for rehabilitation training.

2.1. Adaptation in Rehabilitation Training. The integration of adaptation in rehabilitation training has been the focus of several studies [1–4]. These studies have mainly investigated the integration of adaptivity in robot-assisted rehabilitation training which aimed at providing a personalized training to the patients according to their individual characteristics, needs, and abilities. Moreover, the adaptivity is intended to facilitate an automated training system to minimize the therapist's effort in manually adjusting the rehabilitation training.

Jezernik et al. [1, 4] studied the adaptation in rehabilitation training of locomotion for stroke and spinal cord injured patients. An automated treadmill training system was introduced using a robotic rehabilitation device to increase the training duration and reduce the physiotherapists' effort. A clinical study on six spinal cord injured patients showed that the treadmill training with adaptive gait patterns increases the motivation of the patient and gives him/her the feeling that they are controlling the machine rather than the machine controlling them. Kahn et al. [2] described the integration of adaptive assistance into guided force training as part of the upper extremity rehabilitation for chronic stroke patients. An adaptive algorithm was developed to individually tailor the amount of assistance provided in completing the training task. This algorithm has been evaluated with one patient in a two-month training program which showed significant improvements in the patient's arm function reflected by the performance increase of functional activities of daily living such as tucking a shirt and stabilizing a pillow. Kan et al. [3] presented an adaptive upper-limb rehabilitation robotic system for stroke patients which accounts for the specific needs and abilities of different patients. Using the decision theoretic model, the system autonomously facilitates upper-limb reaching rehabilitation by tailoring the exercise parameters and estimating the patient's fatigue based on the observation in his/her compensation or control of movements. The system performance was evaluated by comparing the decisions made by the system with those of a human therapist. Overall, the therapist agreed with the system decisions approximately 65% of the time and also thought the system decisions were believable and could envision this system being used in both a clinical and home setting.

2.2. Virtual Environments for Rehabilitation Training. Another emerging technology that has been widely applied in rehabilitation is the virtual environment technology. Virtual environments provide a variety of potential benefits for many aspects of rehabilitation training. Schultheis and Rizzo [5] discussed a number of advantages for the use of virtual environments in rehabilitation. One key benefit is that virtual environments are rather naturalistic or "real-life" environments, which may allow the users or patients to be immersed within the environment and "forget" that they are in a rehabilitation training session. Within virtual environments, patients are also facilitated to perform the rehabilitation training tasks using 3D interaction, which gives a close resemblance to the actual movements in the real world. Schultheis and Rizzo [5] also pointed out that virtual environments facilitate the design of individualized training environments where therapists can better tailor the training exercises based on an individual's abilities and needs, and they can also easily apply gradual increments of difficulty and challenge. Another benefit is that virtual environments allow the introduction of gaming factors into the rehabilitation scenario to enhance motivation of patients.

Holden [6] provided a thorough overview of the use of virtual environments in the field of motor rehabilitation. In the context of motor rehabilitation, several studies have

shown that patients with motor impairments are able to train their motor skills in virtual environments and transfer these abilities to the real world. Furthermore, these studies have also indicated that motor learning in a virtual environment may be superior to that in a real environment, for example, a study described in Webster et al. [7] which compared two groups of patients with stroke and unilateral neglect syndrome in a wheelchair training program. The group which had trained in a virtual environment hit significantly fewer obstacles with their wheelchair during the real world obstacle avoidance test than the group which only trained in a real environment. Another study described in Jaffe et al. [8] investigated chronic stroke patients in a training to avoid obstacles during walking. Patients using a virtual environment-based training showed greater improvement in a fast paced velocity test in comparison to the patients who trained in the real world.

In Holden [6], an extensive description of the various virtual environments that have been developed for rehabilitation purposes of patients was provided. This includes rehabilitation for stroke (upper and lower extremity training and spatial and perceptual-motor training), acquired brain injury, Parkinson's disease, orthopedic disorders, vestibular disorders (balance training), wheelchair mobility training, and functional activities of daily living training. A review on these research initiatives showed that a wide variety of clinical applications using virtual environments has been developed and tested. Mainly, the virtual environments consist of scenes that were designed to be simple, therapeutically meaningful tasks to the targeted patients such as making coffee, lifting a cup to the mouth, using an automated teller machine (ATM), and way-finding. Virtual environments have been considered not as a treatment for motor rehabilitation in itself but more as a new technological tool that can be exploited to enhance motor rehabilitation training.

Over the past few years, there is an increasing research interest in the development of virtual environments for use in stroke rehabilitation. Virtual environments are considered beneficial in stroke rehabilitation because they enable more precisely controlled training settings, intensive practice with easier repetition of tasks, automatic recording of training progress, and more enjoyable and compelling interaction for the patients. Some researchers developed virtual environments based on the literal translation of activities of daily living such as self-feeding, bathing, and dressing or grooming. For example, Edmans et al. [9] developed a virtual environment to train a self-feeding task (i.e., making a hot drink). An evaluation study with 50 stroke patients showed that their performance of hot drink-making in the real world and in the virtual environment were correlated, which may indicate the usefulness of such virtual environment as a rehabilitation tool for stroke patients.

Other researchers chose to enclose the rehabilitation tasks in game-like exercises, with the purpose of adding fun and challenges into rehabilitation training to increase or maintain the patient's motivation. For instance, Alankus et al. [10] developed a series of home-based stroke rehabilitation games which make use of inexpensive devices feasible for home use such as Wii remotes and webcams. Two examples of the games are the helicopter game in which the patients have to maneuver a flying helicopter using their arm to avoid hitting buildings and to collect fuel cells in the air and the baseball catch game in which the patients have to differentiate balls and control the baseball glove to catch baseballs and avoid basketballs. The preliminary evaluation with one therapist and four stroke patients showed that the games motivated the patients and they used the right motions required for the rehabilitation training. Saposnik et al. [11] described the first randomized clinical trial on the effectiveness of virtual reality using the Wii gaming system, namely, VRWii, on the arm motor improvement in stroke rehabilitation. The results showed that the VRWii gaming technology represented a feasible, safe, and potentially effective alternative to facilitate rehabilitation therapy and enhance motor function recovery in stroke patients.

2.3. Adaptation in Virtual Environments for Rehabilitation Training. As previously discussed in Section 2.1, it is essential to provide a personalized rehabilitation training which is suited according to the individual characteristics of patients. Patients involved in rehabilitation have a wide range of needs and abilities which may benefit from integrating adaptivity into their rehabilitation training. Adaptivity enables offering a tailored training with minimal efforts from the human therapists as it decreases the dependence on them to continuously monitor the patient's progress and manually adjust the training program.

Several studies mentioned in Section 2.2 have acknowledged the potential of developing virtual environment applications for the purpose of rehabilitation training. These applications may also benefit from adaptivity since it allows to dynamically adjust the parameters of the virtual environment as the training tool to provide a suited, personalized training to every patient based on his/her current needs and abilities. It may also be necessary to integrate adaptivity in virtual environments for rehabilitation training due to the fact that the complex 3D interaction may introduce extra difficulties and eventually influence patients' performance during the training sessions. Adaptivity may reduce this effect by adjusting the virtual environment according to the patient's level of interaction.

This section discusses several previous studies which highlighted the integration of adaptation in virtual environments that were developed for the purpose of rehabilitation training. Ma et al. [12] stated that virtual reality systems for rehabilitation can benefit a group of patients with a great diversity through adaptation. In their study, several adaptive virtual reality games for rehabilitation of stroke patients with upper limb motor disorders have been developed. The information of patient performance is used to enable automatic progression between difficulty levels in the games. The elements of the games are designed to be adaptive and to change dynamically according to how well or badly the patient is performing. An initial evaluation from patients showed positive feedback since they enjoyed training while playing the game and they felt more motivated.

Cameirão et al. [13] have developed an adaptive virtual reality based gaming system for the upper extremities rehabilitation of acute stroke patients. They proposed a multitask adaptive rehabilitation system that provides a task-oriented training with graded complexity. The basic training consists of a virtual reality game where flying spheres move towards the patient. These objects have to be intercepted using the virtual arms which are controlled by the patient's arm movements. As the first task, the patients have to perform the hitting task to train range of movement and speed. The second task is the grasping task to train finger flexure and then finally the placing task to train grasp and release is the last task. Based on the individual performance of the patient during training, the difficulty of the task is adapted by modulating several parameters such as the speed of the spheres, the interval of appearance between consecutive spheres, and the range of dispersion in the field. The impact of the system on the recovery of patients was evaluated with 14 patients. The results suggested that the system induces a sustained improvement during therapy with observed benefits in the performance of activities of daily living.

Barzilay and Wolf [14] developed an online biofeedback-based adaptive virtual training system for neuromuscular rehabilitation. The system employs an artificial intelligence learning system that learns from real-time biofeedback and produces online new patient-specific virtual physiotherapy missions. In the training, the patient is asked to follow the virtual tasks (i.e., trajectories) displayed to him/her by making upper limb movements accordingly. The performance is then modeled by tracking and recording their kinematics and muscle activity (measured through electromyography (EMG) signals) using a motion tracking system. Based on this trained model, the system changes and adapts the task displayed to the patient which results in a new virtual trajectory as the training exercise. This adaptive loop of the system is continuously repeated to provide a real-time adaptive rehabilitation virtual training system for better neuromuscular rehabilitation.

According to Holden [6], the use of mixed reality, which combines physical and virtual environments, in rehabilitation training can provide adaptive scenes for interactive practice and feedback that engage the patient physically and mentally. Duff et al. [15] presented an adaptive mixed reality rehabilitation training system to help improve the reaching movements of patients who suffer hemiparesis from stroke. The system provides real-time, multimodal, customizable, and adaptive feedback based on the movement patterns of the patient's affected arm and torso during the reaching movement. The kinematic data is used to assess the movement and adapt the parameters linked to the feedback presentation and the physical environment that determines the type of task. The feedback is provided via innovative visual and musical forms that present a stimulating, enriched environment for the patient's training. For example, the audio feedback in the form of music is intended to encourage patients to perform the desired reaching movements. The velocity of the patient's hand controls the rhythm of the music; when the patient is moving too slow, the music is played with a slower rhythm and when the patient moves with nonsmooth acceleration or deceleration, there will be abrupt changes in the pace of the music. Additionally, the sequence and intensity of tasks can also be adapted to better address each patient's rehabilitation needs. After training with the interactive mixed reality system, three chronic stroke patients showed improved reaching movements. Integrating mixed reality environments into the training was argued to promote an easier bridging in motor learning between the virtual and physical worlds. In one of their following research, Baran et al. [16] presented the design of a home-based adaptive mixed reality system for stroke rehabilitation. The system, which consists of a custom table, chair, and media center, is designed to be easily integrated into any home to provide an engaging long-term reaching task therapy for stroke patients.

2.4. Summary of Related Work. In this section, we have discussed several research efforts, which have mainly investigated the integration of adaptivity in robot-assisted rehabilitation training. Besides providing a personalized training, the adaptivity integrated in the studies was intended to minimize the dependence from the therapists for manually adjusting the rehabilitation training. Virtual environment technology has been considered to be beneficial and widely applied in rehabilitation. We also have discussed a number of research initiatives that used virtual environments as part of the rehabilitation training platform and demonstrated the patients' ability to train in virtual environments and transfer the trained skills to the real world. Furthermore, we have described several studies which have attempted to integrate adaptivity in the virtual environment training system for achieving better results and patient's engagement in rehabilitation. Mostly, the adaptivity takes form in automatically adjusting the parameters of the virtual environment to alter the difficulty levels in the rehabilitation exercises based on the patient's current training performance and training progress.

We observed that previous studies mainly focused on robot-assisted rehabilitation training for stroke patients. In our work, we aim to develop a haptic-based rehabilitation system (combining robot-assisted rehabilitation and virtual environments technologies) to support a systematic and personalized upper limb rehabilitation training for MS patients.

3. Rehabilitation for Multiple Sclerosis

Rehabilitation for people with MS mainly aims for improving their functional mobility and quality of life, rather than attaining their full recuperation from the disease. This is due to the fact that MS is an incurable illness. In the past, physical training was not advised for MS patients due to the opinion that it would advance the deterioration. Now, however, performing physical training is often part of therapy and rehabilitation efforts for MS patients in parallel with taking medications. A number of studies have shown beneficial effects of physical training in MS regarding lower limb muscle strength, exercise tolerance level, functional mobility (i.e., balance and walking), and quality of life, while no harmful effects were reported [17, 18].

Little research has investigated the therapeutic value of upper limb, in particular arm, rehabilitation for MS patients. Upper limb rehabilitation is considered important since upper extremity dysfunction strongly influences the capacity of MS patients to perform several activities of daily living (ADL) such as self feeding (e.g., eating, filling, or drinking a cup of coffee), bathing, grooming, dressing, and taking medications.

3.1. Robot-Assisted Upper Limb Rehabilitation. Keys to a successful neurological rehabilitation are training duration and training intensity [19]. As time dedicated to upper limb training may be limited in a formal training session, additional therapeutic modalities may be necessary to enable MS patients to train independently of the therapist. Robot-assisted rehabilitation and virtual environment technologies have been considered to be promising to provide an effective, independent upper limb rehabilitation training [20, 21]. Robot-assisted rehabilitation allows high-intensity, repetitive, task-specific, and interactive treatment of the impaired upper limb. Virtual environments facilitate patients to perform the training tasks with their upper limb using 3D interaction, which gives a close resemblance to the real movements in the real world.

In the context of a European research project (INTERREG-IV program "Rehabilitation robotics II"), we investigate the effects of robot-assisted upper limb rehabilitation training for MS patients. Our work combined two technologies, robot-assisted rehabilitation and virtual environments, by first investigating the feasibility of using a phantom haptic device for arm rehabilitation in MS patients [22, 23]. Further, a complete haptic-based rehabilitation system, *I-TRAVLE*, was developed to support a systematic and personalized upper limb rehabilitation training for MS patients [24].

I-TRAVLE (*Individualized, Technology-supported, and Robot-Assisted Virtual Learning Environments*) consists of a hardware and software system setup as depicted in Figure 1. The main component of the hardware system is a haptic robot, the MOOG HapticMaster, that functions as both input and output devices. As an input device, it allows patients to interact with the software applications that deliver the training exercises. As an output device, it provides haptic feedback during the training by guiding or hindering the patient's arm movement with exerted forces. The HapticMaster is equipped with a peripheral device, the ADL Gimbal, where the patients' hand is placed and secured using the attached brace while performing the training exercises. A large display, a full HD 40″ Samsung TV screen, is used as a visual display to project the training exercises and is placed behind the HapticMaster approximately 1.5 m in front of the patient. A complete description of the I-TRAVLE hardware system with the adjustments made for the context of MS training can be found in de Weyer et al. [25].

The main components of the software system of our I-TRAVLE system are the training exercises, the patient interface, the therapist interface, and the central database. Two types of training exercises were developed, namely, the basic and the advanced training exercises. We will discuss the training exercises in Section 3.2. The patient interface, as shown in Figure 2, is created to enable patients to independently start performing and navigating through the exercises predefined by the therapist. Figure 2(a) shows how the patient interface looks like in the basic training and Figure 2(b) shows the interface for the advanced training. Another interface was developed for the therapist, as shown in Figure 3, to manage the user data, personalize therapy sessions, and review the data logged from the performed training exercises. The central database stores all the data about the training exercises and patients' performance. A more detailed description of the I-TRAVLE software system can be found in Notelaers et al. [26].

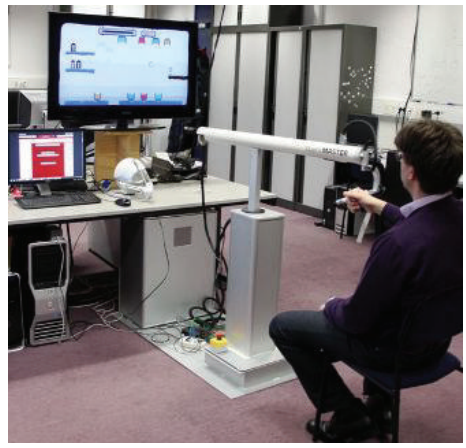

Figure 1: I-TRAVLE system setup.

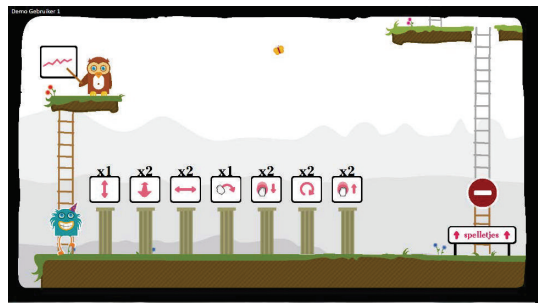

(a) Basic training

(b) Advanced training

Figure 2: The patient interface.

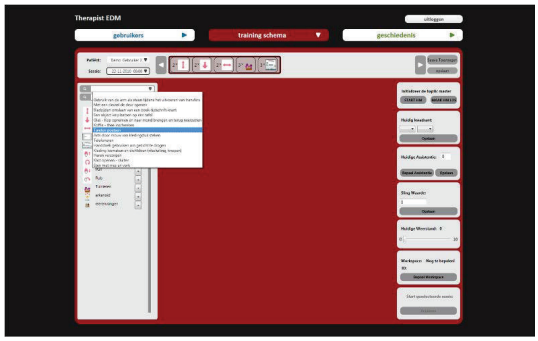

Figure 3: The therapist interface.

Several other researches have been done in the course of the I-TRAVLE system development regarding the influence of visual aspects on the capabilities of MS patients. People with MS often suffer from visual system disorders and cognitive dysfunctions, which may influence their capabilities while navigating in a virtual environment. Van den Hoogen et al. [27] investigated the impact of visual cues such as shading on navigation tasks in a virtual environment for MS patients. The study showed that the addition of shade below patients' current position in the virtual environment improves speed during the task and reduces the time spent on the task. Van den Hoogen et al. [28] discussed a study to comparatively test the effectiveness of two characteristics of virtual environments, namely, the stereo visualization and the graphic environment, in rehabilitation training when utilizing a 3D haptic interaction device. The experiment results showed that the use of stereoscopy within a virtual training environment for neurorehabilitation of MS patients is most beneficial when the task requires movement in depth. Furthermore, the use of 2.5D in the graphic environment implemented showed the highest efficiency and accuracy in terms of patients' movements.

3.2. Individual Training Exercises for Upper Limb Rehabilitation. To keep up the motivation of patients and strive for a successful rehabilitation trajectory, it is essential to give them training exercises that are meaningful in supporting their functional recovery [29]. The development of the I-TRAVLE training approach was inspired by the T-TOAT (technology-supported task-oriented arm training) method of Timmermans et al. [30]. T-TOAT is a technology supported (but not haptic) training which allows integration of daily tasks. Similar to the T-TOAT method, I-TRAVLE divides an activity of daily living (ADL) into skill components and trains the skill components, first every component separately and later several components combined.

The I-TRAVLE training exercises were designed based on the skill components that patients need to train related to their upper limb rehabilitation. Two types of training exercises are provided, namely, basic training exercises which include only one skill component and also advanced training exercises which combine multiple skill components. Seven basic training exercises were developed in I-TRAVLE as follows: pushing, pulling, reaching, turning, lifting, transporting, and rubbing. Figure 4 shows three examples of the basic training exercises: lifting (Figure 4(a)), transporting (Figure 4(b)), and rubbing (Figure 4(c)).

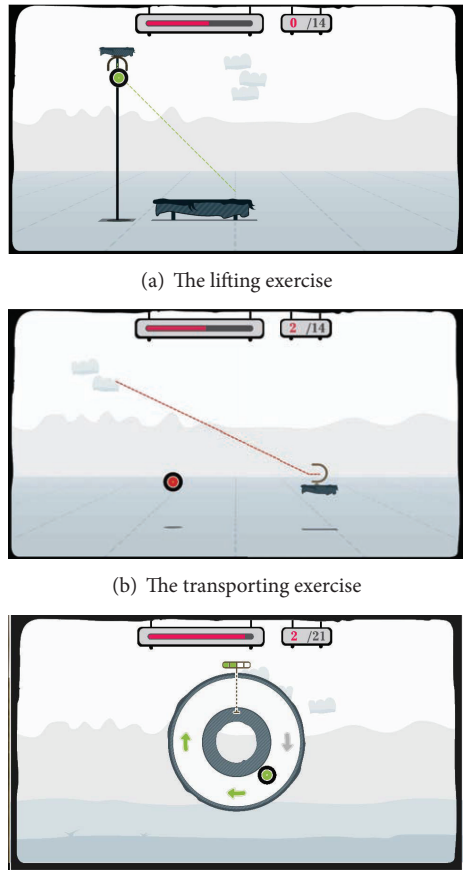

(a) The lifting exercise

(b) The transporting exercise

(c) The rubbing exercise

Figure 4: The basic training exercises for upper limb rehabilitation.

In the advanced training exercises, several skill components were combined into a game-like training exercise as illustrated in Figure 5. Until now, four advanced training exercises have been designed as follows: penguin painting (Figure 5(a)), arkanoid (Figure 5(b)), egg catching, and flower watering. Normally in a therapy session, a patient first trains with several basic training exercises. Depending on the progress of the patient, the therapy session can be continued with the games (i.e., advanced training exercises).

One example of the advanced or game-like training exercises is the penguin painting game as illustrated in Figure 5(a). This game was designed based on two skill components: lifting and transporting. Lifting is one of the important skill components in the upper limb rehabilitation for MS patients. In the penguin painting game, the patient has to collect as many points as possible within a certain time period by painting as many penguins as possible with the right color. Figure 6 illustrates how the penguin painting game is played. On the left side, there are two shelves with penguins waiting to be painted. The patient has to select one penguin from a shelf (Figure 6(a)) and paint it according to

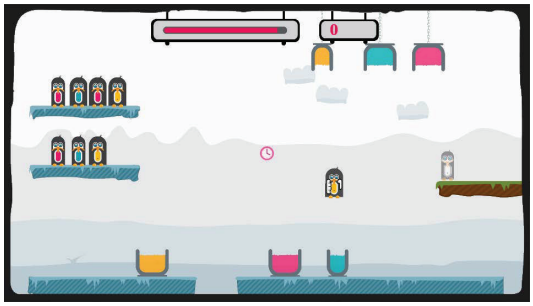

(a) The penguin painting game

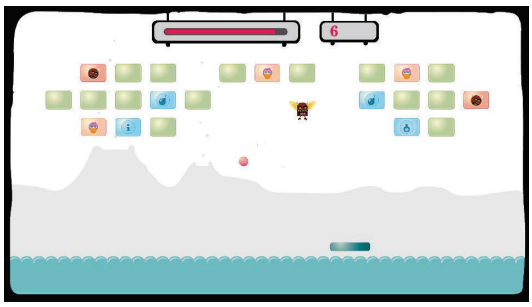

(b) The arkanoid game

Figure 5: The advanced training exercises for upper limb rehabilitation.

the color of its belly. To paint, the patient needs to bring the penguin to the corresponding buckets by dipping it into the bottom to paint the lower part of the penguin (Figure 6(b)) and continue dipping it into the top bucket to paint the upper part of the penguin (Figure 6(c)). While painting, the patient must hold the penguin long enough to effectively apply the color and train for stabilization in this way. At some points during the game, a devil that tries to capture the penguin appears (Figure 6(d)) and must be avoided in order to not lose the penguin already in hand. Every time the patient finishes painting a penguin, the colored penguin must be transported to the exit platform on the right side (Figure 6(e)).

The aforementioned training exercises discussed in this section are designed to be part of individual rehabilitation training for MS patients. This means that the patient will perform the training exercises on his/her own. In this case, the role of the therapist is to determine which training exercises the patient has to perform and also to personalize the therapy sessions according to the patient's current condition and needs. In another case, the therapist will extend his/her role to not only manage the therapy sessions but also take an active part in the therapy sessions by collaborating with the patient in performing the training exercises. This so-called collaborative rehabilitation training will be further discussed in the next section.

3.3. Collaborative Training Exercises for Social Rehabilitation Program. Typically exercises in robot-assisted rehabilitation involve a patient training on his/her own (with a therapist's supervision) and performing repetitive movements for a certain time period predetermined by the therapist. Even when gaming elements are integrated in the training exercises, it is crucial to exploit a variety of motivational techniques to avoid bored patients and patients that are stopping the therapy due to the high intensity and repetitiveness of the exercises. Therefore, we explore different motivational aspects to increase the patient's engagement in the therapy.

Social support has been demonstrated to be beneficial for the engagement and motivation of patients in a rehabilitation context. Van den Hoogen et al. [32] have performed a study on rehabilitation needs of stroke patients, which indicated that social support is critical for patient motivation in order to adhere to the necessary regime of rehabilitation exercises in the chronic phase of stroke. In addition to using games, patient's motivation during rehabilitation can be maintained and further enhanced through the incorporation of social interaction into the training exercises offered in the rehabilitation program.

During rehabilitation, patients can receive social support from different groups in their social network not only from their family members and friends but also from other support groups such as their therapists, caregivers, or fellow patients. These people can extend their form of social support to the patients by actively participating in the therapy sessions. This support can be manifested in two different forms: *sympathy* and *empathy* [33, 34]. Both depend on the types of relationships built based on shared emotions and sense of understanding between the persons. Two possible social scenarios can exist in this context.

(1) *Sympathetic*. This social situation occurs when a person shows the ability to understand and to support the condition or experience of the patient with compassion and sensitivity. For example, healthy family members and close friends may be able to show sympathy towards MS patients.

    One can imagine a situation, where a patient is visited by a family member (e.g., a daughter). This family member could show her sympathetic support through her help in the rehabilitation program by performing the collaborative training exercise together with the patient.

(2) *Empathetic*. This social situation happens when a person shows the ability to coexperience and relate to the thoughts, emotions, or experience of the patient without them being directly communicated. Other fellow patients can easily have empathy towards MS patients due to the resemblance of their condition.

    One can imagine a situation, where two patients are supporting each other by training together at the same time through the collaborative exercise, which makes the training more pleasant and fun.

Social interaction can be incorporated in the rehabilitation training by providing a social play medium which requires a patient to collaborate with his/her supporting partner in performing the training exercises. Thus, the idea is that the patient will keep being engaged and stay motivated

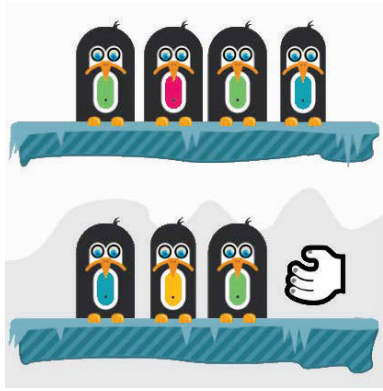

(a) Selecting a penguin from a shelf

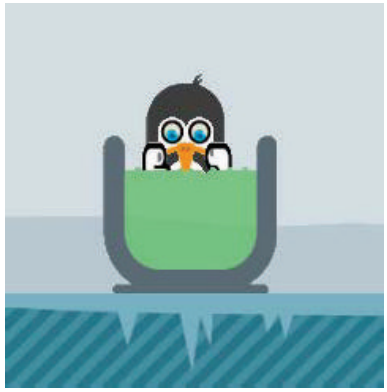

(b) Painting the lower part of the penguin

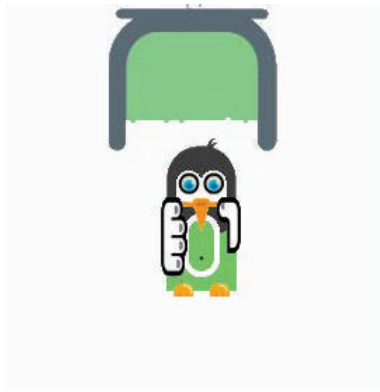

(c) Painting the upper part of the penguin

(d) Avoiding the devil

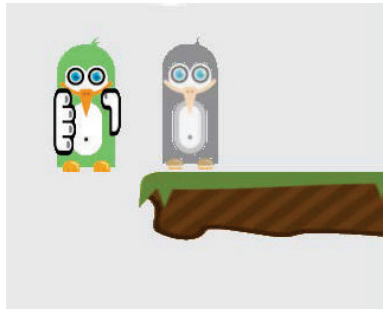

(e) Releasing the painted penguin to the exit platform

Figure 6: Illustration of the penguin painting game.

in training by collaborating with other people as a training partner. By this, we extend the individual rehabilitation training to a collaborative rehabilitation training, where the training exercises involve collaboration and participation of more than only a single MS patient.

Vanacken et al. [31] have explored the possibility of social rehabilitation training by designing a simple collaborative game-like training exercise, as shown in Figure 7. A collaborative balance pump game was created (Figure 7(a)), where two people "play" together during the therapy session. The goal of the game is to collect all stars, which represent points, by hitting them with a ball rolling over a beam. Both players have to collaboratively control and balance the height of both sides of the beam by pumping each side of it in turns. Figure 7(b) illustrates the setup of the social rehabilitation training session in a sympathetic scenario, where a patient plays the collaborative balance pump game with a family member. To produce the pumping gesture, the patient uses a HapticMaster and the healthy person uses a WiiMote as input devices.

An informal user study has revealed that most patients and therapists liked and enjoyed training with the collaborative balance pump game described in Vanacken et al. [31]. Inspired by this, we developed another collaborative training exercise, *social maze*, which has more game elements and variations [35]. This collaborative training game was

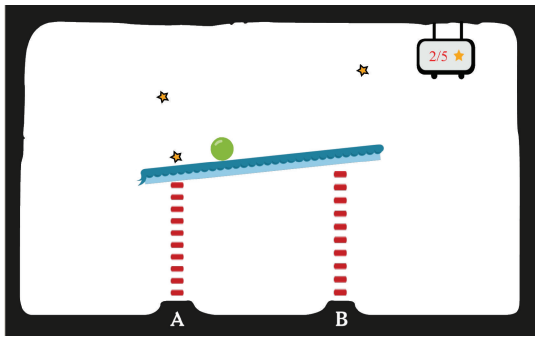

(a) The collaborative balance pump training exercise

(b) Sympathetic social scenario: a patient training in companion of a family member

FIGURE 7: Example of a collaborative training exercise for MS patients. Vanacken et al. [31]

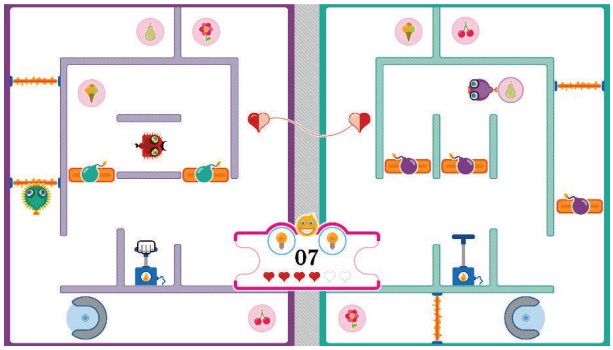

FIGURE 8: The social maze game.

designed based on several skill components (see Section 3.2) that MS patients need to train related to their upper limb rehabilitation: lifting, transporting, turning, pushing, and reaching. Figure 8 depicts our social maze with all game elements. The goal of this game is to collect all symbols, which represent points, by picking up each symbol and bringing it to the collecting bin. The elements of the game were purposively designed so that two players (i.e., a patient and his/her training partner) have to collaborate as such to

(a) Selecting a symbol

(b) Collecting the symbols in the bin

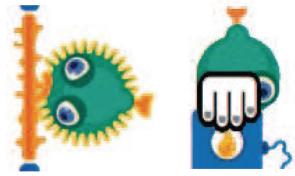

(c) Avoiding the laser beam

(d) Demolishing the bomb

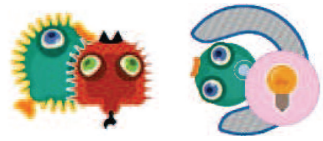

(e) Avoiding the devil

(f) Surmounting the rotator

(g) Gaining lives with the connecting heart

FIGURE 9: Illustration of the social maze game.

achieve the goal. Without collaboration, it is impossible to finish the game.

As can be seen in Figure 8, the game area is divided into two. In each part, the player, represented by a fish-like avatar, can move around his/her own maze to collect the symbols. Figure 9 illustrates how the social maze game is performed. First, the player has to select a symbol (Figure 9(a)). Once the players pick up a symbol, they can place it in the collecting bin (Figure 9(b)) to earn points. Along the way, there are some obstacles such as the laser beams that need to be avoided (Figure 9(c)), the bombs that need to be demolished (Figure 9(d)), the devil that may not be encountered (Figure 9(e)), and the rotators that need to be surmounted (Figure 9(f)). Demolishing the bombs demands a tight collaboration between the players, where one player has to push the bomb trigger (lifting skill component) in order to destroy the bomb blocking the way of the other player. To pass the rotator, the players must enter it and perform the turning movement (turning skill component) to rotate it. When the players are hit by the laser beam or the devil, they will lose a life represented by a heart. To gain more lives, the players must attain the connecting heart (Figure 9(g)).

3.4. Personalization in I-TRAVLE. The diversity of MS patients raises the need for personalization in their rehabilitation training. The differences in physical abilities, MS symptoms, and disease progression bring an influence to the patients' condition and their rehabilitation needs. Therefore, offering the same training trajectory to MS patients is a straightforward, yet unwise, approach. A personalized training that complies to each patient's characteristics becomes a necessity to accommodate the patient diversity and ensure an effective and satisfactory rehabilitation. The I-TRAVLE system has been developed with a concern for supporting personalization in upper limb rehabilitation training for MS patients. An exploratory study on the personalization aspects has been discussed in Notelaers et al. [36]. The first aspect considered in the personalization infrastructure of I-TRAVLE was the workspace determination of patients. Due to the difference in patients' abilities in using their upper limb, some patients may have a smaller range of motion than the others. Based on the measurement of their active range of motion (AROM), the setup of the training program can be adjusted accordingly to ensure that the effort required to perform the training exercises is within the capability of the patient and no impossible or harmful arm movements were necessary.

Within I-TRAVLE, normally the therapist manually determines the training program and its exercise parameters in the therapist interface (see Figure 3) to present suitably challenging, individualized rehabilitation training. The therapist can set up a training program according to the patient's desire to train certain activities of daily living. For example, when the patient prefers to train his/her ability of drinking a cup of coffee (i.e., self feeding), the therapist can choose the suitable skill components such as reaching, lifting, and transporting. Providing customizable parameters of these skill components ensures personalization to better suit the patients' capabilities. A personalized training program with the appropriate difficulty level according to the patients' abilities can be established. For instance, to achieve the training of more fine-grained arm movements, the therapist can customize the parameters of the lifting exercise to a higher difficulty. Several kinds of parameters are adjustable, for instance, related to visual or haptic feedback. The amount of haptic feedback that is given when the patient has to follow a certain path in the virtual world influences how easy or how difficult it is for the patient to stay on the path. Figure 4(a) shows the lifting exercise. The green line shows the ideal path the patient has to follow to bring the green disc to the target through the HapticMaster. When the patient deviates too much from the ideal path, the line and disc become orange and finally red (as shown for the transporting exercise in Figure 4(b) to encourage the patient to correct her path. Another example of feedback that is parameterized is illustrated for the skill component rubbing in Figure 4(c). The patient has to move the disc between the two walls of the tube. Haptic feedback makes the inside of the walls either smooth or course grained, so that it is either easy or hard for the patient to slide the disc next to the walls.

Not only the parameters of the skill components can be customized but also personalization can take place in the gaming level. Figure 5(a) shows the penguin painting game. To make the lifting easier, the weight of the penguins can be adjusted. In the arkanoid game (Figure 5(b)), the viscosity of the bar pushing back the ball is also an adjustable haptic parameter.

However, the customization of exercise parameters is dependent on the therapist's judgement and requires the therapist to monitor the difficulty levels and preset parameters during the training session and to intervene to adjust if needed. There might be times when the therapist is not aware of the need for adjusting the training program according to the patient's progress or when the therapist finds a limited time to set up a new training program customized to the patient's current ability. This dependency can be minimized without a conscious effort from the therapist through the integration of adaptivity. Adaptivity enables the system to automatically adjust itself in such a way to support the different context of each patient's rehabilitation training. Tailoring the right training challenge in the right time without any interference from the therapist can be provided by automatically adjusting the difficulty level of the training exercises according to the patient's current training performance [37].

4. Towards Adaptive Personalized Rehabilitation Training: *Automatic Difficulty Level Adjustment*

The focus in this work is how we can enhance our personalization strategy by integrating adaptivity into the rehabilitation training, both in individual and collaborative training exercises, for MS patients. Due to the diversity of MS patients, every patient has a different physical ability and condition which may influence the course of their training. For example, one patient might find it very difficult to perform a specific training task, while the other finds it quite easy to perform it. We also have to take into account that every patient progresses differently. It could be the case that one patient may progress slower than the other in performing the rehabilitation training tasks. With adaptation, we aim to keep the patients continue on training at their ease and ensure no major barriers inhibit their interaction during training. For that purpose, we propose the adaptivity of automatically adjusting the difficulty level of the training exercise to be investigated in this study.

To achieve an optimal training experience for MS patients, we were inspired by the flow theory of Csikszentmihalyi [38] to keep the balance between difficulty level and patient performance. As illustrated in Figure 10, we would like to make sure that a patient stays within the "optimal training zone," where the difficulty level of exercise given to a patient is balanced with his current performance. In the optimal zone, the patient will not experience overtraining or undertraining [39]. Overtraining happens when the patient is asked to perform the exercises with a high difficulty level while his/her performance is still low; thus, the patient is most likely to find the training too difficult and may not be able to perform the training. On the other hand, undertraining happens when a low difficulty level is given to a patient who

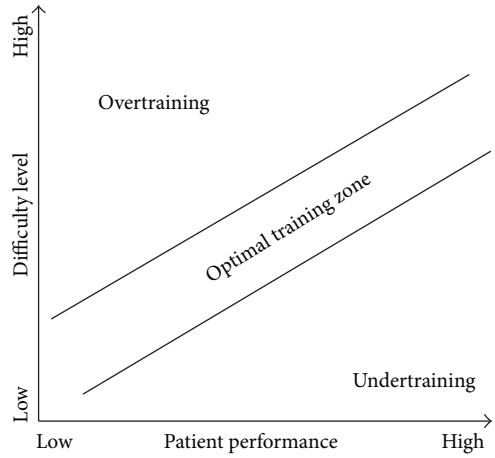

Figure 10: Balancing the difficulty level and patient performance.

has a high performance which makes the training not that challenging anymore.

As an optimization strategy to achieve such personalized training, we propose providing the ability to automatically and dynamically adjust the difficulty of the exercise to avoid boredom, provide suitable challenge, and minimize the therapist's involvement as well. This can be done by creating automatic difficulty adjustments according to the patient's performance and progress in the exercise. For this purpose, we need to establish a user model by capturing the patient's performance metrics (e.g., task completion times, scores, and errors) during the exercises and making use of that information to infer the short-term training progress of the patient. This can be considered as a sort of performance-evaluation mechanism. Once established, we can put the user model into practice by applying it to enable adapting the difficulty level whenever necessary. Based on the information from the user model, we can adjust the difficulty of the exercise by making it harder or easier.

In this study, we investigate the possibility of providing automatic difficulty level adjustment in two training exercises of our I-TRAVLE system, namely, the penguin painting game and the social maze game, through two user studies that we have carried out with several MS patients.

5. Adaptive Difficulty in Individual Training: *The Penguin Painting Game*

The penguin painting game is an individual training exercise that was designed as part of the upper limb rehabilitation for MS patients and focuses on training the skill components of lifting and transporting. The goal of this game is to paint penguins with the right color as many as possible within a certain time period (see Section 3.2). At the beginning of the training, every patient starts from an initial level as shown in Figure 11. After two consecutive training sessions, the training progress of the patient is determined based on his/her performance in each session.

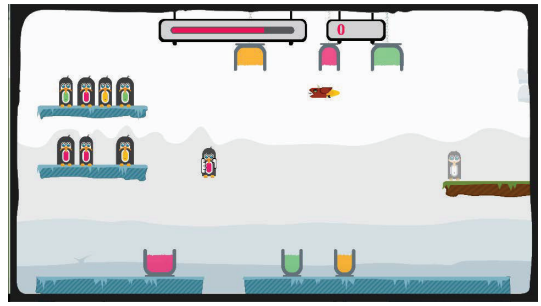

Figure 11: The penguin painting game: initial level.

If no significant difference of the performance is shown between the training sessions, it is considered that the patient is training on an appropriate level and adaptation will not be triggered. If the patient shows a decrease in his/her performance between the sessions, a lower difficulty level will be automatically offered to the patient in the next session. On the other hand, if an increase of the patient's performance is shown between the training sessions, the system will automatically provide a level with a higher difficulty in the next session.

We define seven different difficulty levels by altering the following game parameters accordingly (see Table 1):

(i) *size of penguin*: how big the penguins are (small/large);

(ii) *speed of devil*: how fast the devil moves (slow/medium/fast);

(iii) *frequency of devil*: how frequent the devil appears (infrequent/normal/frequent);

(iv) *length of stabilization*: the time required to hold the penguin still (short/normal/long);

(v) *obstacle wall*: addition of an obstacle wall along the way (no/yes);

(vi) *amount of coloring buckets*: how many coloring buckets exist (2/3/4);

(vii) *width of coloring bucket*: how big the coloring buckets are (narrow/wide);

(viii) *exit platform*: addition of another exit platform which requires patients to place the colored penguins to the size-corresponding platforms (no/yes).

As shown in Figure 12, three different levels are designed as the easy levels in the penguin painting game. Level −1 (Figure 12(a)) is easier than the initial level. Then, one level easier is Level −2 (Figure 12(b)) with Level −3 (Figure 12(c)) being the easiest level. Figure 14 illustrates the three difficult levels in the penguin painting game. Level 1 (Figure 13(a)) is more difficult than the initial level. Then, one level higher is Level 2 (Figure 13(b)) with Level 3 (Figure 13(c)) being the most difficult level.

Table 1: Overview of the penguin painting game parameters in the different difficulty levels.

Game parameter	Difficulty level						
	Level −3	Level −2	Level −1	Level 0	Level 1	Level 2	Level 3
Size of penguin	All small	90% small 10% large	70% small 30% large	50% small 50% large	30% small 70% large	10% small 90% large	All large
Speed of devil	Slow	Slow	Medium	Medium	Medium	Fast	Fast
Frequency of devil	Infrequent	Infrequent	Normal	Normal	Normal	Frequent	Frequent
Length of stabilization	Short	Short	Normal	Normal	Normal	Long	Long
Obstacle wall	No	No	No	No	No	Yes	Yes
Amount of coloring bucket	2	2	3	3	3	4	4
Width of coloring bucket	All wide	Bottom: 1 wide, 1 narrow Top: 1 wide, 1 narrow	Bottom: 2 wide, 1 narrow Top: 2 wide, 1 narrow	Bottom: 1 wide, 2 narrow Top: 2 wide, 1 narrow	Bottom: 1 wide, 2 narrow Top: 1 wide, 2 narrow	Bottom: 2 wide, 2 narrow Top: All narrow	All narrow
Exit platform	No	No	No	No	Yes	Yes	Yes

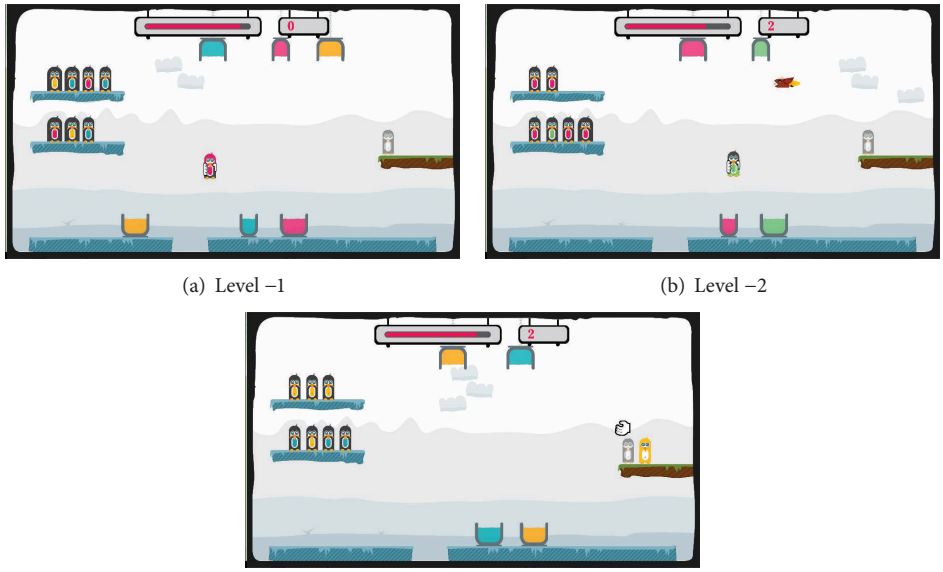

(a) Level −1 (b) Level −2

(c) Level −3

Figure 12: The easy levels in the penguin painting game.

To determine the patient's training progress, it is necessary to obtain information of his/her training performance and make a comparison over the last two training sessions. The patient's performance of each training session is calculated as a function of the following performance metrics.

(1) *Task Completion Time.*

How much time does the patient take to complete one task (i.e., select and transport a penguin)?

How much is the slope of task completion times in one training session?

(2) *Score.*

What score does the patient achieve in one game session?

(3) *Error.*

How many times does the patient make errors (i.e., hitting the devil, painting with the wrong color)?

(4) *Pause.*

How many times does the patient make pause actions (i.e., motionless period between steps for longer than 2 seconds)?

(5) *Distance.*

What is the distance traveled by the patient to complete one task (i.e., select and transport a penguin)?

How much is the slope of the distance traveled in one training session?

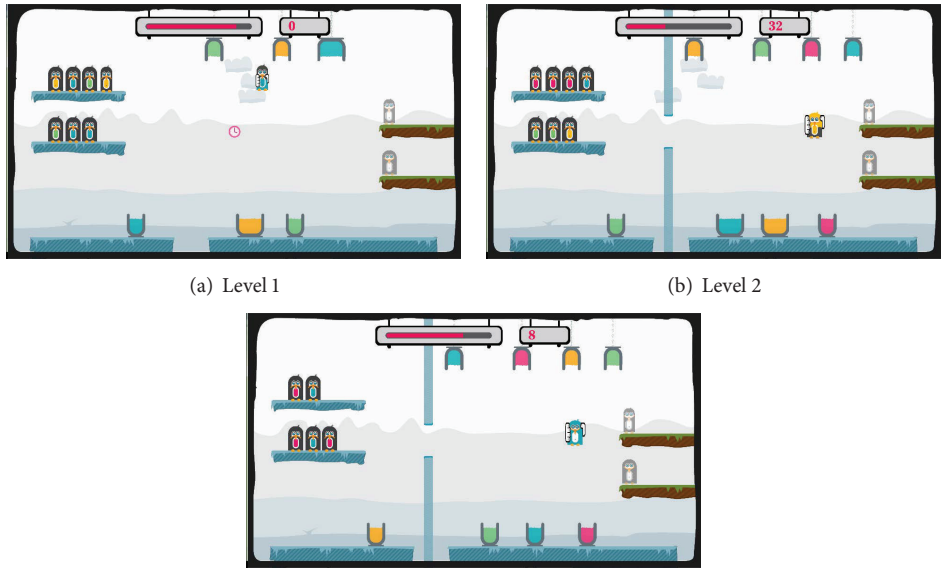

(a) Level 1 (b) Level 2

(c) Level 3

Figure 13: The difficult levels in the penguin painting game.

5.1. User Study 1: Automatic Adjustment of Difficulty Level in the Penguin Painting Game. We have integrated the adaptation of automatic adjustment of difficulty levels in the penguin painting game. This results in seven difficulty levels which differ in the exercise parameters as described in Section 5 (see Table 1). We expect that supporting adaptivity in the adjustment of difficulty levels of the training exercises will not only deliver a personalized training to each MS patient but also provide suitable challenge, enable less boredom, and minimize the therapist's involvement. Therefore, we carried out a user study to investigate the outcome of integrating adaptive difficulty into the penguin painting game.

5.1.1. Participants. For the user studies in this research, we recruited a group of participants which consists of nine patients of the Rehabilitation and MS Centre in Overpelt (Belgium) who all suffer from upper limb dysfunction due to MS and were willing to participate in both user studies. The patients were 6 males and 3 females with an average age of 60 years, ranging from 47 to 72 years old. The duration since the MS diagnosis varies between 3 and 34 years, with an average of 20.5 years. Six of them used the left hand to operate the HapticMaster in training, while the other three used their right hand. Table 2 shows the personal information of each MS patient participating in this research. To have an overview of the severity of their upper limb dysfunction, we obtained their clinical measures as shown in Table 3: upper limb strength (motricity index [40]), upper limb functional capacity (action research arm test [41]), and arm motor function scores (Brunnstrom Fugl-Meyer proximal and distal [42]).

In this first user study, only 8 patients of the group participated. Patient 9 was unable to participate due to his health condition.

Table 2: Personal information of MS patients in the user studies.

Patient	Gender	Age (years)	Diagnosis duration (years)	Training hand
1	Male	64	14	Left
2	Female	58	3	Left
3	Male	71	10	Right
4	Female	47	14	Right
5	Male	57	27	Left
6	Male	55	27	Left
7	Female	64	25	Right
8	Male	56	30	Left
9	Male	72	34	Left

Table 3: Clinical characteristics of MS patients in the user studies.

Patient	MI	ARAT	BFM-prox	BFM-dist
1	76	41	25	40
2	83	56	36	29
3	84	46	32	28
4	76	56	36	30
5	55	41	23	21
6	47	7	18	24
7	72	18	31	25
8	60	30	27	24
9	50	1	12	7

MI: motricity index (maximal score = 100); ARAT: action research arm test (maximal score = 57); BFM-prox: Brunnstrom Fugl-Meyer proximal score (maximal score = 66); BFM-dist: Brunnstrom Fugl-Meyer distal score (maximal score = 66).

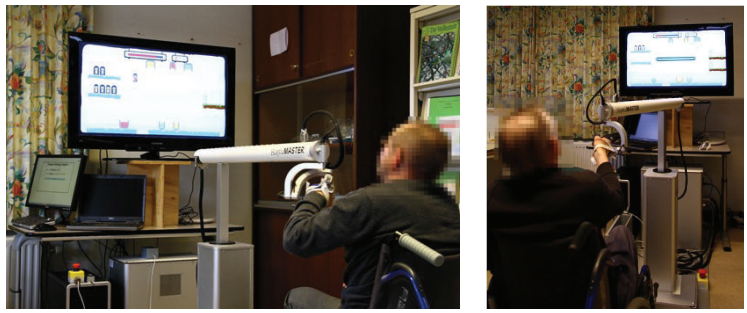

(a) The patient trained at the initial level

(b) The patient's training was adapted to a higher difficulty level

FIGURE 14: The setup of user study: automatic difficulty level adjustment in the penguin painting game (e.g., 2 exit platforms in the difficult level).

5.1.2. Procedure. The user study consisted of seven sessions: two elicitation sessions and five adaptive sessions; all took place on the same day. In the elicitation sessions, participants were asked to perform the penguin painting game in the initial level (see Figures 11 and 14(a)). After two elicitation sessions, the performance metrics of the participant were calculated to determine the progress of his/her training. Based on the information about the training progress over these elicitation sessions, it will be determined for the first adaptive session whether or not the difficulty level should be adapted. Throughout the adaptive sessions, participants were offered an adaptive personalized training in terms of the adjustment of difficulty levels. Three possibilities can happen over the course of five adaptive sessions: *stay at the same level*, *go one level lower*, or *go one level higher* (see Figure 14(b)).

The duration of each session is 3 minutes. After each adaptive session, participants were asked to rate their subjective perception on enjoyment, boredom, challenge, frustration, and fun, on a 5-point scale rating (e.g., *1 not at all* to *5 very much*) based on their experience of performing the adaptive penguin painting game. Averagely, the user study lasted for about 30 minutes per participant. Figure 14 illustrates the setup of this user study.

5.1.3. Results. We have applied the adaptation of automatic difficulty level adjustment in the penguin painting game, which provided an adaptive personalized training for each participant. Consequently, the training trajectory was different for every participant during the five adaptive sessions. For each session, the participant can experience staying at the same difficulty level, going to a lower level, or going to a higher level, depending on his/her individual performance. Figure 15 shows the personalized training trajectory for each patient as a result of integrating the adaptive difficulty level adjustment in the penguin painting game. As can be observed, no patient had the same trajectory as the other patient due to the fact that every patient progressed differently. This finding confirms the need for adaptation. Further, we analyzed how adaptation influenced the subjective perception on enjoyment, boredom, challenge, frustration, and fun, across the sessions. Due to the small number of samples and observations in this user study, we used the nonparametric methods for the statistical analysis.

Based on the patients' subjective responses, we calculated the average ratings of enjoyment, boredom, challenge, frustration, and fun, for the three conditions of adaptation (go to a lower level, stay at the same level, and go to a higher level) as shown by Figure 16. Kruskal-Wallis test showed that no significant differences were found for *Enjoyment*, *Frustration*, and *Fun* between the different conditions of adaptations. This indicates that patients perceived the same level of enjoyment, frustration, and fun eventhough the system introduced an automatic adaptation of difficulty levels in the training exercises. Patients rated a high level of enjoyment and fun (above 4) and a low level of frustration (below 2) in all the conditions.

However, there is a significant difference found for *Boredom* ($H(2) = 15.651$, $P < 0.001$; 2 for condition 1, 1.33 for condition 2, and 1 for condition 3) and *Challenge* ($H(2) = 24.376$, $P < 0.001$; 2 for condition 1, 2.89 for condition 2, and 4.25 for condition 3). Mann-Whitney pairwise comparison tests showed that patients felt significantly less bored and more challenged when the training was adapted to a higher level compared to when they had to adapt to a lower level or stayed at the same level ($P < 0.001$).

Furthermore, we observed that some patients have noticed the automatic adaptation to be related to their training progress and they liked the diversity of difficulty levels. We did not inform about the implemented adaptation to the patients before or during the user study. A couple of therapists appreciated the automatic adaptation as it provided the patients with more variety in the training and also gave them more freedom to train on their own without any interference from the therapist to manually adjust the exercise parameters. This kind of adaptation could be useful to determine an appropriate level to start training on a certain day according to the patients condition on that day, thus less determined by the previous training or the therapist.

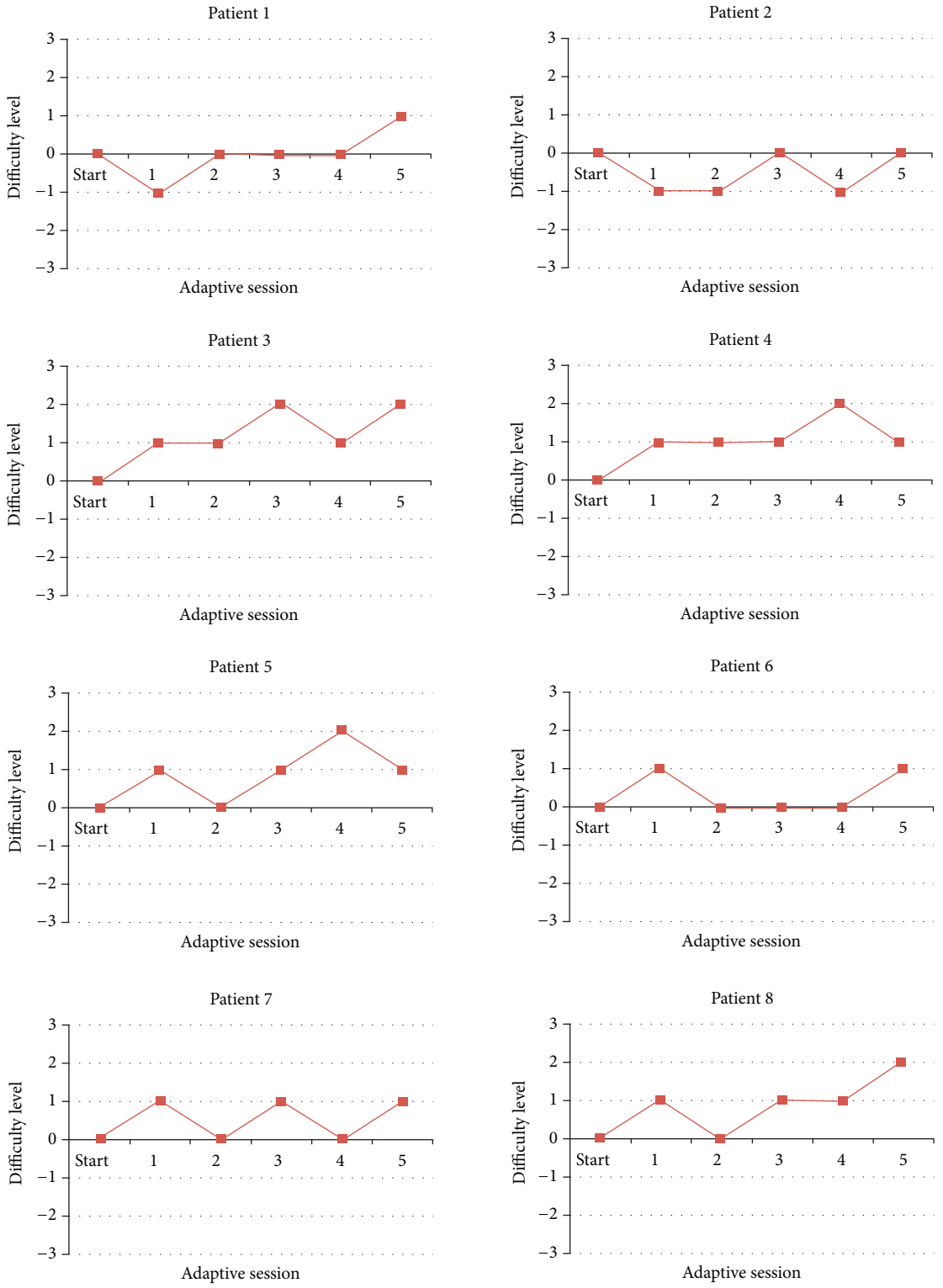

Figure 15: Adaptive personalized training trajectory in the penguin painting game.

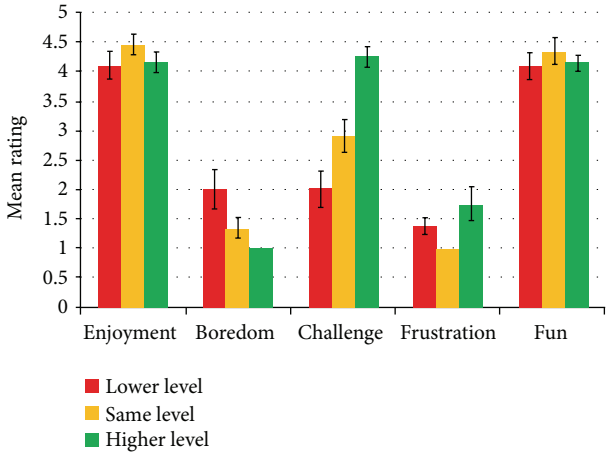

Figure 16: Patient's subjective rating with respect to adaptation.

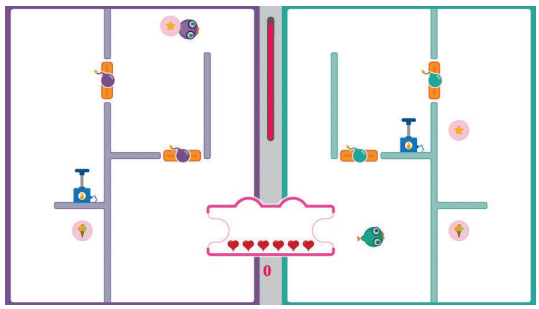

Figure 17: The social maze game: initial level.

6. Adaptive Difficulty in Collaborative Training: The Social Maze Game

The social maze game is a collaborative training exercise that was designed to train several skill components such as lifting, transporting, turning, pushing, and reaching. The goal of this game is to collect all symbols by picking up each symbol and bringing it to the collecting bin (see Section 3.3). To achieve this, the patient should pair and closely collaborate with his/her training partner (e.g., a therapist, family member, or fellow patient). At the beginning of the training, every pair starts from an initial level as depicted in Figure 17.

The same performance-evaluation and adaptation mechanism with the penguin painting game is implemented. First, we obtain an indication of the patient's training progress by comparing the training performance of the last two training sessions. When no training progress is indicated, no adaptation will be triggered and the pair will stay at the same level. When a training progress is indicated, a higher difficulty level will be automatically offered to the pair in the next session. When a training decline is indicated, the system will automatically switch to a lower difficulty level in the next session. It is important to mention here that although collaborative training exercises involve two persons, we mainly focus the adjustment of difficulty level based on the patients' progress in the training since they hold the core function in the rehabilitation. Particularly in the sympathetic scenario, we do not take into account the progress of a healthy person as the training partner since his/her role is solely supporting the rehabilitation training of the patient.

We define eight difficulty levels ranging from very easy to very difficult. As shown in Figure 18, three different levels are designed as the easy levels in the social maze game with Level −3 (Figure 18(c)) being the easiest level. Figure 19 illustrates the four difficult levels in the social maze game with Level 4 (Figure 19(d)) being the most difficult level.

To adjust the difficulty levels, we alter the following game parameters in each level accordingly (see Table 4):

(i) *viscosity of movement*: how high the viscosity is (very low/low/normal/high/very high);

(ii) *speed of devil*: how fast the devil moves (slow/medium/fast);

(iii) *length of laser beam*: how long the laser beam lasts (short/normal/long);

(iv) *friction of bomb*: the degree of friction that the bomb has (no friction/less friction/much friction);

(v) *friction of wall*: the degree of friction that the wall has (no friction/less friction/much friction).

In the social maze game, four performance metrics are employed to determine the patient's training progress as follows.

(1) *Speed.*

How fast can the patient complete one task (i.e., select and transport a symbol)?

(2) *Score.*

What score does the patient achieve in one game session?

(3) *Error.*

How many times does the patient make errors (i.e., hitting the devil, hitting the laser beam)?

(4) *Pause.*

How many times does the patient make pause actions (i.e., motionless period between steps for longer than 2 seconds)?

6.1. User Study 2: Automatic Adjustment of Difficulty Level in the Social Maze Game. We have integrated the adaptation of automatic adjustment of difficulty levels in the social maze game. To investigate how patients perceive the outcome of this adaptation, we carried out the second user study with our group of participants as described in Section 5.1.1.

6.1.1. Participants. All nine patients of the group participated in this user study. More information on these participants can be found in Table 2 for their personal information and Table 3 for their clinical characteristics. In this user study, we applied the sympathetic scenario of social rehabilitation training, where a patient collaborates with his/her therapist in

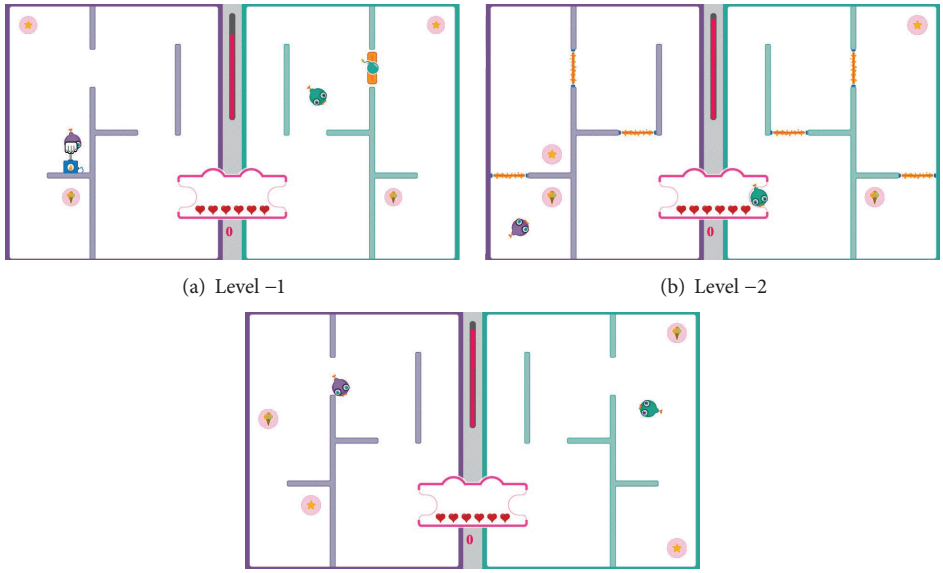

(a) Level −1 (b) Level −2

(c) Level −3

Figure 18: The easy levels in the social maze game.

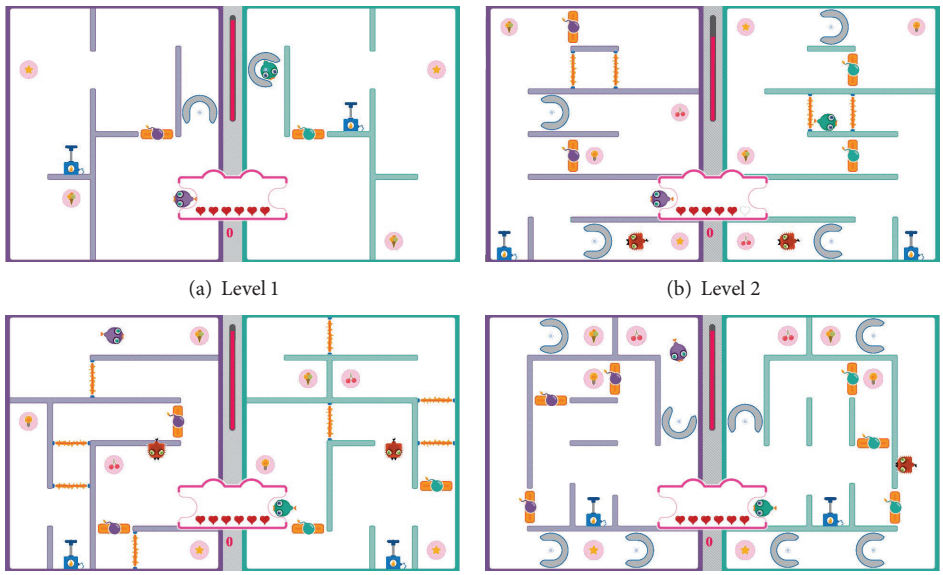

(a) Level 1 (b) Level 2

(c) Level 3 (d) Level 4

Figure 19: The difficult levels in the social maze game.

Table 4: Overview of the social maze game parameters in the different difficulty levels.

Game parameter	Difficulty level							
	Level −3	Level −2	Level −1	Level 0	Level 1	Level 2	Level 3	Level 4
Viscosity of movement	Very low	Low	Low	Normal	Normal	High	High	Very high
Speed of devil	Slow	Slow	Slow	Medium	Medium	Fast	Fast	Fast
Length of laser beam	Short	Short	Short	Normal	Normal	Long	Long	Long
Friction of bomb	No	No	No	Less	Less	Much	Much	Much
Friction of wall	No	No	No	Less	Less	Much	Much	Much

Figure 20: The setup of user study: automatic difficulty level adjustment in the social maze game.

performing the social maze game. Only one therapist, whom every patient has a good relationship with, participated in this user study. The Novint Falcon was used as the input device for the therapist. All patients used the HapticMaster as the input device.

6.1.2. Procedure. Similar to the previous study described in Section 5.1.2, the user study consisted of seven sessions: two elicitation sessions and five adaptive sessions. In the elicitation sessions, pairs of participants (i.e., one patient and the therapist) were asked to perform the social maze game in the initial level (see Figure 17). After two elicitation sessions, the performance metrics of the patient were calculated to determine the progress of his/her training. Depending on the observation of the training progress, the system will determine how the difficulty level should be adjusted throughout the adaptive sessions. There can be three possible results of the adaptation: *stay at the same level*, *go one level lower*, or *go one level higher*.

After each adaptive session, patients were asked to rate their subjective perception on difficulty and enjoyment, on a 5-point scale rating (e.g., *1 not at all* to *5 very much*) based on their experience of performing the social maze game. Averagely, the user study lasted for about 30 minutes per participant. Figure 20 illustrates the setup of this user study.

6.1.3. Results. We have applied the adaptation of automatic difficulty level adjustment in the social maze game. Since the adaptation resulted in a personalized training, each patient had a unique training trajectory which differs from each other during the adaptive sessions. Figure 21 shows the personalized training trajectory for each pair of participants as a result of integrating adaptive difficulty in the social maze game. No pair of participants had exactly the same trajectory as the other, which confirms the need for adaptation based on the patient's individual performance. We analyzed how adaptation influenced the subjective perception on difficulty and enjoyment across the sessions. We used the nonparametric statistics because of the small number of samples and observations in this user study.

Based on the patients' subjective responses, we calculated the average ratings of perceived difficulty and perceived enjoyment, for the three conditions of adaptation as shown by Figure 22. Kruskal-Wallis test showed that significant differences were found for *perceived difficulty* ($H(2) = 13.062$, $P < 0.001$; 1.64 for condition 1, 2.08 for condition 2, and 2.96 for condition 3) and *perceived enjoyment* ($H(2) = 9.439$, $P < 0.05$; 3.91 for condition 1, 3.67 for condition 2, and 3.09 for condition 3). This indicates that patients perceived the difficulty and enjoyment differently across the conditions of adaptation. Mann-Whitney pairwise comparison tests showed that patients perceived the training to be more difficult and less enjoyable when the training was adapted to a higher level compared to when they had to adapt to a lower level ($P < 0.05$).

The finding which showed that as the levels got more difficult the patients perceived the training to be less enjoyable is somewhat different than our previous finding where patients perceived the same high level of enjoyment despite the change in difficulty levels. We think that social effect plays a role in this case. In a collaborative training session, the patients might have felt more social pressure to perform as good as the training partner. They might have feared that they will hinder the collaboration if they perform less well. However, additional investigation is needed to confirm this thought. Another possible explanation is that the differences among the difficulty levels were quite prominent. This calls for a further investigation to find a subtler difference of difficulty that maintains the patient's enjoyment in training.

With regard to social interaction, we believe that the social maze game has become a social play medium between patients and their therapist. We have observed some relevant behaviors which indicated the development of social interaction during the collaborative rehabilitation training. Figure 23 depicts two examples of behaviors shown by the pairs of participants throughout the training sessions. The most shown behavior during the social maze game was the act of discussing strategy (Figure 23(a)). It was pretty obvious that the nature of the training exercise requires the two participants to closely collaborate and discuss their strategy and necessary actions. This behavior happened throughout the whole session, sometimes followed by the act of looking

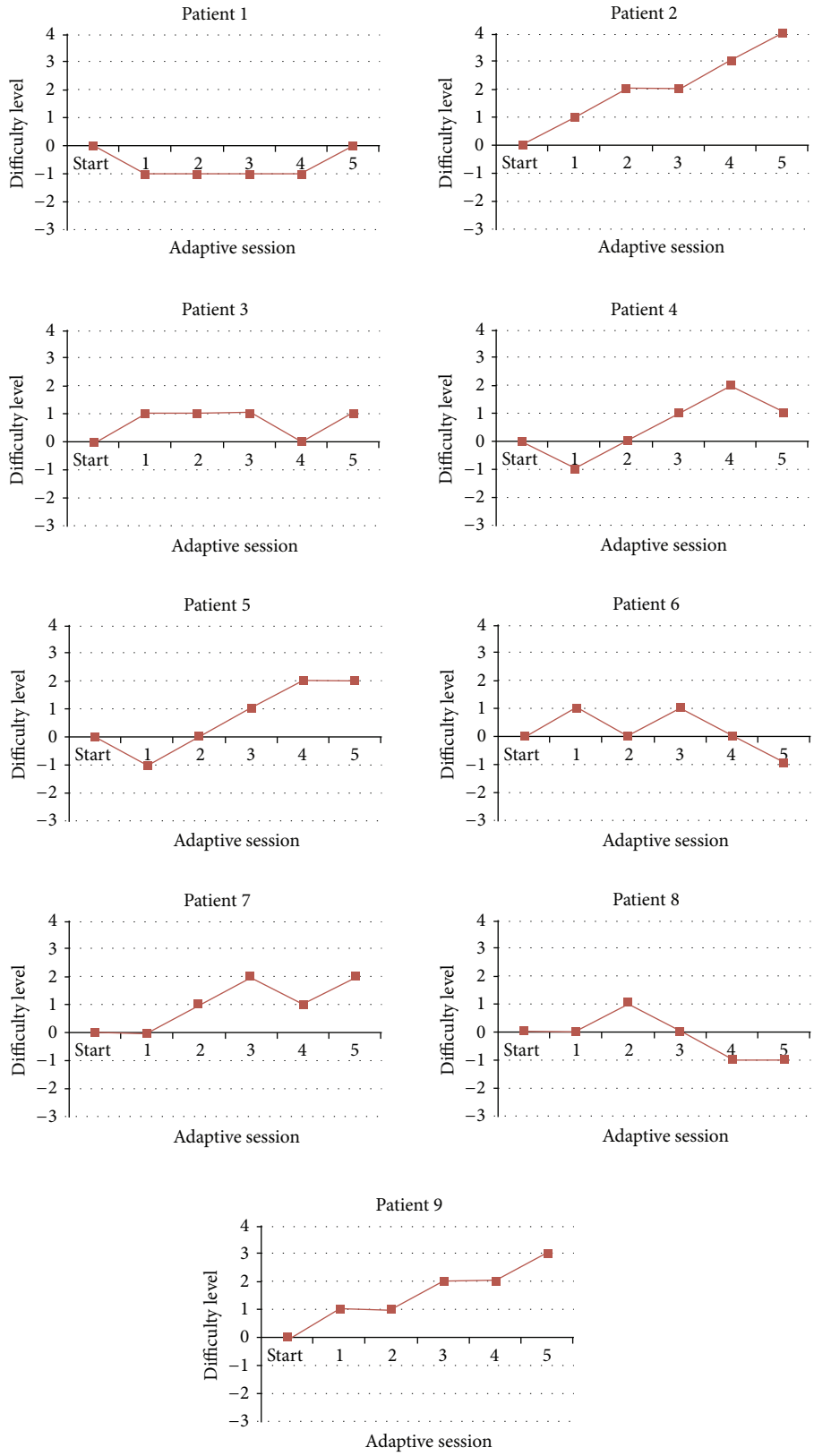

Figure 21: Adaptive personalized training trajectory in the social maze game.

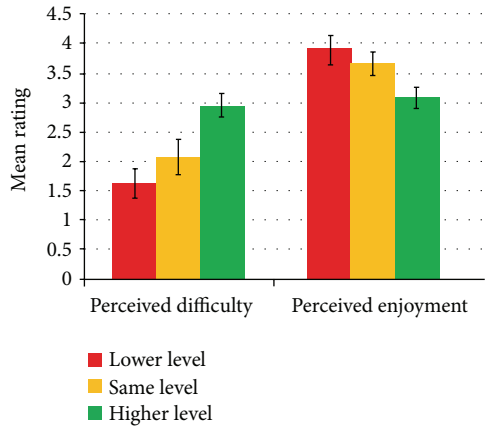

Figure 22: Patient's subjective rating with respect to adaptation.

(a) Discussing strategy at the end of a session

(b) Mimicking each other

Figure 23: Different behaviors observed during the social maze game.

at each other. At the beginning and during the session, participants discussed what actions they should perform and the best way to perform them. At the end of the session, participants briefly reviewed their previous session and how they should perform better on the next session. In some participants, we can also observe the behavior of unconsciously mimicking each other during the strategy discussion (Figure 23(b)). Throughout the sessions, we can observe that all participants showed other behaviors such as smiling, laughing, and chuckling. This mostly happened when one of them made an error such as encountering the devil or hitting the laser beam. A couple of participants tended to make jokes during the training session that resulted in both of them laughing at each other.

7. Discussion

Our work has presented an investigation to integrate adaptivity and personalization into individual rehabilitation training and collaborative rehabilitation training for MS patients. Typically rehabilitation training is individual, where a MS patient performs the training exercises alone under the supervision of a therapist. However, rehabilitation training can take place in a collaborative setting as well, where performing the training exercises involves more than only a single MS patient. By changing the nature of rehabilitation training to be collaborative, we can enhance the patient's motivation and also support social interaction between the patient and his/her training partner (e.g., a family member, friend, or therapist).

We have discussed and implemented the adaptation of automatic difficulty level adjustment in both individual training (i.e., the penguin painting game) and collaborative training (i.e., the social maze game). Two user studies have been carried out to investigate the outcome of this adaptation. Overall, we can conclude that providing adaptive difficulty in the training exercises has delivered an adaptive personalized training to each MS patient according to his/her own individual training progress. Patients and the therapist have appreciated the automatic adaptation of difficulty levels and considered it to provide more variety in the training and also give the patients more freedom to train on their own without any interference from the therapist to manually adjust the exercise parameters. This kind of adaptation could be useful to determine an appropriate level to start training on a certain day according to the patient's condition on that day, thus less determined by the previous training or the therapist.

Moreover, we have observed the development of social interaction between patients and their training partner during the course of the collaborative rehabilitation training exercises. While performing the social maze game collaboratively, they have showed several particular behaviors such as smiling, laughing or chuckling, looking at each other, and discussing strategy. We realized that the adaptation in

the collaborative training exercise has been implemented with a focus on the patient's needs and characteristics despite the existence of a training partner. In the sympathetic social scenario, it may be interesting to investigate how or what kinds of adaptation can facilitate the family member or the therapist to achieve a more engaging and motivating collaboration with the patient. For the empathetic social scenario, we also need to investigate how the different types of adaptation can accommodate the needs and characteristics of another patient as a training partner.

It is not our focus to carry out an in-depth investigation on the adaptation algorithm used in these user studies. We were more interested to observe the patients' response with respect to the automatic adjustment of difficulty levels. We realize that a more accurate and well-defined algorithm could be provided. Therefore, further investigation is needed to optimize the adaptation algorithm which also matches the judgment of therapists on the trigger and timing of adaptation. Another next step is to extend our investigation of integrating adaptivity and personalization into MS rehabilitation training to other types of adaptation that may help patients during the course of their training, for example, automatically adjusting the assistance level based on the detected muscle fatigue. In some cases, the muscle fatigue might develop during long training; thus, it might be necessary to provide the patients with some assistance to help them perform the task and continue their training.

8. Conclusion

This paper has discussed our investigation on the notion of integrating adaptivity and personalization into individual and collaborative rehabilitation training for MS patients. We have strived for developing adaptive personalized training games by introducing the automatic adjustment of difficulty levels in the penguin painting game (individual training) and the social maze game (collaborative training). The user studies showed that none of the MS patients experienced the same training trajectory as the other. This confirms that every patient progresses differently, which encourages the need for adaptation. Adaptive personalized training, which was delivered to every MS patient according to his/her own individual training progress, has shown to be beneficial and much appreciated. The automatic adjustments of difficulty levels in the training games were also considered to provide more variety in the training and more freedom to train independently.

Conflict of Interests

The authors declare that there is no conflict of interests regarding the publication of this paper.

Acknowledgments

The authors acknowledge the INTERREG-IV program, in particular "rehabilitation robotics II" (Project no. IVA-VLANED-1.14, Euregio Benelux) and "I-TRAVLE" (Project no. IVA-VLANED-1.58 and the consortium partners (see http://i-travle.tumblr.com/). The authors greatly appreciate Geert Alders for his valuable insights, Tom De Weyer for his abundant help, and Karel Robert for his graphical design. The authors thank all participants for their contribution to the user studies.

References

[1] S. Jezernik, R. Schärer, G. Colombo, and M. Morari, "Adaptive robotic rehabilitation of locomotion: a clinical study in spinally injured individuals," *Spinal Cord*, vol. 41, no. 12, pp. 657–666, 2003.

[2] L. E. Kahn, W. Z. Rymer, and D. J. Reinkensmeyer, "Adaptive assistance for guided force training in chronic stroke," in *Proceedings of the 26th Annual International Conference of the IEEE Engineering in Medicine and Biology Society (EMBC '04)*, pp. 2722–2725, San Francisco, Calif, USA., September 2004.

[3] P. Kan, R. Huq, J. Hoey, R. Goetschalckx, and A. Mihailidis, "The development of an adaptive upper-limb stroke rehabilitation robotic system," *Journal of NeuroEngineering and Rehabilitation*, vol. 8, no. 1, article 33, 2011.

[4] S. Jezernik, G. Colombo, and M. Morari, "Automatic gait-pattern adaptation algorithms for rehabilitation with a 4-DOF robotic orthosis," *IEEE Transactions on Robotics and Automation*, vol. 20, no. 3, pp. 574–582, 2004.

[5] M. T. Schultheis and A. A. Rizzo, "The application of virtual reality technology in rehabilitation," *Rehabilitation Psychology*, vol. 46, no. 3, pp. 296–311, 2001.

[6] M. K. Holden, "Virtual environments for motor rehabilitation: review," *Cyberpsychology & Behavior*, vol. 8, no. 3, pp. 187–211, 2005.

[7] J. S. Webster, P. T. McFarland, L. J. Rapport, B. Morrill, L. A. Roades, and P. S. Abadee, "Computer-assisted training for improving wheelchair mobility in unilateral neglect patients," *Archives of Physical Medicine and Rehabilitation*, vol. 82, no. 6, pp. 769–775, 2001.

[8] D. L. Jaffe, D. A. Brown, C. D. Pierson-Carey, E. L. Buckley, and H. L. Lew, "Stepping over obstacles to improve walking in individuals with poststroke hemiplegia," *Journal of Rehabilitation Research and Development*, vol. 41, no. 3, pp. 283–292, 2004.

[9] J. A. Edmans, J. R. F. Gladman, S. Cobb et al., "Validity of a virtual environment for stroke rehabilitation," *Stroke*, vol. 37, no. 11, pp. 2770–2775, 2006.

[10] G. Alankus, A. Lazar, M. May, and C. Kelleher, "Towards customizable games for stroke rehabilitation," in *Proceedings of the 28th Annual CHI Conference on Human Factors in Computing Systems (CHI '10)*, pp. 2113–2122, Atlanta, Ga, USA, April 2010.

[11] G. Saposnik, R. Teasell, M. Mamdani et al., "Effectiveness of virtual reality using wii gaming technology in stroke rehabilitation: a pilot randomized clinical trial and proof of principle," *Stroke*, vol. 41, no. 7, pp. 1477–1484, 2010.

[12] M. Ma, M. McNeill, D. Charles et al., "Adaptive virtual reality games for rehabilitation of motor disorders," in *Universal Access in Human-Computer Interaction. Ambient Interaction*, C. Stephanidis, Ed., vol. 4555 of *Lecture Notes in Computer Science*, pp. 681–690, Springer, 2007.

[13] M. S. Cameirão, S. Bermúdez i Badia, E. D. Oller, and P. F. M. J. Verschure, "Using a multi-task adaptive VR system for upper limb rehabilitation in the acute phase of stroke," in *Proceedings*

of the International Conference on Virtual Rehabilitation (ICVR '08), pp. 2–7, Vancouver, Canada, 2008.

[14] O. Barzilay and A. Wolf, "An adaptive virtual biofeedback system for neuromuscular rehabilitation," in *Proceedings of the 11th IUPESM World Congress on Medical Physics and Biomedical Engineering*, pp. 1291–1294, Munich, Germany, September 2009.

[15] M. Duff, Y. Chen, S. Attygalle et al., "An adaptive mixed reality training system for stroke rehabilitation," *IEEE Transactions on Neural Systems and Rehabilitation Engineering*, vol. 18, no. 5, pp. 531–541, 2010.

[16] M. Baran, N. Lehrer, D. Siwiak et al., "Design of a home-based adaptive mixed reality rehabilitation system for stroke survivors," in *Proceedings of the 33rd Annual International Conference of the IEEE Engineering in Medicine and Biology Society (EMBS '11)*, pp. 7602–7605, Boston, Mass, USA, September 2011.

[17] U. Dalgas, E. Stenager, and T. Ingemann-Hansen, "Multiple sclerosis and physical exercise: recommendations for the application of resistance-, endurance- and combined training," *Multiple Sclerosis*, vol. 14, no. 1, pp. 35–53, 2008.

[18] R. W. Motl and J. L. Gosney, "Effect of exercise training on quality of life in multiple sclerosis: a meta-analysis," *Multiple Sclerosis*, vol. 14, no. 1, pp. 129–135, 2008.

[19] G. Kwakkel, R. C. Wagenaar, J. W. R. Twisk, G. J. Lankhorst, and J. C. Koetsier, "Intensity of leg and arm training after primary middle-cerebral-artery stroke: a randomised trial," *The Lancet*, vol. 354, no. 9174, pp. 191–196, 1999.

[20] G. Kwakkel, B. J. Kollen, and H. I. Krebs, "Effects of robot-assisted therapy on upper limb recovery after stroke: a systematic review," *Neurorehabilitation and Neural Repair*, vol. 22, no. 2, pp. 111–121, 2008.

[21] J. H. Burridge and A.-M. Hughes, "Potential for new technologies in clinical practice," *Current Opinion in Neurology*, vol. 23, no. 6, pp. 671–677, 2010.

[22] K. Coninx, C. Raymaekers, J. D. Boeck et al., "Using the phantom device for rehabilitation of the arm in MS patients: a case study," in *Proceedings of the 6th International Conference onMethods and Techniques in Behavioral Research (Measuring Behavior '08)*, pp. 148–149, Maastricht, The Netherlands, 2008.

[23] P. Feys, G. Alders, D. Gijbels et al., "Arm training in multiple sclerosis using phantom: clinical relevance of robotic outcome measures," in *Proceedings of the 11th IEEE International Conference on Rehabilitation Robotics (ICORR '09)*, pp. 576–581, Kyoto, Japan, June 2009.

[24] I-TRAVLE, "Revalidatierobotica II, an Interreg IV project," 2011, http://www.i-travle.eu.

[25] T. de Weyer, S. Notelaers, K. Coninx et al., "Watering the flowers: virtual haptic environments for training of forearm rotation in persons with central nervous deficits," in *Proceedings of the 4th International Conference on Pervasive Technologies Related to Assistive Environments (PETRA '11)*, pp. 1–6, Crete, Greece, 2011.

[26] S. Notelaers, T. de Weyer, C. Raymaekers, K. Coninx, H. Bastiaens, and I. Lamers, "Data management for multimodal rehabilitation games," in *Proceedings of the 21st International Workshop on Database and Expert Systems Applications (DEXA '10)*, pp. 137–141, Bilbao, Spain, September 2010.

[27] W. M. van den Hoogen, I. Lamers, K. Baeten et al., "Effects of shading and droplines on object localization in virtual rehabilitation for patients with neurological conditions," in *Proceedings of the International Conference on Virtual Rehabilitatio (ICVR '11)*, pp. 1–6, Zurich, Switzerland, June 2011.

[28] W. van den Hoogen, P. Feys, I. Lamers et al., "Visualizing the third dimension in virtual training environments for neurologically impaired persons: beneficial or disruptive?" *Journal of NeuroEngineering and Rehabilitation*, vol. 9, article 73, 2012.

[29] H. Woldag and H. Hummelsheim, "Evidence-based physiotherapeutic concepts for improving arm and hand function in stroke patients: a review," *Journal of Neurology*, vol. 249, no. 5, pp. 518–528, 2002.

[30] A. A. A. Timmermans, R. P. J. Geers, J. A. Franck et al., "T-TOAT: a method of task-oriented arm training for stroke patients suitable for implementation of exercises in rehabilitation technology," in *Proceedings of the IEEE 11th International Conference on Rehabilitation Robotics (ICORR '09)*, pp. 98–102, Kyoto, Japan, June 2009.

[31] L. Vanacken, S. Notelaers, C. Raymaekers et al., "Game-based collaborative training for arm rehabilitation of MS patients: a proof-of-concept game," in *Proceedings of GameDays*, pp. 65–75, 2010.

[32] W. van den Hoogen, W. IJsselsteijn, and Y. de Kort, "Yes Wii can! Using digital games as a rehabilitation platform after stroke—the role of social support," in *Proceedings of the International Conference on Virtual Rehabilitation (ICVR '09)*, p. 195, Haifa, Israel, July 2009.

[33] J. Decety and T. Chaminade, "Neural correlates of feeling sympathy," *Neuropsychologia*, vol. 41, no. 2, pp. 127–138, 2003.

[34] J. Decety and P. L. Jackson, "The functional architecture of human empathy," *Behavioral and Cognitive Neuroscience Reviews*, vol. 3, no. 2, pp. 71–100, 2004.

[35] T. de Weyer, K. Robert, J. Hariandja, G. Alders, and K. Coninx, "The social maze: a collaborative game to motivate ms patients for upper limb training," in *Proceedings of the 11th international conference on Entertainment Computing*, pp. 476–479, Springer, Berlin, Germany, 2012.

[36] S. Notelaers, T. de Weyer, J. Octavia, K. Coninx, H. Bastiaens, and P. Feys, "Individualized robot-assisted training for ms- and stroke patients in i-travle," *BIO Web of Conferences*, vol. 1, article 00069, 2011.

[37] J. R. Octavia, K. Coninx, and P. Feys, "As i am not you: accommodating user diversity through adaptive rehabilitation training for multiple sclerosis patients," in *Proceedings of the 24th Australian Computer-Human Interaction Conference*, pp. 424–432, ACM, New York, NY, USA, 2012.

[38] M. Csikszentmihalyi, *Flow: The Psychology of Optimal Experience*, Harper & Row, 1990.

[39] M. L. O'Toole, "Overreaching and overtraining in endurance athletes," in *Overtraining in Sport*, R. B. Kreider, A. C. Fry, and M. L. O'Toole, Eds., pp. 3–18, Human Kinetics, 1998.

[40] D. T. Wade, "Measuring arm impairment and disability after stroke," *Disability and Rehabilitation*, vol. 11, no. 2, pp. 89–92, 1989.

[41] W. J. G. de Weerdt, "Measuring recovery of arm-hand function in stroke patients: a comparison of the Brunnstrom-Fugl-Meyer test and the action research arm test," *Physiotherapy Canada*, vol. 37, no. 2, pp. 65–70, 1985.

[42] P. W. Duncan, M. Propst, and S. G. Nelson, "Reliability of the Fugl-Meyer assessment of sensorimotor recovery following cerebrovascular accident," *Physical Therapy*, vol. 63, no. 10, pp. 1606–1610, 1983.

Hindawi Publishing Corporation
BioMed Research International
Volume 2014, Article ID 632765, 10 pages
http://dx.doi.org/10.1155/2014/632765

Research Article

Metabolic Demand and Muscle Activation during Different Forms of Bodyweight Supported Locomotion in Men with Incomplete SCI

Alyssa M. Fenuta and Audrey L. Hicks

Department of Kinesiology, McMaster University, 1280 Main Street West, Hamilton, ON, Canada L8S 4L8

Correspondence should be addressed to Audrey L. Hicks; hicksal@mcmaster.ca

Received 27 December 2013; Revised 18 April 2014; Accepted 23 April 2014; Published 21 May 2014

Academic Editor: Belinda Lange

Body weight supported locomotor training uses neuroplasticity principles to improve recovery following a spinal cord injury (SCI). Steady state locomotion using the same body weight support (BWS) percent was compared in 7 males (42.6 ± 4.29 years) with incomplete SCI and matched (gender, age) noninjured controls (42.7 ± 5.4 years) using the Lokomat, Manual Treadmill, and ZeroG. The VO2000, Polar Heart Rate (HR) Monitor, and lower limb electromyography (EMG) electrodes were worn during the 2-minute sessions. Oxygen uptake (VO_2) and HR were expressed as percentage of peak values obtained using progressive arm ergometry; VO_2 was also expressed relative to resting metabolic equivalents (METS). Filtered EMG signals from tibialis anterior (TA), rectus femoris (RF), biceps femoris (BF), and medial gastrocnemius (MG) were normalized to ZeroG stepping. The Lokomat required 30% of VO_2 peak (2METS) compared to ~54% (3METS) for Manual Treadmill and ZeroG sessions. HR was 67% of peak during Lokomat sessions compared to ~83% for Manual Treadmill and ZeroG. Muscle activation was higher in treadmill conditions compared to the ZeroG primarily due to increased BF activity. At the same level of BWS, locomotion using the Manual Treadmill or the ZeroG is more aerobically demanding than the Lokomat. Treadmill modalities encourage greater hip extensor activation compared to overground locomotion.

1. Introduction

Body weight supported locomotor training (e.g., treadmill) is a modern approach to spinal cord injury (SCI) rehabilitation, which provides an interactive, task-specific training environment that is believed to promote "rewiring" of synaptic connections [1–3]. The amount of loading experienced by an individual is manipulated in an attempt to compensate for uncontrolled spinal reflexes and motor losses associated with the injury. In doing so, these interventions offer the possibility of including gait retraining earlier in rehabilitation programming. Research suggests that the eventual transfer to unsupported overground walking is limited to those with incomplete SCI (American Spinal Injury Association Scale (AIS) C-D) as they benefit from retained brain-body connections, particularly with the cerebellum [4]. Presently, there are a variety of training devices available for individuals to consider using during rehabilitation (Figure 1). Alexeeva and colleagues [5] suggest that an effective intervention to improve locomotor ability in this subpopulation is overground locomotor training with 30% body weight support (BWS) that takes place 1 hour per day, 3 times per week, for 10 weeks in duration. It is important to note, however, that *optimal* training strategies to enhance locomotor function have yet to be established for individuals with incomplete SCI.

Locomotion targets the lower limbs and has an associated metabolic cost, which can be reduced by unloading an individual through the use of a harness. Following treadmill training, normalization of the gait pattern is possible allowing individuals to become more efficient at completing the task of walking [6, 7]. In fact, there is evidence to suggest metabolic cost decreases by as much as 68% following training in individuals with SCI [8]. To our knowledge, only one study [9] has *simultaneously* collected metabolic and EMG measurements during robotic and therapist assisted treadmill locomotion in individuals with incomplete SCI.

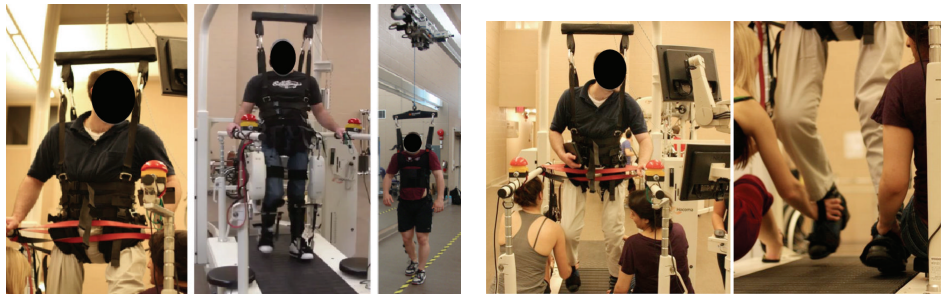

(a) (b)

Figure 1: (a) Body weight supported training devices used during walking sessions; from left to right: Manual Treadmill, Lokomat, and ZeroG. All devices provided body weight support (BWS) through a harness. The Andago GmbH treadmill (Loko) was used for robotic assisted (Lokomat) and unassisted (Manual Treadmill) walking sessions. The ZeroG had a custom series elastic actuator that traveled along an overhead trolley, which provided dynamic BWS while individuals performed overground walking sessions. (b) Manual Treadmill sessions normally completed with therapist assistance (not provided in this study) at both legs. The Andago GmbH treadmill is used during these sessions without the robotic orthosis providing individuals with greater degrees of freedom during training.

These researchers determined that *voluntary* effort is required during robotic-assisted locomotion to achieve metabolic costs and hip flexor activity similar to those associated with therapist-assisted locomotion. It was suggested that therapist-assisted treadmill training programs should be used as progressions from robotic-assisted sessions.

The purpose of this study was to investigate oxygen demand and muscle activation patterns at the *same* level of BWS while individuals with incomplete SCI completed a locomotor training session using (a) the treadmill with robotic assistance (Lokomat), (b) the treadmill *without* therapist assistance (Manual Treadmill), and (c) an overground training system (ZeroG). It was hypothesized that the highest levels of oxygen uptake and muscle activation would occur during locomotion using the ZeroG and this would be higher in persons with incomplete SCI versus gender and age matched able-bodied adults.

2. Methods

2.1. Participants. Adults (18–65 years of age) with SCI were eligible to participate if their injury was (a) chronic (1 + year) or (b) incomplete (AIS C-D, sensory and/or motor function at S4/5) and (c) if they could comfortably complete walking sessions using the Andago GmbH treadmill (Loko, Germany) with manual and robotic (LokomatPro, Hocoma, Switzerland) assistance, as well as overground using the ZeroG (ZeroG; Aretech, LLC, Ashburn, VA). Each participant with a SCI was gender and age (±5 years) matched to an able-bodied adult, who served as the control group. For the ZeroG session, participants were required to be able to walk with less than or equal to 68 kg (150 lbs) offset, as this was the maximum amount of dynamic BWS (constant rope tension) the machine could provide. Participants did not consume any food (except water) in the four hours preceding testing and did not consume caffeine or alcohol or participate in strenuous exercise in the 24 hours prior. Familiarization with the laboratory environment, equipment, and test procedures occurred during prescreening. Written informed consent was obtained from all participants with a protocol approved by the McMaster Research Ethics Board.

2.1.1. Baseline Assessments. At the first session, demographic and anthropometric measures of height (cm) and weight (kg) were recorded. Lower length measurements were taken to properly fit individuals to the Lokomat and individuals were fitted to harnesses for the respective devices. The amount of BWS to be used for all walking sessions was determined to be the percentage of body weight offset that allowed individuals to take steps using the ZeroG without excessive knee flexion.

Participants performed a VO_2 peak test to volitional fatigue on an electronically braked arm ergometer (Angio V2; Lode BV, Groningen, The Netherlands) using a previously described protocol [10]. Oxygen uptake (AEI Metabolic System (Moxus) software, Pittsburgh, PA) and heart rate (Polar T31 Heart Rate Monitor; Polar Electro Inc., Woodbury, NY, USA) were sampled at 30-second epochs and rating of perceived exertion (RPE) using Borg's 0–10 scale [11] was assessed every minute to gauge subjective perception of physical effort both centrally (heart and breathing) and peripherally (arms).

Following peak arm ergometry testing, participants were strapped into the robotic limbs of the Lokomat and completed maximal lower limb isometric strength measures of hip and knee flexion/extension using the L-FORCE v2.0 software module (Lokomat System V5.0). The L-FORCE v2.0 has been technically and clinically validated [12].

2.1.2. Body Weight Supported Walking Sessions. The subsequent 3 body weight supported walking sessions all used the same amount of support that had been established at the first session using the ZeroG (see *Baseline Assessments*). Participants completed walking trials in a *randomized* order using the Andago GmbH treadmill system (with or without the Lokomat) or overground ZeroG. EMG electrodes (Delsys Trigno Wireless EMG Surface Electrodes, Delsys, Boston, MA) were placed on tibialis anterior (TA), rectus femoris (RF), biceps femoris (BF), and medial gastrocnemius (MG)

muscles of both legs. Footswitches (Delsys Wireless Force Sensitive Resistors, Delsys, Boston, MA) were placed on the bottom of both feet (sensor on base of first toe and calcaneus, resp.) to synchronize the muscle activation signals with heel strike as the subject walked. The subjects put on a Polar HR Monitor and then were fitted to the appropriate harness and device settings based on the prescreening evaluation and randomization order. Then the participant was attached to the portable metabolic cart (MedGraphics V02000, Medical Graphics Corp., St. Paul, MN) using the patented preVent mask. Resting measures (5 minutes) were taken before and after each walking session; oxygen uptake (sampled in 30-second epochs), HR, and brachial blood pressure were recorded at 1, 3, and 5 minutes. Participants walked at a comfortable self-selected speed at the same level of BWS regardless of the device until steady state exercise conditions (stabilized oxygen uptake and heart rate values; ±5 mL/kg/min and ±5 BPM, resp.) were achieved (~2 minutes). Participants were then asked to complete additional 2 minutes of steady state walking to allow for collection of oxygen uptake, HR, RPE, and muscle activity. Oxygen uptake and HR were recorded at 30-second epochs and RPE (central and peripheral; anchored to VO_2 peak test) using Borg's 0–10 scale was monitored every minute. Muscle activity was continuously monitored throughout steady state walking sessions and collected using EMGworks Acquisition software program (Delsys EMGworks 4.0, Delsys, Boston, MA). For the Lokomat walking trial, all participants were asked to contribute as much as possible to the "walking motion"; the Guidance Force Control system was set to 100% for all sessions indicating full robotic assistance. When the robotic orthosis was not used, participants stepped on the treadmill *without* assistance and no corrections were made by assisting therapists to normalize stepping patterns. Participants were allowed to use the bilateral handrails on the treadmill to maintain postural stability, although they were asked to minimize upper-extremity weight bearing. Following all sessions, regardless of randomization order, participants were required to take a couple of steps using the ZeroG in order to have muscle activity data to normalize and control for potential day-to-day variation in EMG signal conduction and/or electrode placement. For all walking trials, able-bodied participants completed 2-minute steady state sessions (a) at baseline (0 BWS) and (b) at a percentage of BWS determined by their matched SCI participant (% BWS).

2.2. Data Analysis. MOXUS (AEI Metabolic System (Moxus) software, Pittsburgh, PA) and VO2000 (Medical Graphics Corp., St. Paul, MN) software programs were used for analysis of peak and walking VO_2 metabolic measures, respectively. Oxygen consumption during walking sessions using the Lokomat, Manual Treadmill, and ZeroG devices was expressed relative to resting metabolic equivalents (METS), which are considered 2.7 mL/kg/min and 3.5 mL/kg/min for SCI and CON, respectively [13]. EMGworks Analysis (Delsys EMGworks 4.0, Delsys, Boston, MA) was used for analysis and filtering of muscle activity signals; the rectified EMG records were low-pass filtered using a second order Butterworth filter.

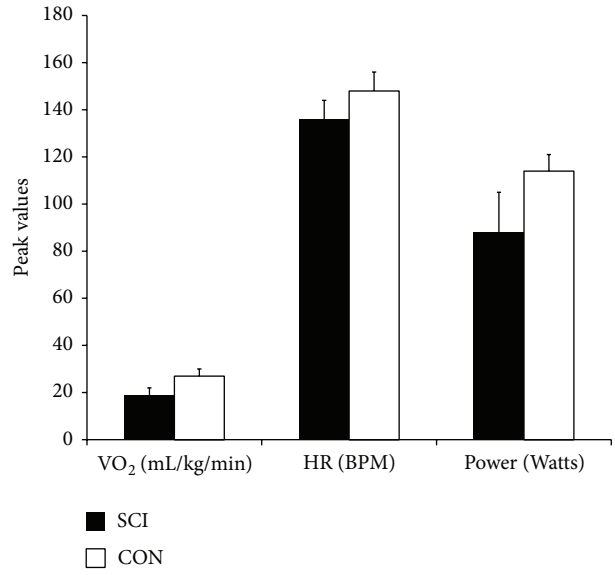

Figure 2: VO_2 peak test variables for SCI and CON. Relative VO_2 peak (mL/kg/min), peak heart rate (HR) expressed in beats per minute (BPM), and maximum power achieved (Watts). Values are mean ± SE.

2.2.1. Statistical Analysis. SPSS 17.0 (Chicago, IL) software program was used for statistical analysis of acquired data. The Shapiro-Wilk test was used to test for normality of the data due to the small sample size; nonparametric statistics were used where appropriate. Statistical significance was set at $P < 0.05$ for all analyses. Bonferroni's correction was used for post hoc testing when necessary. All reported values are expressed as mean ± standard error.

Repeated measures ANOVAs were conducted on the steady state cardiovascular data normalized to (a) resting (METS) and (b) VO_2 peak. Repeated measures ANOVAs were conducted on the filtered root mean square (RMS) muscle activity signals over 3 consecutive gait cycles normalized to ZeroG filtered activity signals at the *same* level of BWS for each given day. For CON, this analysis was completed for both baseline (0 BWS) and matched (% BWS) conditions. Bivariate correlations (Pearson) were conducted for participants with SCI to investigate potential relationships between the amount of required BWS and flexion: extension isometric strength at the hip and knee, respectively. One-way ANOVAs were used to look at differences between SCI and CON.

3. Results

3.1. Baseline Assessments. Seven individuals with incomplete SCI and seven gender-and-age matched controls participated in the study. No significant differences were found between SCI and CON with respect to demographic or aerobic peak measures from the arm ergometer test (Table 1, Figure 2). The average amount of BWS that was used for the walking sessions

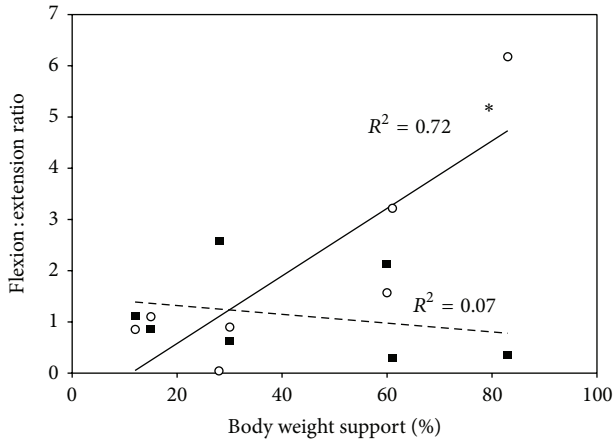

Figure 3: Relationship of the lower limb flexion: extension strength ratios (at the hip and knee) determined using LForce on the Lokomat with the percentage of body weight support (BWS) required for locomotion using the ZeroG in participants with SCI. Open circles and solid line indicate the relationship at the *hip*. Closed squares and dashed line indicate the relationship at the *knee*. $P < 0.05 = *$.

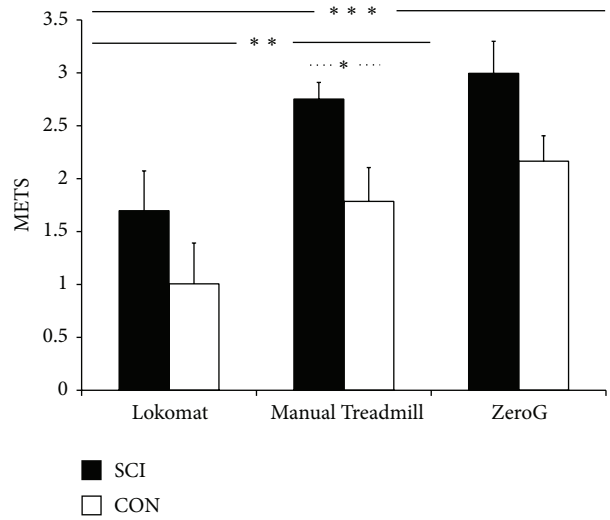

Figure 4: Metabolic equivalents (METS) for SCI and CON during locomotion with body weight support (BWS). Solid line indicates significance between *device* comparisons, and dashed line indicates significance between *group* comparisons. $P < 0.05 = *$, $P < 0.01 = **$, and $P < 0.001 = ***$.

was 41.3% ± 10.16% (Table 1). A strong positive correlation ($R^2 = 0.72$) was found between the flexion: extension strength ratio at the hip in participants with SCI and the amount of BWS required to complete the overground walking session; the higher the flexion: extension ratio, the more support that was required (Figure 3). The greater contributor to this relationship at the hip joint was the decrease in isometric hip extension strength compared to flexion strength ($R^2 = -0.69$ versus $R^2 = -0.36$).

3.2. Body Weight Supported Walking Sessions. All 7 matched pairs completed the Manual Treadmill and ZeroG walking sessions; one participant in the SCI group did not complete the Lokomat walking session due to spasticity (exaggerated stretch reflexes). All participants reached steady state within 2 minutes of walking.

3.2.1. Aerobic Demand Expressed Relative to Resting Values. Lokomat sessions resulted in significantly lower MET values when compared to the Manual Treadmill or ZeroG sessions (Figure 4). The highest MET values were attained during ZeroG walking, although these were not statistically different compared to the Manual Treadmill, for both SCI and controls (3.0 ± 0.30 versus 2.8 ± 0.16 and 2.2 ± 0.24 versus 1.8 ± 0.32, resp.). Individuals with SCI achieved a significantly higher MET value compared to CON during the Manual Treadmill session (2.8 ± 0.16 versus 1.8 ± 0.32).

3.2.2. Aerobic Demand Expressed Relative to Peak Values. Cardiovascular measures were expressed relative to percentage of peak values obtained during the arm ergometer test (Figure 5).

VO_2. The Lokomat session was significantly less demanding compared to the Manual Treadmill and ZeroG sessions (e.g., 30.1% ± 10.06% versus 52.9% ± 17.60% versus 54.7% ± 16.42%, resp.) for participants with SCI (Figure 5(a)). Differences between groups existed during the Lokomat session only, with participants with SCI requiring a significantly greater percentage of peak VO_2 compared to CON (30.1% ± 10.06% versus 14.4% ± 6.32%).

HR. Lokomat sessions resulted in significantly lower HRs (expressed as a percentage of peak) in comparison to the Manual Treadmill or ZeroG sessions (e.g., 67.3% ± 4.77% versus 80.8% ± 1.95% versus 84.7% ± 3.03%, resp.) for participants with SCI (Figure 5(b)). Individuals with SCI achieved a significantly higher percentage of peak HR values compared to CON during all 3 walking sessions (average of 77.7% ± 3.57% versus 52.3% ± 1.09% across trials).

RPE. Lokomat sessions were perceived to be significantly less demanding when compared to the Manual Treadmill or ZeroG sessions (e.g., central RPE: 0.5 ± 0.19 versus 3.7 ± 1.28 versus 3.8 ± 1.14; peripheral RPE: 0.7 ± 0.18 versus 4.1 ± 0.64 versus 5.1 ± 1.18) for participants with SCI. Additionally, individuals with SCI perceived the Manual Treadmill and ZeroG sessions to be significantly more demanding compared to CON (e.g., central RPE: 3.7 ± 1.28 versus 0.9 ± 0.14; 3.76 ± 1.14 versus 1.0 ± 0.00; peripheral RPE: 4.1 ± 0.64 versus 0.9 ± 0.86; 5.1 ± 1.18 versus 1.0 ± 0.00).

3.2.3. Muscle Activity Expressed Relative to Walking While Using the ZeroG. Nonstatistically significant differences in muscle activity gait parameters were found between the three devices (Figures 6 and 7). For individuals with SCI, average muscle activation tended to be higher for both treadmill conditions compared to the ZeroG session, which could be attributed to increases in TA and BF activity. Conversely,

Table 1: Demographic variables for SCI and CON.

	SCI		CON		Between groups (P-value)
	Mean ± Standard error	Range	Mean ± Standard error	Range	
Age (years)	42.6 ± 4.29	23–55	42.7 ± 5.40	20–58	0.98
Height (cm)	179.1 ± 1.56	173–184	177.5 ± 2.91	168–190	0.84
Weight (kg)	89.6 ± 6.39	81.2–107.6	84.8 ± 5.88	69.4–112.1	0.52
BMI (kg/m^2)	27.9 ± 2.03	20.6–36	26.1 ± 1.46	20.6–31.1	0.48
BWS (kg)	37.8 ± 9.62	10–68	32.8 ± 7.40	10–68	0.67
BWS (%)	41.3 ± 10.16	12–83	41.3 ± 10.16	12–83	1.00
Time since injury (years)	4.0 ± 0.62	2–7	N/A		N/A

SCI: incomplete spinal cord injury; CON: matched controls; BMI: body mass index; BWS: body weight support.

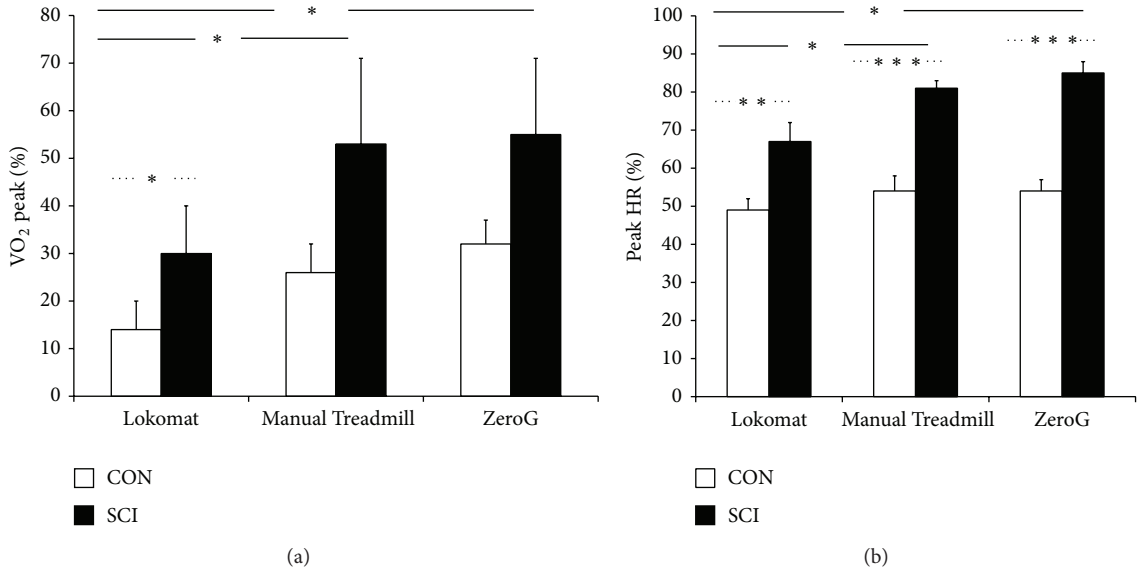

Figure 5: Cardiovascular measures ((a) VO_2, (b) HR) during locomotion with body weight support (BWS) expressed as percentage of peak values obtained from the arm ergometer test. Solid line indicates significance between *device* comparisons, and dashed line indicates significance between *group* comparisons. $P < 0.05 = *$, $P < 0.01 = **$, and $P < 0.001 = ***$.

the ZeroG session tended to require greater muscle activation compared to the treadmill sessions for CON. The only statistically significant difference between groups occurred during the Lokomat session, which elicited greater relative TA activation for participants with SCI compared to CON (128.3% ± 35.07% versus 36.0% ± 8.22%).

4. Discussion

The main objective of this study was to compare physiological responses during 2 minutes of steady state locomotion at the *same* level of BWS while using the Lokomat, Manual Treadmill, and ZeroG. It was hypothesized that ZeroG locomotion would be the most physiologically demanding session for individuals with incomplete SCI as it most resembles unsupported overground walking. As expected walking sessions were physiologically more demanding for individuals with SCI compared to CON. Contrary to what was hypothesized, both the Manual Treadmill and ZeroG sessions were considered significantly more demanding compared to the Lokomat, with no significant differences between the two sessions.

4.1. Baseline Assessments. VO_2 peak values obtained from the men with incomplete SCI (1.7 ± 0.27 L/min) were compared to normative physical capacity values. There was no difference in VO_2 peak between individuals with paraplegia or tetraplegia whose capacities were fair and excellent, respectively, based on the literature [14]. Peak VO_2 values from able-bodied participants (2.2 ± 0.15 L/min) were similar to those reported by van Loan and colleagues [15] (2.1 L/min) and more recent unpublished data from our lab (2.4 L/min). Interestingly, the peak aerobic data in this study was similar between the two groups, which are contrary to other studies indicating that those with SCI usually obtain lower values [16] due to a decreased amount of active muscle mass and sympathetic tone limiting venous "muscle pumping" action and the ability to increase oxygen uptake [17]. Zwiren and

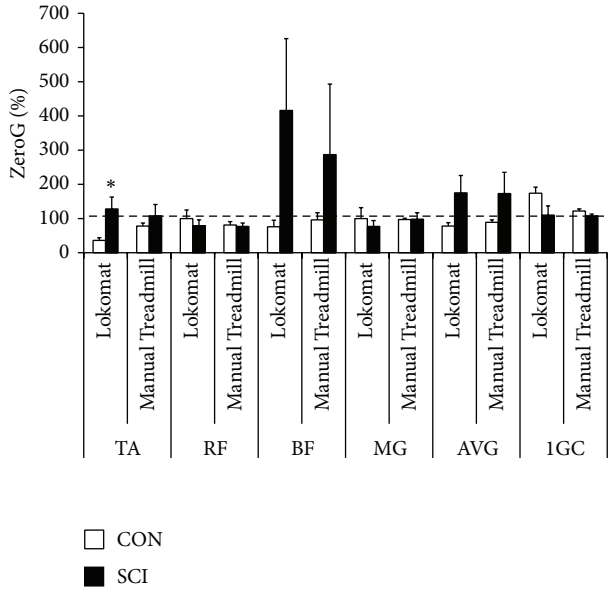

Figure 6: Muscle activity of independent muscle groups during treadmill locomotion with body weight support (BWS) normalized to ZeroG stepping with the same BWS. TA indicates tibialis anterior, RF indicates rectus femoris, BF indicates biceps femoris, MG indicates medial gastrocnemius, AVG indicates average muscle activity over a gait cycle, and 1GC indicates gait cycle completion time. Dashed line at 100 = value obtained while walking on the ZeroG. Statistically significant between group (SCI versus CON) comparisons $P < 0.05 = *$.

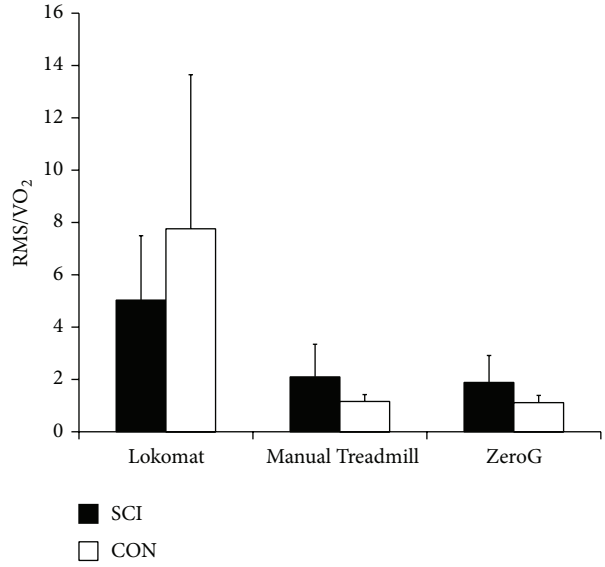

Figure 7: Ratio of root mean square (RMS) muscle activity across all muscle groups (μV) to oxygen uptake (%VO_2 peak) between devices for SCI and CON. Mean ± standard error.

Bar-Or [18], however, found no significant differences in VO_2 max in matched wheelchair-active and normal active subjects, suggesting that conditioning levels of the participants in the current study may have been more similar than typically expected (e.g., two participants with SCI were competitive athletes).

We used the L-Force module in the Lokomat to assess lower extremity isometric strength of the hip and knee. The reduced hip extension and knee flexion strength measures obtained from participants with SCI compared to CON are in agreement with previous studies which suggest that this population has difficulty voluntarily activating muscle below the lesion level making weight bearing and toe-clearance during gait difficult [19]. Further investigation into the flexion: extension strength ratio at both the hip and knee determined that a positive correlation existed between flexion: extension strength at the hip (primarily due to a reduction in hip extensor isometric strength) and the percentage of BWS required to complete an overground walking session using the ZeroG. The importance of the hip extensors for locomotion is in agreement with a study by Yang and colleagues [20], who found that manual muscle testing scores for the hamstrings in addition to the quadriceps were the strongest predictors of responsiveness to body weight supported gait training. In fact, responders on average had twice the volitional muscle strength as that of nonresponders. Whether the isometric strength measures obtained from the L-Force module of the Lokomat are able to predict responsiveness to body weight supported gait training, however, requires further investigation. This may provide a useful tool to therapists in terms of exercise prescription, determining readiness for locomotor training, as well as monitoring rehabilitation progression.

4.2. Randomized Body Weight Supported Sessions

4.2.1. Body Weight Support. The average amount of BWS used during the walking sessions was 41.3%, with only three of the seven participants with SCI able to complete walking sessions with the recommended less than 30% BWS [1]. These lower levels of support have been shown to better resemble independent overground walking patterns while allowing individuals to better maintain upright posture.

4.2.2. Metabolic Demand. Previous research has indicated the robotic orthosis results in lower metabolic costs (approximately 20%) compared to the Manual Treadmill [21], with the potential to minimize these differences if the participant is encouraged to exert maximal effort [9]. In this study, despite encouraging participants to maximally contribute to the walking motion in all walking conditions differences in metabolic costs were evident, with the Lokomat resulting in the lowest metabolic demand (approximately 23.8% of VO_2 peak for the SCI group) compared to the Manual Treadmill and ZeroG sessions, which had similar oxygen costs. While this may suggest that perhaps participants were not providing maximal efforts during these sessions, it is also important to note that in order to standardize walking conditions between participants 100% Guidance Force was set on the robotic orthosis which may have limited the ability for our participants to exert a maximal effort. Further, the study

by Israel and colleagues [9] provided therapist assistance during treadmill sessions, an option that was not provided for participants in this study. Other features of the Lokomat that could have contributed to the differences in metabolic costs include posterior support assisting with forward propulsion and stability at the pelvis and trunk. The evidence from this study suggests that the use of the robotic orthosis is not entirely passive, with increases in oxygen uptake evident during training sessions, which according to Krewer and colleagues [22] can be attributed to loading during stance phase resulting in associated muscle activation.

In order to complete a walking session using the overground device at the same level of BWS, the participants with SCI required three times resting metabolic rate while their matched controls only required double. The walking sessions completed with the ZeroG and Manual Treadmill sessions required greater than 50% of VO_2 peak values for the SCI group (e.g., 55% and 53% of VO_2 peak, resp.). This would suggest that walking using the aforementioned devices may be above the anaerobic threshold [23, 24] for people with SCI, resulting in reduced endurance and earlier onset of fatigue. In contrast, the ZeroG and Manual Treadmill sessions required only 32% and 26% of peak oxygen uptake for the CON group. This is consistent with evidence obtained by Waters and colleagues [25] who found that individuals without mobility impairments require minimal effort during walking with rates of oxygen consumption of 30% of maximum aerobic capacity. The similarity in oxygen costs between the treadmill session without the robotic orthoses and the overground walking session in CON is in agreement with evidence in able-bodied populations which suggest that no significant differences exist in energy expenditure between treadmill and overground walking at controlled velocities [23]. It is important to note that walking velocity in this study was not controlled, although all participants received the same instruction to walk at a comfortable speed. Oxygen uptake while walking overground in this study was 41.8% higher in SCI compared to noninjured adults, which is similar to earlier work which found the rate of oxygen uptake while walking to be 38% higher in SCI compared to CON [26]. In the present study individuals with incomplete SCI had 36.5% higher HR compared to CON during overground walking sessions which is slightly greater than the 24% greater increase found during walking by Teixeira da Cunha-Filho and colleagues [27].

4.2.3. Muscle Activity. Muscle activity for SCI tended to be greater with the treadmill than the ZeroG due to increases in TA and BF activity. For the SCI group, the "foot lifters" used with the Lokomat may have provided afferent feedback to the spinal cord during gait encouraging dorsiflexion. Evidence from this study supports this as Lokomat sessions resulted in greater TA activation in SCI compared to CON. While the "foot lifters" used with the robotic orthosis may have provided beneficial feedback for the SCI group, reduced EMG activity of TA during gait in the CON group may have occurred using this same device as the foot lifters may have inhibited normal activation of this muscle group.

It has been suggested that muscles with greater cortical projections such as TA and more proximal muscles such as the hamstrings [28] are the most affected in individuals with SCI following body weight supported training [29]. Improved hip extension with training is common with treadmill training as the belt encourages hip extension forcing individuals to "pull up" (e.g., increasing knee flexion) during swing. The large variability in BF activation in this study may be an indicator of potential responders to body weight supported training. Gorassini and colleagues [7] showed increased TA and hamstring muscle activation during treadmill walking only in responders. While responders increased amplitude of hamstring activity, burst duration decreased resulting in less cocontraction with quadriceps activation. Thus, the ability to modify muscle activation patterns after SCI may predict responsiveness to training.

Unlike the SCI group, muscle activity for CON tended to be greater with overground sessions rather than treadmill sessions, as well as having higher TA activation during supported Manual Treadmill versus Lokomat sessions. Muscular work associated with forward propulsion is thought to be a primary determinant of the metabolic costs of walking in subjects without neurological injury [9] which would be greater when using the ZeroG compared to the treadmill sessions, especially when the robotic orthosis is used. As previously mentioned, "foot lifters" used with the robotic orthosis may have inhibited normal activation of TA for the CON group, resulting in the obtained differences between the two treadmill modalities.

While both groups were able to successfully complete all walking sessions greater muscle activity was evident during treadmill sessions in the SCI group compared to during ZeroG sessions for the CON group. This may provide evidence in support of the idea of motor equivalence [30]. Essentially this principle suggests that a given motor task goal (e.g., walking) can be achieved using different muscle synergies. This is advantageous for individuals with lesions to the spinal cord as they can take advantage of the redundancies of the neuromuscular system to accomplish motor tasks. For example, individuals with SCI may require use of their arms and/or axial muscles for support during swing phase, essentially completing the same phase of gait but at a greater energy cost due to the involvement of additional musculature. As an individual progresses with training, neuronal coupling of movement (e.g., incorporation of arm swing) will provide additional sensory feedback to help generate temporally appropriate muscle activity patterns [31]. From a therapeutic perspective, therefore, body weight supported training interventions help individuals to learn to produce new motor strategies in a controlled setting with the hopes of transferring this rehearsed pattern to unsupported overground walking.

4.3. Limitations. The number of participants in this study was arguably small; however, the inclusion criteria of having the ability to take independent steps using the ZeroG limited the available sample pool. Therefore, the generalizability of these findings may be applicable only to individuals with higher levels of motor function following an incomplete SCI.

It has been demonstrated in the literature that gait kinematics similar to baseline walking (0% BWS) can be maintained when 30 percent or less support is provided [5]. Recent work from our lab, specifically looking at changes in muscle activation with increased amounts of BWS using the ZeroG in able-bodied adults, found significant reductions in muscle activity when 40 or more percent of body weight was offset by the device without altering the muscle activation pattern during gait [31]. It is important to note that 3 of the 7 participants with incomplete SCI would have been unable to independently complete the walking sessions if <40% BWS was provided on the ZeroG. Whether these individuals can obtain the recommended ranges of support with training is an area of future investigation and will help determine if the comparison between devices is minimized at lower levels of support.

The Lokomat was programmed to provide maximal assistance to the legs during all phases of gait (e.g., 100% Guidance Force) in order to standardize the Guidance Force, therefore these results are only relevant to Lokomat sessions completed under these conditions. It is anticipated that decreasing the Guidance Force will increase physiological demand; however, whether these changes result in statistically nonsignificant differences between the two treadmill conditions has yet to be determined.

Participants were allowed to use the treadmill handrails or the arms of the therapist during the overground session for balance but were discouraged to use them for weight bearing. Without the use of arm swing, individuals were unable to take advantage of neuronal coupling, which may have influenced lower extremity muscle activity [32]. While attempts were made to ensure consistent upper-extremity use across stepping conditions no objective measures of force (e.g., force plates on handrails) were made to ensure this.

Finally, the inability to control walking speed, particularly with respect to the overground walking session, may have influenced the results obtained, as reduced speed has been associated with increased signal variability and decreased muscle activation. According to Winter [33], changes in walking speed affect the acceleration of lower limbs during gait, primarily activity at the hip and knee versus the ankle. Therefore, while our EMG recordings may have been differentially affected by not having control over this factor (e.g., RF and BF greater than TA and MG), it would have been close to impossible to control walking speed during the ZeroG sessions.

5. Conclusions

The objective of this study was to compare oxygen demand and muscle activation between the Lokomat, Manual Treadmill, and ZeroG. Consistent with our hypothesis, walking sessions were more demanding for participants with SCI compared to CON. Contrary to our hypothesis the ZeroG was not considered the most physiologically demanding session, with both the ZeroG and Manual Treadmill sessions eliciting significantly greater VO_2 values compared to the Lokomat. In addition, contrary to what was expected, the ZeroG did not elicit significantly greater lower limb muscle activity in the four muscle groups included in this investigation. The evidence from this study would suggest a benefit to using the Lokomat to work on isolated hip extension strength. Therapists can take advantage of the feedback system of the device, the greater BF activation of this treadmill-based exercise, as well as having the ability to conduct longer sessions due to the decreased cardiovascular and muscular demands imposed on the patient using the robotic device. The Manual Treadmill and ZeroG should then be used as more intense progressions where hip extension can continue to be encouraged while using the treadmill and additional components of gait (e.g., balance and torso stability) can be focused on while using the overground device.

Abbreviations

ADL:	Activities of daily living
ANOVA:	Analysis of variance
AIS:	American Spinal Injury Association Impairment Scale
BF:	Biceps femoris
BMI:	Body mass index
BPM:	Beats per minute
BWS:	Body weight support
CON:	Able-bodied controls
EMG:	Electromyography
HR:	Heart rate
MET:	Metabolic equivalent
MG:	Medial gastrocnemius
RF:	Rectus femoris
RMS:	Root mean square
ROM:	Range of motion
RPE:	Rating of perceived exertion
SCI:	Spinal cord injury
TA:	Tibialis anterior
VO_2:	Metabolic rate of oxygen consumption.

Conflict of Interests

The authors declare that there is no conflict of interests regarding the publication of this paper.

Authors' Contribution

Alyssa M. Fenuta (M.S. degree) and Audrey L. Hicks (Ph.D. degree) collaborated in designing the study. A. Fenuta was responsible for testing the participants and analyzing the data under Dr. Hicks' supervision. Finally, A. Fenuta compiled the paper with Dr. Hicks providing editorial guidance.

Acknowledgment

This study was supported by an ONF-REPAR partnership grant.

References

[1] A. M. Fenuta and A. L. Hicks, "Body weight-supported treadmill training after spinal cord injury: is there an ideal prescription for intervention?" *Critical Reviews in Physical and Rehabilitation Medicine*, vol. 23, no. 1–4, pp. 1161–4174, 2011.

[2] H. Barbeau and S. Rossignol, "Recovery of locomotion after chronic spinalization in the adult cat," *Brain Research*, vol. 412, no. 1, pp. 84–95, 1987.

[3] V. Dietz and S. J. Harkema, "Locomotor activity in spinal cord-injured persons," *Journal of Applied Physiology*, vol. 96, no. 5, pp. 1954–1960, 2004.

[4] P. Winchester, R. McColl, R. Querry et al., "Changes in supraspinal activation patterns following robotic locomotor therapy in motor-incomplete spinal cord injury," *Neurorehabilitation and Neural Repair*, vol. 19, no. 4, pp. 313–324, 2005.

[5] N. Alexeeva, C. Sames, P. L. Jacobs et al., "Comparison of training methods to improve walking in persons with chronic spinal cord injury: a randomized clinical trial," *Journal of Spinal Cord Medicine*, vol. 34, no. 4, pp. 362–379, 2011.

[6] V. Dietz, "Body weight supported gait training: from laboratory to clinical setting," *Brain Research Bulletin*, vol. 76, no. 5, pp. 459–463, 2008.

[7] M. A. Gorassini, J. A. Norton, J. Nevett-Duchcherer, F. D. Roy, and J. F. Yang, "Changes in locomotor muscle activity after treadmill training in subjects with incomplete spinal cord injury," *Journal of Neurophysiology*, vol. 101, no. 2, pp. 969–979, 2009.

[8] E. J. Protas, S. A. Holmes, H. Qureshy, A. Johnson, D. Lee, and A. M. Sherwood, "Supported treadmill ambulation training after spinal cord injury: a pilot study," *Archives of Physical Medicine and Rehabilitation*, vol. 82, no. 6, pp. 825–831, 2001.

[9] J. F. Israel, D. D. Campbell, J. H. Kahn, and T. G. Hornby, "Metabolic costs and muscle activity patterns during robotic- and therapist-assisted treadmill walking in individuals with incomplete spinal cord injury," *Physical Therapy*, vol. 86, no. 11, pp. 1466–1478, 2006.

[10] A. T. Hol, J. J. Eng, W. C. Miller, S. Sproule, and A. V. Krassioukov, "Reliability and validity of the six-minute arm test for the evaluation of cardiovascular fitness in people with spinal cord injury," *Archives of Physical Medicine and Rehabilitation*, vol. 88, no. 4, pp. 489–495, 2007.

[11] G. Borg, "A category scale with ratio properties for intermodal and interindividual comparisons. Psychophysical Judgement and the process of perception," in *Proceedings of the 22nd International Congress of Psychology*, H. G. Geissler and P. Petzol, Eds., pp. 25–34, North Holland, Amsterdam, The Netherlands, 1980.

[12] M. Bolliger, L. Lunenburger, S. Bircher, G. Colombo, and V. Dietz, "Reliability of measuring isometric peak torque in the driven gait orthosis 'Lokomat'," *Neurorehabilitation & Neural Repair*, vol. 20, 2006.

[13] E. G. Collins, D. Gater, J. Kiratli, J. Butler, K. Hanson, and W. E. Langbein, "Energy cost of physical activities in persons with spinal cord injury," *Medicine and Science in Sports and Exercise*, vol. 42, no. 4, pp. 691–700, 2010.

[14] T. W. J. Janssen, A. J. Dallmeijer, D. Veeger, and L. H. V. van der Woude, "Normative values and determinants of physical capacity in individuals with spinal cord injury," *Journal of Rehabilitation Research and Development*, vol. 39, no. 1, pp. 29–39, 2002.

[15] M. D. van Loan, S. McCluer, J. M. Loftin, and R. A. Boileau, "Comparison of physiological responses to maximal arm exercise among able-bodied, paraplegics and quadriplegics," *Paraplegia*, vol. 25, no. 5, pp. 397–405, 1987.

[16] K. Cerny, R. Waters, H. Hislop, and J. Perry, "Walking and wheelchair energetics in persons with paraplegia," *Physical Therapy*, vol. 60, no. 9, pp. 1133–1139, 1980.

[17] W. T. Phillips, B. J. Kiratli, M. Sarkarati et al., "Effect of spinal cord injury on the heart and cardiovascular fitness," *Current Problems in Cardiology*, vol. 23, no. 11, pp. 641–716, 1998.

[18] L. D. Zwiren and O. Bar-Or, "Responses to exercise of paraplegics who differ in conditioning level," *Medicine and Science in Sports and Exercise*, vol. 7, no. 2, pp. 94–98, 1975.

[19] J. Ditunno and G. Scivoletto, "Clinical relevance of gait research applied to clinical trials in spinal cord injury," *Brain Research Bulletin*, vol. 78, no. 1, pp. 35–42, 2009.

[20] J. F. Yang, J. Norton, J. Nevett-Duchcherer, F. D. Roy, D. P. Gross, and M. A. Gorassini, "Volitional muscle strength in the legs predicts changes in walking speed following locomotor training in people with chronic spinal cord injury," *Physical Therapy*, vol. 91, no. 6, pp. 931–943, 2011.

[21] T. G. Hornby, C. R. Kinnaird, C. L. Holleran, M. R. Rafferty, K. S. Rodriguez, and J. B. Cain, "Kinematic, muscular and metabolic responses during exoskeletal-, elliptical-, or therapist-assisted stepping in people with incomplete spinal cord injury," *Physical Therapy*, vol. 92, pp. 1278–1291, 2012.

[22] C. Krewer, F. Müller, B. Husemann, S. Heller, J. Quintern, and E. Koenig, "The influence of different Lokomat walking conditions on the energy expenditure of hemiparetic patients and healthy subjects," *Gait and Posture*, vol. 26, no. 3, pp. 372–377, 2007.

[23] R. L. Waters and S. Mulroy, "The energy expenditure of normal and pathologic gait," *Gait and Posture*, vol. 9, no. 3, pp. 207–231, 1999.

[24] P. Cerretelli, G. Ambrosoli, and M. Fumagalli, "Anaerobic recovery in man," *European Journal of Applied Physiology and Occupational Physiology*, vol. 34, no. 3, pp. 141–148, 1975.

[25] R. L. Waters, H. J. Hislop, and J. Perry, "Comparative cost of walking in young and old adults," *Journal of Orthopaedic Research*, vol. 1, no. 1, pp. 73–76, 1983.

[26] R. L. Waters and B. R. Lunsford, "Energy cost of paraplegic locomotion," *Journal of Bone and Joint Surgery A*, vol. 67, no. 8, pp. 1245–1250, 1985.

[27] I. T. da Cunha-Filho, H. Henson, H. Qureshy, A. L. Williams, S. A. Holmes, and E. J. Protas, "Differential responses to measures of gait performance among healthy and neurologically impaired individuals," *Archives of Physical Medicine and Rehabilitation*, vol. 84, no. 12, pp. 1774–1779, 2003.

[28] B. Brouwer and P. Ashby, "Corticospinal projections to upper and lower limb spinal motoneurons in man," *Electroencephalography and Clinical Neurophysiology*, vol. 76, no. 6, pp. 509–519, 1990.

[29] P. R. Lucareli, M. O. Lima, F. P. S. Lima, J. G. de Almeida, G. C. Brech, and J. M. D'Andréa Greve, "Gait analysis following treadmill training with body weight support versus conventional physical therapy: a prospective randomized controlled single blind study," *Spinal Cord*, vol. 49, no. 9, pp. 1001–1007, 2011.

[30] R. Grasso, Y. P. Ivanenko, M. Zago et al., "Distributed plasticity of locomotor pattern generators in spinal cord injured patients," *Brain*, vol. 127, no. 5, pp. 1019–1034, 2004.

[31] A. Fenuta and A. L. Hicks, "Muscle activation during body weight-supported locomotion while using the ZeroG," *Journal*

of Rehabilitation Research and Development, vol. 51, no. 1, pp. 51–58, 2014.

[32] D. P. Ferris, H. J. Huang, and P.-C. Kao, "Moving the arms to activate the legs," *Exercise and Sport Sciences Reviews*, vol. 34, no. 3, pp. 113–120, 2006.

[33] D. A. Winter, "Biomechanical motor patterns in normal walking," *Journal of Motor Behavior*, vol. 15, no. 4, pp. 302–330, 1983.

Hindawi Publishing Corporation
BioMed Research International
Volume 2014, Article ID 904985, 11 pages
http://dx.doi.org/10.1155/2014/904985

Research Article

Kinematic Metrics Based on the Virtual Reality System Toyra as an Assessment of the Upper Limb Rehabilitation in People with Spinal Cord Injury

Fernando Trincado-Alonso,[1] Iris Dimbwadyo-Terrer,[1] Ana de los Reyes-Guzmán,[1] Patricia López-Monteagudo,[2] Alberto Bernal-Sahún,[2] and Ángel Gil-Agudo[1]

[1] *Biomechanics and Technical Aids Department, National Hospital for Spinal Cord Injury, Finca la Peraleda s/n, 45071 Toledo, Spain*
[2] *Indra Sistemas, Avenida de Bruselas, 33-35, Alcobendas, 28108 Madrid, Spain*

Correspondence should be addressed to Fernando Trincado-Alonso; fernandotrin@gmail.com

Received 27 December 2013; Revised 11 February 2014; Accepted 20 February 2014; Published 23 April 2014

Academic Editor: Alessandro De Mauro

The aim of this study was to develop new strategies based on virtual reality that can provide additional information to clinicians for the rehabilitation assessment. Virtual reality system Toyra has been used to record kinematic information of 15 patients with cervical spinal cord injury (SCI) while performing evaluation sessions using the mentioned system. Positive correlation, with a moderate and very strong association, has been found between clinical scales and kinematic data, considering only the subscales more closely related to the upper limb function. A set of metrics was defined combining these kinematic data to obtain parameters of reaching amplitude, joint amplitude, agility, accuracy, and repeatability during the evaluation sessions of the virtual reality system Toyra. Strong and moderate correlations have been also found between the metrics reaching and joint amplitude and the clinical scales.

1. Introduction

It has been estimated that the prevalence of spinal cord injury (SCI) is 223–755 per million inhabitants, with an incidence of 10.4–83 per million inhabitants per year [1]. Fifty percent of the patients with SCI are diagnosed as complete, and in one-third of the patients, the SCI is reported as tetraplegic.

In patients with tetraplegia, the arm and hand function is affected to a different degree, depending on the level and severity of the injury [2].

Several studies have shown that the improvement in upper extremity function is one of the greatest needs in patients with tetraplegia [3]. In this respect, therapy of the upper extremities in people with tetraplegia plays a key role during the rehabilitation.

Virtual reality (VR) has emerged in the rehabilitation context in an effort to promote task oriented and repetitive movement training of motor skills while using a variety of stimulating environments [4]. This approach can increase patient motivation, while extracting objective and accurate information enables the patient's progress to be monitored.

The aim of VR is to create a feeling of immersion within the simulated environment so that the patient's behaviour during the game resembles as much as possible the one that he would have in the real world.

There are different technologies of motion capture that permit the transfer of the actual movement of the patient to a virtual environment. One of them is the inertial measurement technology. There are several advantages of using inertial measurement systems (IMUs) as motion capture systems for VR applications, since they are compact, light, resistant to environmental interference, and easy to wear.

VR technology increases the range of possible tasks, partly automating and quantifying therapy procedures and improving patient motivation using real-time task evaluation and reward [5]. It also permits the standardization of tasks

and the recording of kinematic data during the execution of these tasks, making it an interesting tool for assessment of the rehabilitation progress.

Evaluation of the SCI patient's functional status is usually carried out by means of clinical scales, although they have a high subjective component depending on the observer who scores the test. Therefore, a better understanding of human movement requires more objective testing and accurate analysis of motion to describe the arm movements more precisely and specifically during functional testing. Kinematic analysis is one such method [6].

Clinical scales are not very sensitive to slight improvements in functionality and also they are not able to establish the biomechanical characteristics that explain the clinical changes in the scores obtained by the patients during their rehabilitation. Thus, it is important to find the kinematic parameters that correlate with clinical scales. In a previous study from our group, correlations were already found between kinematic data and clinical scales [7]. These scales inform about global disability, but they include specific items related to upper limb impairment. Therefore it seems relevant to go deeper in the analysis trying to obtain a more specific correlation between kinematics and functionality.

It is important to underline that kinematic data by themselves are not always sufficiently clear and understandable for clinicians in order to reliably evaluate a patient. However, combining them to obtain new metrics could enhance their potentiality as tools for physical assessment.

The objectives of the present study are (i) to analyze the correlations between kinematic data after performing upper limb tasks included in the VR system Toyra and upper limb clinical scales; (ii) to define kinematic metrics based on data recorded by the VR system Toyra that could offer additional information to clinicians; and (iii) to analyze the correlation between the defined kinematic metrics and clinical scales by applying them to a group of 15 patients with tetraplegia.

2. State-of-the-Art

2.1. Kinematic Metrics. Quantification of upper extremity movements has been researched since many years ago. One of the first studies in this field was carried out by Fitts in 1954 with the aim of analyzing the speed-accuracy trade-off and, as a result, calculating the performance and an index of difficulty of a task from three parameters: the time spent on performing the movement, the distance, and the size of the object to be reached [8].

The interest in obtaining parameters that could provide relevant information to clinicians from the quantification of the upper extremity movements is relatively recent. To this aim, there are some studies that analyzed the movements performed by patients with neurological disorders during reaching tasks and also while drawing [9–11]. There are also studies in which a basic activity of daily living (ADL) has been analyzed, such as the drinking task, in people with stroke [12] or SCI [13].

Some of the kinematic parameters calculated to obtain information that could be clinically relevant are the time spent on the task, velocity, and range of motion during the movement [6, 13, 14]; the correlation between shoulder and elbow joint angles, that indicates the coordination during reaching tasks [11–13]; and the number of peaks in the speed profile of the hand during the movement, with lower values indicating smoother trajectories [12].

In neurological rehabilitation, the assessment of upper limb motor recovery should include smoothness, efficacy, and efficiency of the movement [10]. In this study, metrics related to these characteristics of the movement have been proposed.

(i) Efficacy: the percentage of the task successfully completed by patient's voluntary movement.

(ii) Accuracy: the spatial deviation between the path followed by the patient's hand and the theoretical trajectory (in other studies it has been named "trajectory error").

(iii) Efficiency: it is a measure of the ratio between the length of the hand's path during the movement and the length of the theoretical trajectory.

(iv) Smoothness: it is computed from the speed profile of the hand during the movement as the number of peaks.

These metrics are more easily applicable to reaching movements in which the theoretical hand's path is considered as the straight line between the starting point and the target location.

Most of the metrics proposed are a measure of the error or deviation between two variables. So, for example, smoothness as the number of peaks is a measure of error, since a higher number of peaks are related to a less smooth movement. The same occurs in accuracy and efficiency metrics, in which a decrease in these metrics indicates an improvement in motor performance for a functional task. For that reason, it seems necessary to obtain parameters that could be directly proportional to the patient's functional status [15].

2.2. Clinical Scales. There are plenty of scales in the literature which pretend to assess the patients in order to detect functional changes during the upper limb rehabilitation process [16]. These assessment scales include grasping, holding, and manipulating objects, which require the recruitment and complex integration of muscle activity from shoulder to fingers.

The upper extremity motor function tests are classified in the following categories: (1) strength tests; (2) functional tests; and (3) ADL tests [17]. In this section, only the clinical scales that were used in this study and those that will be mentioned in the "Discussion" section are described.

2.2.1. Strength Tests. The evaluation of key muscle groups is important to identify the motor level in patients with tetraplegia. Motor index gives a rapid overall indication of a patient's limb impairment using principal components analysis (Hotelling's method), where the large number of movements was reduced to one movement at each joint which represented the general strength of movement at the joint [18].

2.2.2. Functional Tests. Jebsen Taylor Test of Hand Function [19] is a scale which pretends to assess the hand disability and improvement in hand function gained by therapeutic procedures in patients with hand disabilities, but due to the kind of activities proposed in the test it is necessary to have a relatively high degree of dexterity to complete it.

The Action Research Arm (ARA) test provides a rapid yet reliable and standardized performance test appropriate for use in assessing recovery of upper limb but it is solely used in stroke patients.

The Fugl-Meyer Assessment (FMA) was developed to measure sensorimotor stroke recovery based on Twitchell and Brunnstrom's concept of sequential stages of motor return in patients with hemiplegic stroke [20].

The Motor Activity Log (MAL) is a scripted, structured interview that was developed by Taub et al. to measure the effects of constraint-induced movement (CI) therapy on use of the more-impaired arm outside the laboratory in individuals with stroke [21].

2.2.3. ADL Tests. Two of the most used ADL evaluations for patients with tetraplegia are the functional independence measure (FIM) and the spinal cord independence measure II (SCIM II). These tests are validated and reliable and show strong correlation with each other [22].

The purpose of the FIM is the measurement of the severity of the patient's disability and the outcomes of medical rehabilitation in patients. The FIM has a good clinical interrater agreement in patients undergoing inpatient medical rehabilitation (ICC = 0.97). FIM scores were significantly lower in complete C4 tetraplegics than in C6 tetraplegics, which indicated that the FIM is sensitive enough to differentiate between different levels of injury [17].

The SCIM scale was developed specifically for SCI persons in order to make the functional assessments of persons with paraplegia or tetraplegia more sensitive to changes. The SCIM has a good interrater reliability ($r = 0.98$). Besides, the sensitivity of the SCIM is higher than the sensitivity of the FIM, showing in patients with tetraplegia that this scale missed 22% of the functional changes detected by the SCIM [17].

Regarding the kind of patients of this study, with a complete SCI at levels between C5 and C8, motor index, FIM, and SCIM tests were considered as the most suitable and, therefore, they have been chosen for this study.

3. New Assessment Metrics

3.1. Captured Raw Kinematic Data. For the kinematic capture process, a motion capture system based on inertial sensors, MTx Xsens Company (Xsens Inc., Netherlands), has been used. In this application, 5 inertial sensors were located on the head, trunk, arm, forearm, and hand. The placement of the sensors can be seen in Figure 1.

A biomechanical model was developed, previously reported, based on inertial sensor data and upper limb (UL) anthropometric data. The MTx includes triaxis accelerometers, gyroscopes, and magnetometers. As long as the inertial sensors only provide information on the orientation of each body segment, a biomechanical model is required to calculate the angular magnitudes of clinical relevance on the basis of each orientation. The kinematic model used was based on the Euler method; thus the results depend on the sequence of rotations used. The kinematic chain proposed in this model consists of 7 DoF: three in the shoulder joint (flexion-extension, abduction-adduction, and external-internal rotation); two in the elbow joint (flexion-extension and pronation-supination); and two in the wrist (palmar-dorsal flexion and radial-ulnar deviation). More details about this biomechanical model applied here have been previously described [23].

The kinematic assessment protocol consists of the execution of an Evaluation Session with the VR System Toyra. This session comprises 14 exercises whose principal objective is to assess the patient's functional capacity, based on the record of the kinematic variables during the execution of analytical movements of the UL joints in each of its degrees of freedom. The same therapist carried out the Evaluation Sessions on all patients in order to minimize the errors due to the different placements of the sensors by different therapists. In Figure 2, the position of a patient in front of the screen during the execution of a session with Toyra can be seen.

Joint ranges of motion (ROM) of shoulder, elbow, and wrist were analysed with the mathematics software tool MATLAB (Matrix House, Cambridge, UK), thus obtaining 14 different kinematic variables: step-by-step shoulder abduction (AbdshoulderS), complete shoulder abduction (AbdshoulderC), step-by-step shoulder flexion (FlexshoulderS), complete shoulder flexion (FlexshoulderC), shoulder rotation (Rotshoulder), step-by-step elbow flexion (FlexelbowS), complete elbow flexion (FlexelbowC), elbow extension (Extelbow), elbow supination (Supelbow), elbow pronation (Proelbow), wrist extension (Extwrist), wrist flexion (Flexwrist), wrist radial deviation (Raddevwrist), and wrist ulnar deviation (Uldevwrist). The "step-by-step" variables have been measured during exercises in which the goals that the patients have to reach appear on the screen sequentially from the bottom to the top of the screen in such a way that they have to perform discrete movements and stay in the object for one second, approximately, thus requiring a certain degree of control of the muscles involved in this movement, whereas for the "complete" variables, all goals are displayed at the same time, so that the patients perform a continuous trajectory. The reason to measure separately these two kinds of variables is that "step-by-step" movements require holding the arm in a fixed position, so that the patient needs to exert the task with greater control movement. Depending on the level of SCI, some patients can be able to perform complete movements but not the step-by-step ones.

Ranges of Motion (ROM) have been calculated from the 14 kinematic variables previously mentioned as the difference between the maximum and the minimum value reached by the patients during each specific exercise.

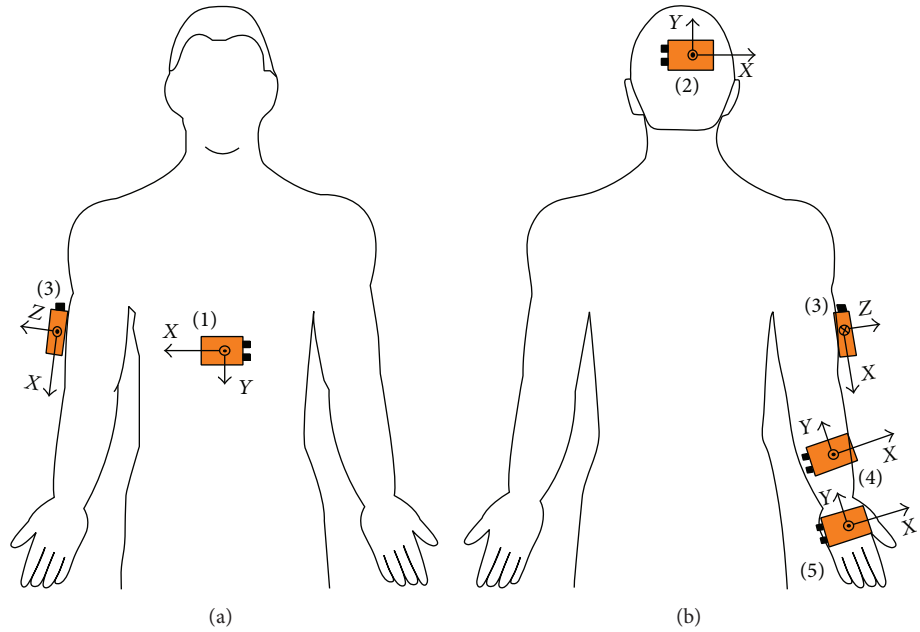

Figure 1: Placement of inertial sensors: (a) frontal view; (b) posterior view. The sensors were located on the trunk (1), the back of the head (2), the right arm (3), the forearm (4), and the hand (5) [23].

Figure 2: Patient performing a Toyra session.

3.2. New Kinematic Metrics. Five different metrics have been defined based on the kinematic data obtained during the Toyra sessions.

(i) Joint Amplitude. It has been defined as the sum of the ROMs obtained by a patient normalized by the corresponding ROM obtained by a healthy subject, defined as "ideal ROM":

$$\mathrm{JA} = \frac{\sum_{i=1}^{i=14} k_i \cdot \mathrm{ROM}_i}{\sum_{i=1}^{i=14} k_i \cdot \mathrm{idealROM}_i} \cdot 100\,[\%]\,, \tag{1}$$

where ROM_i (°) = degrees covered by the joint under study (it is important to remark that each exercise of the session has been designed to check the performance of a single joint. For example, the exercise of shoulder abduction will measure the shoulder's ability, despite the fact that some other joints are, to a lesser extent, also involved in this movement) and k_i = weighting coefficients of the exercises, chosen to give more importance to the ones that are more linked with the motor abilities of the patient.

(ii) Reaching Amplitude. It has been defined as the range that the patient is able to reach at the three different axes (X, Y, Z). The X-axis has been established horizontally, parallel to the screen, the Y-axis horizontally, perpendicular to the screen, and the Z-axis is vertical, parallel to the screen.

It is expected that, as long as a patient with SCI is able to reach further the objects that surround him, he would get more autonomy and functionality.

It is calculated at each axis as the difference between the maximum and the minimum value of the position of the patient's hand, getting a range of reaching for each exercise while the patient is carrying out the three-dimensional movements required by the task. Then, these ranges of reaching are summed and normalized by the sum of ranges obtained by a healthy subject. Finally, the three values obtained for each of the three axes are weighted according to their contribution:

$$\mathrm{RA} = \sum_{j=1}^{j=3} k_j \cdot \frac{\sum_{i=1}^{i=14} \max\left(h_{j_i}\right) - \min\left(h_{j_i}\right)}{\sum_{i=1}^{i=14} \max\left(\mathrm{ideal}\, h_{j_i}\right) - \min\left(\mathrm{ideal}\, h_{j_i}\right)} \cdot 100\,[\%]\,, \tag{2}$$

where k_j = weighting coefficient to assign to each axis a different contribution to the total reach amplitude and

h_{j_i} = trajectory of the hand's position at each axis j for each exercise i carried out by the patient. Ideal h_{j_i} = trajectory of the hand's position at each axis j for each exercise i carried out by a healthy subject.

Depending on the value assigned to k_j (where $j = 1$ the X-axis, $j = 2$ the Y-axis, and $j = 3$ the Z-axis), it is possible to compute the *reaching amplitude* separately for each direction.

(iii) Accuracy. It has been calculated considering 2 parameters: mean distance from the trajectory performed by the patient's hand to the ideal trajectory of the hand performed by a healthy subject (d_{mean}) and the maximum distance between these 2 trajectories (d_{max}). Consider

$$\text{Ac} = 100 - \sum_{i=1}^{i=14} 2 \cdot d_{\text{mean}_i} \cdot \left(1 + \frac{d_{\text{mean}_i}}{d_{\text{max}_i}}\right). \tag{3}$$

The idea of this formula is to penalize the accuracy of those trajectories that present several peaks of deviation in respect to the ideal trajectory. If they have a few peaks, d_{mean} will not be affected to a great extent by these peaks, so that $d_{\text{mean}} \ll d_{\text{max}}$, and thus the penalization for the accuracy would be approximately $2d_{\text{mean}}$.

However, if there are a lot of peaks of deviation, d_{mean} will be affected by these values, so that d_{mean} will increase. Consider as an example an extreme case in which there were so many peaks of deviation that $d_{\text{mean}} \approx d_{\text{max}}$; then the penalization for the accuracy would be $4d_{\text{mean}}$, much higher than in the previous case.

In order to obtain values in percentages, as in the previous metrics, accuracy has been normalized by the value of accuracy obtained by a healthy subject:

$$\text{Ac}_{\text{norm}} = \frac{\text{Ac}}{\text{Ac}_{\text{ideal}}} \cdot 100\,[\%]\,. \tag{4}$$

(iv) Agility. It has been considered that an agile movement should not only be fast but also precise. To this aim, this metric takes into consideration three parameters: accuracy (as defined in the previous metric), angular velocity, and time needed to execute the task. Consider

$$\text{Ag} = 100 - \sum_{i=1}^{i=14} \left(20 \cdot \left(d_{\text{mean}_i}/d_{\text{max}_i}\right) + 30 \cdot \left(v_{\text{max}_i}/v_{\text{mean}_i}\right) + 50 \cdot \left(t_i/t_{\text{ideal}_i}\right)\right) \times 100^{-1}, \tag{5}$$

where d_{mean_i} (m) = mean distance from the trajectory performed by the patient's hand to the ideal trajectory of the hand performed by a healthy subject, d_{max_i} (m) = maximum distance between the trajectory performed by the patient's hand and the ideal trajectory of the hand performed by a healthy subject, v_{max_i} (°/s) = maximum angular velocity of the joint under study in each exercise, v_{mean_i} (°/s) = mean angular velocity of the joint under study in each exercise, t_i (s) = time spent by the patient on performing the exercise i, and t_{ideal} (s) = time spent by a healthy subject on performing the exercise i.

The first term of the agility penalization is the one regarding the accuracy error and it has been already explained in the previous metric.

The second term is regarding angular velocity. A very high maximum angular velocity is considered as a penalization, unless the mean velocity is also high. The reason to calculate it in this way is that patients with a badly preserved functionality will carry out the exercises quite slowly, obtaining a low mean angular velocity, but they will also carry out uncontrolled movements, for example, dropping the arm, thus getting a high maximum angular velocity. Therefore, it is important to evaluate the relationship between the maximum and the mean angular velocity, not only one of them separately.

The third term takes into account the time spent by the patient on performing the exercise in relation with the time spent by a healthy subject on performing the same exercise.

In order to obtain values in percentages, as in the previous metrics, agility has been normalized by the value of accuracy obtained by a healthy subject:

$$\text{Ag}_{\text{norm}} = \frac{\text{Ag}}{\text{Ag}_{\text{ideal}}} \cdot 100\,[\%]\,. \tag{6}$$

(v) Repeatability. It computes the inverse of the area comprised between the upper and the lower envelopes of the repetitions of the same movement during a session:

$$R = k \cdot \sum_{i=1}^{i=8} \frac{k_0}{A_i \cdot \left(1 + \left(1/n_{\text{rep}}\right)\right)}, \tag{7}$$

where A_i = area comprised between the upper and the lower envelopes of the repetitions of the exercise I and k, k_0 = normalizing coefficients used to adjust the scale. Here $k = 1000$ and k_0 have been used. n_{rep} = number of repetitions for each exercise (it is necessary that all exercises have the same number of repetitions).

For this metric, only exercises 1 to 8 have been used. They are step-by-step shoulder abduction, complete shoulder abduction, step-by-step shoulder flexion, complete shoulder flexion, step-by-step elbow flexion, complete elbow flexion, elbow extension, and shoulder rotation. These exercises are the ones that require the patient to perform a determined trajectory to accomplish the task, so the trajectories of different repetitions should be similar if the task has been correctly executed. Area A_i has been computed by calculating the upper and the lower envelopes along time of all repetitions of the kinematic variable corresponding to exercise i. For example, for the first exercise, shoulder abduction curve along time has been used, as it can be seen in Figures 3 and 4.

Area comprised in each exercise is being weighted by the number of repetitions (n_{rep}) because the area tends to increase with the number of repetitions used.

The idea is that, as long as the patient improves his performance, he should be able to repeat more accurately the same task; thus the area between the envelopes should decrease.

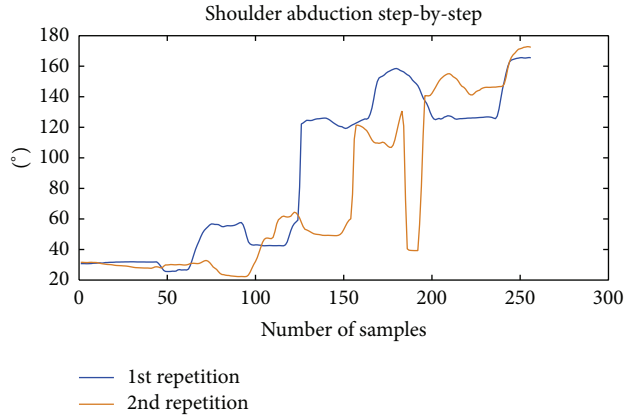

Figure 3: Example of the curves of shoulder abduction recorded during 2 repetitions of the same movement by a patient.

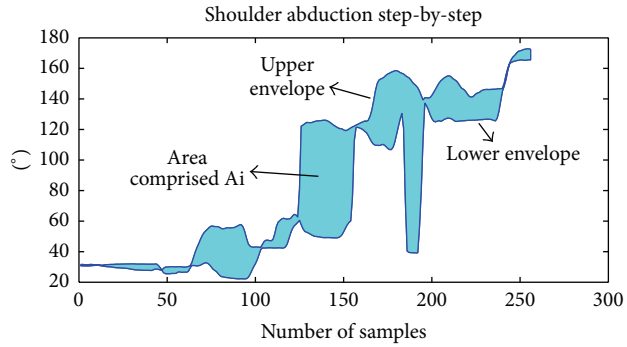

Figure 4: Example illustrating the calculation of the *repeatability* for the 2 repetitions previously shown in Figure 3.

4. Evaluation Method

4.1. Participants. Fifteen subjects (11 males and 4 females with complete spinal cord injury; mean age 35.33 ± 14.4 years, 4.8 ± 2.37 months since injury) participated in the study. Subject's demographic and clinical characteristics are shown in Table 1.

Eligible participants met the following criteria: (1) at least 18 years of age; (2) less than 12 months from the injury; (3) motor complete spinal cord injury according to the ASIA's impairment scale at the level of C5 to C8 (A-B ASIA level [24]); (4) no history of traumatic or cognitive pathology that can affect the Upper Limb (UL) movements; (5) normal or corrected-to-normal vision and hearing; (6) no history of technology addiction; and (7) no history of epilepsy and pregnancy. Each subject gave informed consent voluntarily which were approved by the Local Ethics Committee.

4.2. Data Collection and Analysis. Subjects remained seated in their own wheelchair in front of the screen. A total of five MTx IMUs were used to capture movements of the dominant UL, wirelessly connected (Bluetooth) to a computer via a digital data bus (Master Xbus), which was responsible for the synchronization, data collection, and transmission. The IMUs were strategically placed on the trunk, the back of the head, the arm, the forearm, and the hand [23]. Each subject received an explanation about how to perform the activity, which consisted of reaching the different goals that appear sequentially on the screen. Subjects were instructed to perform each of the 14 analytic movements required including complete and step-by-step shoulder, elbow, and wrist motion required. A sampling frequency of 25 Hz was used for the MTx IMUs recordings. The subjects cyclically executed each exercise three times. The mean of these three recordings yielded the final measurement value for each subject.

As it has been described in the "new kinematic metrics" section, some of the metrics require some data recorded from healthy subjects in order to compare the results of the metrics with a reference value, thus yielding a final value expressed in percentage with respect to the healthy reference. In order to obtain these reference values, a group of five healthy subjects (2 males and 3 females, mean age of 29 years and standard deviation of 6.041) was previously registered. The following parameters were extracted from the healthy subjects and then averaged to obtain the reference values: ROMs, trajectories, time spent on each exercise, and absolute value for the metrics.

Neurological examinations of all the patients were performed according to the ASIA standards [24]. The functional examination was done by using three scales. The first scale was SCIM II, which has 16 items divided into three functional areas: self-care, respiration and sphincter management, and mobility. Total score can vary from 0 (minimal) to 100 (maximal) [25]. Only the self-care subscore has been considered in this study, because it has been previously shown to be more closely related with the upper limb function [26]. From now on, this subscale will be named self-care SCIM.

The second assessment scale was the UL part of motor index scale (UL MI), which assesses power and range of the following movements: shoulder abduction, elbow flexion, and pinch between the thumb and index finger. The total score is rated between 0 (no movement) and 100 (normal movement [27]. The total score of the scale and also each of the subscores: shoulder abduction (UL MI AbdShoulder), elbow flexion (UL MI Flexelbow), and pinch (UL MI Pinch) has been evaluated.

The third scale was functional independence measure (FIM), which consists of 18 items organized in six categories, four corresponding to motor functions (self-care items, sphincter control, mobility items, and locomotion) and two corresponding to cognitive functions (communication and social cognition). The lowest and highest scores of the total ranged from 18 to 126 [28]. As in the SCIM, only the self-care subscore has been taken into account. From now on, this subscale will be named self-care FIM.

Both the kinematic assessment with Toyra and the clinical evaluation were carried out for each patient with a maximum difference of 2 days.

Descriptive analysis including means and standard deviations (SD) for continuous variables was initially performed to characterize each subject and also each group of subjects considering the neurological level of injury (C5–C8). The Pearson correlation coefficient was used to correlate kinematic ROMs with clinical and functional variables.

Table 1: Demographic and clinical characteristics of the sample analysed.

Sex (male)†	11 (73.33)			
Age (years)*	35.33 (14.40)			
Time since injury (months)*	4.80 (2.37)			
Dominance (right)†	9 (60)			
ASIA (A)†	9 (60)			
Etiology (trauma)†	14 (93.33)			
Level of neurological injury (C5–C8)†	C5 = 7 (46.66)	C6 = 4 (26.66)	C7 = 3 (20)	C8 = 1 (6.66)

*Continuous variables are expressed as mean and standard deviation values. †Categorical variables are expressed as frequency and percentage of the sample analyzed.

Table 2: Shoulder kinematics per level of injury (mean ± SD).

	AbdshoulderS	AbdshoulderC	FshoulderS	FshoulderC	Rotshoulder
C5 $n = 7$	73.184 ± 28.436	72.402 ± 36.022	103.506 ± 53.465	107.957 ± 41.308	114.707 ± 31.245
C6 $n = 4$	95.903 ± 34.925	122.465 ± 26.207	157.989 ± 28.381	138.222 ± 56.126	89.824 ± 22.948
C7 $n = 3$	102.218 ± 52.31	113.985 ± 45.117	165.138 ± 32.002	152.904 ± 21.112	108.454 ± 47.901
C8 $n = 1$	137.787 ± 12.10	152.151 ± 13.21	178.582 ± 12.34	175.32 ± 14.25	130.843 ± 12.120

Table 3: Elbow kinematics per level of injury (mean ± SD).

	FelbowC	Extelbow	FelbowS	Supelbow	Proelbow
C5 $n = 7$	118.624 ± 15.864	126.714 ± 19.974	111.632 ± 27.046	162.411 ± 85.775	146.391 ± 17.788
C6 $n = 4$	129.835 ± 10.935	145.311 ± 25.908	125.537 ± 22.501	126.215 ± 9.024	185.726 ± 58.672
C7 $n = 3$	132.846 ± 6.68	145.044 ± 9.539	131.95 ± 2.635	142.297 ± 31.714	178.916 ± 39.569
C8 $n = 1$	112.46 ± 13.23	151.505 ± 32.12	116.905 ± 12.23	122.997 ± 24.12	183.384 ± 21.14

A significance level of P less than 0.05 has been used. All statistical analysis was performed with Matlab (The Mathworks Inc., Natick, MA, USA).

5. Results

Kinematics recorded by Toyra (the 14 kinematic variables already mentioned) were obtained for each patient and averaged by levels of neurological injury. These averages can be seen in Tables 2, 3, and 4.

Values obtained by all patients in the clinical scales SCIM, UL MI, and FIM have also been obtained and averaged by level of injury, showing the results in Table 5.

Positive strong correlations between kinematic variables and clinical scales have been found in the following parameters: self-care SCIM and shoulder flexion step-by-step ($r = 0.776$, $P = 0.00067$), self-care SCIM, and complete shoulder flexion ($r = 0.74$, $P = 0.0016$), UL MI and shoulder flexion step-by-step ($r = 0.714$, $P = 0.0028$), and UL MI and complete shoulder flexion ($r = 0.712$, $P = 0.0029$).

Positive moderate correlations between kinematic variables and clinical scales have been found in the following parameters: self-care SCIM and shoulder abduction step-by-step ($r = 0.548$, $P = 0.034$), self-care SCIM and complete shoulder abduction ($r = 0.518$, $P = 0.048$), self-care SCIM and ulnar deviation ($r = 0.551$, $P = 0.033$), UL MI and shoulder abduction step-by-step ($r = 0.547$, $P = 0.035$), self-care FIM and shoulder abduction step-by-step ($r = 0.675$, $P = 0.0113$), and self-care FIM and complete shoulder flexion ($r = 0.618$, $P = 0.0243$). Results are shown in Table 6.

The metrics developed were applied to patients group. In Figures 5, 6, 7, and 8 the results are shown averaging the values of the metrics by levels of injury.

The metrics developed in this study have been applied to 15 patients; then the obtained values with the clinical scales' scores were compared. As it can be seen in Table 7, strong positive correlation has been found between the metric *joint amplitude* and the self-care SCIM ($r = 0.797$, $P = 0.000375$) and between this metric and the subscale UL MI AbdShoulder ($r = 0.861$, $P = 0.00003$).

Table 4: Wrist kinematics per level of injury (mean ± SD).

	Extwrist	Flexwrist	Raddevwrist	Uldevwrist
C5 $n = 7$	57.204 ± 11.602	44.053 ± 17.086	24.878 ± 10.11	23.155 ± 11.656
C6 $n = 4$	44.275 ± 21.867	47.589 ± 13.546	20.796 ± 8.173	25.851 ± 15.579
C7 $n = 3$	77.045 ± 9.831	65.793 ± 8.925	36.476 ± 2.415	42.669 ± 1.238
C8 $n = 1$	56.002 ± 12.02	54.004 ± 11.23	23.656 ± 11.21	34.868 ± 10.25

Table 5: Clinical subscales of self-care SCIM, UL MI, and self-care FIM per level of injury (mean ± SD).

	Self-care SCIM	UL MI	Self-care FIM
C5 $n = 7$	2 ± 1.414	66.429 ± 20.999	10 ± 2.828
C6 $n = 4$	3 ± 1.414	64.25 ± 17.115	13 ± 9.539
C7 $n = 3$	5 ± 1.732	69 ± 19.079	12 ± 2
C8 $n = 1$	8 ± 0	93 ± 0	16 ± 0

Table 6: Correlations found between kinematic variables recorded by VR system Toyra and clinical subscales.

	Self-care SCIM	UL MI	Self-care FIM
AbdshoulderS	$r = 0.548^{*}$ $P = 0.034$	$r = 0.547^{*}$ $P = 0.035$	$r = 0.675^{*}$ $P = 0.0113$
AbdshoulderC	$r = 0.518^{*}$ $P = 0.048$	$r = 0.385$ $P = 0.157$	$r = 0.551$ $P = 0.074$
FshoulderS	$r = 0.776^{***}$ $P = 0.00067$	$r = 0.714^{**}$ $P = 0.0028$	$r = 0.476$ $P = 0.1$
FshoulderC	$r = 0.74^{**}$ $P = 0.0016$	$r = 0.712^{**}$ $P = 0.0029$	$r = 0.618^{*}$ $P = 0.0243$
Udwrist	$r = 0.551^{*}$ $P = 0.033$	$r = 0.336$ $P = 0.221$	$r = 0.165$ $P = 0.59$

$^{*}P < 0.05$.
$^{**}P < 0.01$.
$^{***}P < 0.001$.

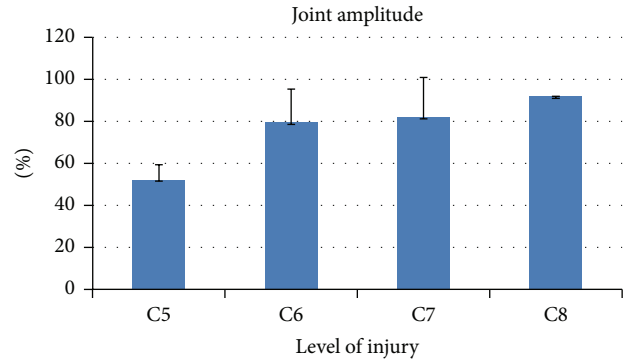

Figure 5: Kinematic metric *joint amplitude* per level of injury (mean ± SD). It is expressed in percentage with respect to the reference value of healthy subjects.

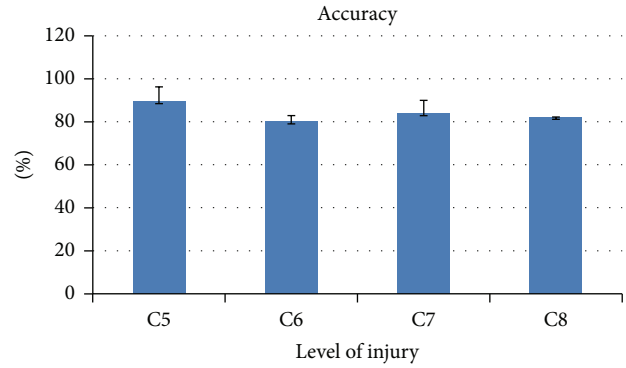

Figure 6: Kinematic metric *accuracy* per level of injury (mean ± SD). It is expressed in percentage with respect to the reference value of healthy subjects.

There were moderate positive correlations between the following parameters: *joint amplitude* and self-care FIM ($r = 0.591$, $P = 0.0335$), *reaching amplitude (Y-axis)* and self-care FIM ($r = 0.708$, $P = 0.00673$), *reaching amplitude (Z-Axis)* and UL MI ($r = 0.552$, $P = 0.0457$), *reaching amplitude (Z-Axis)* and UL MI AbdShoulder ($r = 0.551$, $P = 0.0332$), *reaching amplitude (Z-Axis)* and UL MI Flexelbow ($r = 0.52$, $P = 0.0467$), and *reaching amplitude (Z-Axis)* and self-care FIM ($r = 0.681$, $P = 0.01$).

There was also a moderate negative correlation between *agility* and UL MI AbdShoulder ($r = -0.536$, $P = 0.0397$).

6. Discussion

The present study shows that the kinematic data recorded by VR system Toyra correlate with clinical scales specific for the upper limb function, which is in line with preliminary results of our group [7]. Some metrics have been defined based on these kinematic data, showing promising results in terms of clinically relevant information, as it has been demonstrated by the correlation found between some of the metrics and the self-care subscales.

Table 7: Correlations between kinematic metrics and clinical subscales.

	Self-care SCIM	UL MI	UL MI AbdShoulder	UL MI Flexelbow	UL MI Pinch	Self-care FIM
Joint amplitude	$r = 0.797^{***}$	$r = 0.513$	$r = 0.861^{***}$	$r = 0.292$	$r = 0.276$	$r = 0.591^{*}$
	$P = 0.000375$	$P = 0.05$	$P = 0.00003$	$P = 0.291$	$P = 0.32$	$P = 0.0335$
Reaching amplitude (total)	$r = -0.068$	$r = 0.376$	$r = -0.041$	$r = -0.024$	$r = 0.346$	$r = 0.539$
	$P = 0.811$	$P = 0.167$	$P = 0.883$	$P = 0.931$	$P = 0.207$	$P = 0.057$
Reaching amplitude (X-axis)	$r = -0.374$	$r = 0.05$	$r = -0.393$	$r = -0.23$	$r = 0.14$	$r = 0.019$
	$P = 0.17$	$P = 0.858$	$P = 0.147$	$P = 0.409$	$P = 0.0619$	$P = 0.952$
Reaching amplitude (Y-axis)	$r = 0.217$	$r = 0.4$	$r = 0.258$	$r = 0.005$	$r = 0.315$	$r = 0.708^{**}$
	$P = 0.17$	$P = 0.139$	$P = 0.354$	$P = 0.986$	$P = 0.252$	$P = 0.0067$
Reaching amplitude (Z-axis)	$r = 0.474$	$r = 0.523^{*}$	$r = 0.551^{*}$	$r = 0.52^{*}$	$r = 0.315$	$r = 0.681^{*}$
	$P = 0.075$	$P = 0.0457$	$P = 0.0332$	$P = 0.0467$	$P = 0.252$	$P = 0.01$
Accuracy	$r = -0.239$	$r = -0.174$	$r = -0.364$	$r = -0.442$	$r = -0.062$	$r = -0.283$
	$P = 0.391$	$P = 0.535$	$P = 0.182$	$P = 0.099$	$P = 0.828$	$P = 0.349$
Agility	$r = -0.259$	$r = -0.248$	$r = -0.536^{*}$	$r = -0.463$	$r = -0.081$	$r = -0.338$
	$P = 0.351$	$P = 0.373$	$P = 0.0397$	$P = 0.082$	$P = 0.775$	$P = 0.26$

$^{*}P < 0.05$.
$^{**}P < 0.01$.
$^{***}P < 0.001$.

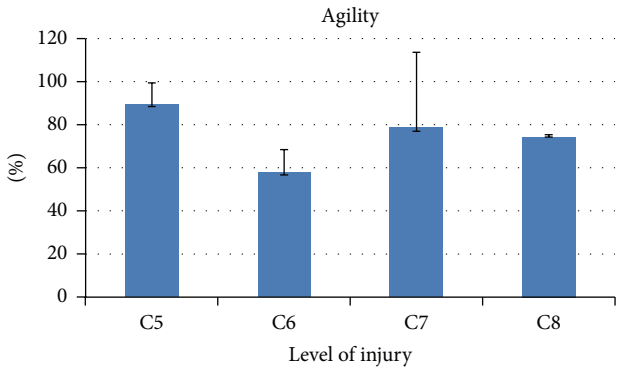

Figure 7: Kinematic metric *agility* per level of injury (mean ± SD). It is expressed in percentage with respect to the reference value of healthy subjects.

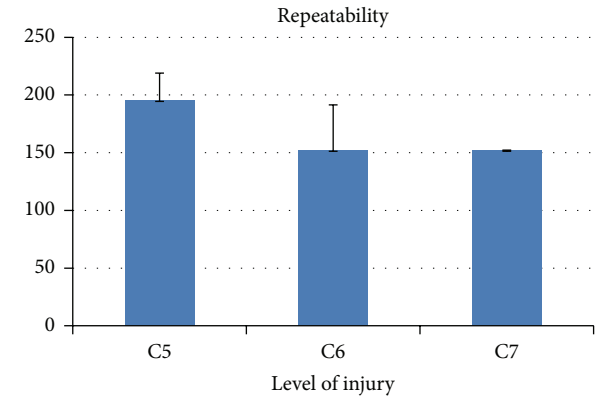

Figure 8: Kinematic metric *repeatability* per level of injury (mean ± SD). It is expressed in absolute value. It has been calculated only for levels C5, C6, and C7 because the number of registers for C8 level was not sufficient to establish a reliable value. For the same reason, the reference value of healthy subjects for this metric has not been calculated.

This study supports the use of such VR systems not only as rehabilitation tools but also as an objective assessment tool of the user's performance, providing data with potential clinical relevance. The different degree of correlation found between the clinical scales and the kinematic variables yields interesting information that can be used in two directions. One is to analyse in minute resolution the patients' physical state, trying to use this information to complement the clinical scales scores and to design treatments that encourage the training of the joints more linked with a functional improvement. The second one would be to develop predictive models that could offer the clinician an estimation of the clinical scale score expected for a patient, thus adding objective data that could facilitate the and to follow the progression of a patient. Some previous studies go in this direction [9, 29].

The highest positive correlation between clinical scales and kinematic variables was found in the step-by-step shoulder flexion. As it was previously mentioned, the step-by-step kinematic variables require higher muscle control, and this could be the reason of the high correlation of this variable with the functionality. Together with the moderate correlations found in the shoulder abduction, these results suggest the importance of the shoulder range or movement in patients with SCI, which is consistent with previous studies that established that shoulder muscle strength, in patients with tetraplegia, is an important determinant of functional ability level [30].

In a previous study in which correlations between kinematics and clinical scales were also studied [22], no correlation was found between shoulder range of motion and any clinical scales. However, the methodology that was used in that study is quite different than the one presented here, because the patients performed only one kind of reaching and grasp task, without using any VR system, so that

the reaching and grasp task did not encourage them to reach their maximum values of range of motion in all directions. In contrast with that study, here the patients carry out a wide variety of tasks, because the goals to reach are displayed in some different locations around the patient. This is one of the advantages of VR, which permits measurement of the patient's kinematics during different tasks without the difficulties of setting up a new physical environment for each task.

The only kinematic variable not related with the shoulder that showed positive correlation with clinical scales was the ulnar wrist deviation. This result could be due to the tenodesis effect, an anatomical consequence of the SCI very common in patients with level of injury C6 or C7 that entails a high wrist range of motion during the execution of the activities of daily living (ADL) [31].

Regarding the kinematic metrics developed in this study, the higher correlation obtained between the *joint amplitude* and the clinical scales, in comparison with any of the correlations obtained between the same scales and the isolated kinematic variables, suggests that the combination of kinematic variables could offer more clinically relevant information than when individually presented.

The strong positive correlation between *joint amplitude* and the SCIM scale and also the upper limb abduction shoulder subscore shows that this metric could be a good indicator of functionality. A similar result was obtained in [29], where the range of motion was found to affect to a large extent the performance of a model that predicts the clinical score from the kinematic recordings of a therapeutic robotic arm.

Reaching amplitude along the Z-axis shows moderate correlations with four of the clinical scores or subscores (UL MI global, UL MI Abdshoulder, UL MI Flexelbow, and self-care FIM scale). As it has been defined, the Z-axis goes vertically upwards, so that the movements in this direction require a higher force, and thus this ability could be closely related to the clinical measurements. Also *reaching amplitude* along the Y-axis shows a positive correlation with self-care FIM scale. The Y-axis was defined horizontally, perpendicular to the screen, and it is thereby the direction in which some of the ADL considered in the FIM scale take place, like eating or grooming. This could be the rationale of this correlation.

The negative correlation that showed the *agility* with the UL MI AbdShoulder was unexpected, and it could indicate that the normalization by the mean velocity used to calculate this metric could not have been enough to counteract the presence of involuntary movements, very common in patients with SCI, that usually lead to the appearance of high velocity peaks. Further filtering strategies and an optimization of the metric's parameters will be necessary to improve this metric.

With respect to the metric *accuracy*, no correlation with clinical scores was found, in contrast with a previous report, where there were strong correlations between a metric called "trajectory error," with similar foundations to the one presented here [32]. We believe that the clinical scales (self-care SCIM, self-care FIM, and UL MI) used in our study do not encompass the specific information that this metric provides. Maybe other methods could be used in further researches to evaluate its validity. For example, in the mentioned study, clinical scales Fugl-Meyer, Motor Activity Log, Action Research Arm Test, and Jebsen-Taylor Hand Function Test were used. These scales are likely to measure aspects more related to the accuracy of movements than the ones used here.

These metrics present some limitations, such as the different number of patients in each group of injury. Therefore, it will be necessary in future researches to increase the number of patients in order to have a sufficient number to compare the averages of each level of injury. It could be also interesting to apply this metrics and kinematic analysis when the patients are performing more functional tasks such as ADLs in VR environments, not only analytical movements as in the evaluation session presented here.

7. Conclusions

It has been shown that some of the kinematic data extracted by a VR system based on IMUs motion capture systems have a clinical meaning. It has also been shown that the combination of these variables could provide more information than when separately used. For this purpose, a set of kinematic metrics has been defined, showing promising results in some of them. It seems very important to give clinicians the chance to obtain clinical relevant information from technological applications of rehabilitation. This could facilitate the use of such devices in clinical settings.

Conflict of Interests

Each author has read and concurs with the content of the final paper and was fully involved. The material herein has not been and will not be submitted for publication elsewhere. No commercial party having a direct financial interest in the results of the research supporting this paper has or will confer a benefit upon the author(s) or upon any organization with which the author(s) is/are associated.

Acknowledgments

The authors thank the consortium including Foundation Rafael del Pino, Foundation of the Spanish National Hospital for Paraplegic Research and Integration (FUHNPAIIN), and INDRA Systems for funding this research.

References

[1] M. Wyndaele and J.-J. Wyndaele, "Incidence, prevalence and epidemiology of spinal cord injury: what learns a worldwide literature survey?" *Spinal Cord*, vol. 44, no. 9, pp. 523–529, 2006.

[2] L. A. Harvey, J. Batty, R. Jones, and J. Crosbie, "Hand function of C6 and C7 tetraplegics 1–16 years following injury," *Spinal Cord*, vol. 39, no. 1, pp. 37–43, 2001.

[3] G. J. Snoek, M. J. Ijzerman, H. J. Hermens, D. Maxwell, and F. Biering-Sorensen, "Survey of the needs of patients with spinal cord injury: impact and priority for improvement in hand

function in tetraplegics," *Spinal Cord*, vol. 42, no. 9, pp. 526–532, 2004.

[4] J. C. Stewart, S.-C. Yeh, Y. Jung et al., "Intervention to enhance skilled arm and hand movements after stroke: a feasibility study using a new virtual reality system," *Journal of NeuroEngineering and Rehabilitation*, vol. 4, article 21, 2007.

[5] K. Eng, E. Siekierka, P. Pyk et al., "Interactive visuo-motor therapy system for stroke rehabilitation," *Medical and Biological Engineering and Computing*, vol. 45, no. 9, pp. 901–907, 2007.

[6] M. A. Murphy, K. S. Sunnerhagen, B. Johnels, and C. Willén, "Three-dimensional kinematic motion analysis of a daily activity drinking from a glass: A Pilot Study," *Journal of NeuroEngineering and Rehabilitation*, vol. 3, article 18, 2006.

[7] I. Dimbwadyo-Terrer, F. Trincado-Alonso, A. De los Reyes-Guzmán et al., "Clinical, functional and kinematic correlations using the virtual reality system toyra as upper limb rehabilitation tool in people with spinal cord injury," in *Proceedings of the International Congress on Neurotechnology, Electronics and Informatics (NEUROTECHNIX '13)*, A. R. Londral, P. Encarnaçao, and J. L. Pons, Eds., pp. 81–88, SCITEPRESS-Science and Technology, 2013.

[8] P. M. Fitts, "The information capacity of the human motor system in controlling the amplitude of movement," *Journal of Experimental Psychology*, vol. 47, no. 6, pp. 381–391, 1954.

[9] C. Bosecker, L. Dipietro, B. Volpe, and H. I. Krebs, "Kinematic robot-based evaluation scales and clinical counterparts to measure upper limb motor performance in patients with chronic stroke," *Neurorehabilitation and neural repair*, vol. 24, no. 1, pp. 62–69, 2010.

[10] R. Colombo, F. Pisano, S. Micera et al., "Assessing mechanisms of recovery during robot-aided neurorehabilitation of the upper limb," *Neurorehabilitation and Neural Repair*, vol. 22, no. 1, pp. 50–63, 2008.

[11] L. Dipietro, H. I. Krebs, S. E. Fasoli et al., "Changing motor synergies in chronic stroke," *Journal of Neurophysiology*, vol. 98, no. 2, pp. 757–768, 2007.

[12] M. A. Murphy, C. Willén, and K. S. Sunnerhagen, "Kinematic variables quantifying upper-extremity performance after stroke during reaching and drinking from a glass," *Neurorehabilitation and Neural Repair*, vol. 25, no. 1, pp. 71–80, 2011.

[13] A. De los Reyes-Guzmán, A. Gil-Agudo, B. Peñasco-Martín, M. Solís-Mozos, A. del Ama-Espinosa, and E. Pérez-Rizo, "Kinematic analysis of the daily activity of drinking from a glass in a population with cervical spinal cord injury," *Journal of Neuroengineering and Rehabilitation*, vol. 7, p. 41, 2010.

[14] S. Namdari, G. Yagnik, D. D. Ebaugh et al., "Defining functional shoulder range of motion for activities of daily living," *Journal of Shoulder and Elbow Surgery*, vol. 21, no. 9, pp. 1177–1183, 2012.

[15] A. De los Reyes-Guzmán, I. Dimbwadyo-Terrer, S. Pérez-Nombela, F. Trincado-Alonso, D. Torricelli, and A. Gil-Agudo, "Objective metrics for functional evaluation of upper limb during the ADL of drinking: application in SCI," in *Proceedings of the 13th Mediterranean Conference on Medical and Biological Engineering and Computing*, L. M. . Roa Moreno, Ed., vol. 41 of *IFMBE Proceedings*, pp. 1751–1754, Springer, 2014.

[16] A. de los Reyes-Guzmán, S. Pérez-Nombela, I. Dimbwadyo-Terrer, and D. Torricelli, "Functional upper limb evaluation of daily activities in people with neurological disorders," in *Functional Upper Limb Evaluation of Daily Activities in People with Neurological Disorders*, C. V. Jean Baptiste Giroux, Ed., pp. 55–76, Nova Science Publishers, 2013.

[17] J. H. Van Tuijl, Y. J. M. Janssen-Potten, and H. A. M. Seelen, "Evaluation of upper extremity motor function tests in tetraplegics," *Spinal Cord*, vol. 40, no. 2, pp. 51–64, 2002.

[18] C. Collin and D. Wade, "Assessing motor impairment after stroke: A Pilot Reliability Study," *Journal of Neurology Neurosurgery and Psychiatry*, vol. 53, no. 7, pp. 576–579, 1990.

[19] R. H. Jebsen, N. Taylor, R. B. Trieschmann, M. J. Trotter, and L. A. Howard, "An objective and standardized test of hand function," *Archives of Physical Medicine and Rehabilitation*, vol. 50, no. 6, pp. 311–319, 1969.

[20] M. H. Rabadi and F. M. Rabadi, "Comparison of the action research arm test and the fugl-meyer assessment as measures of upper-extremity motor weakness after stroke," *Archives of Physical Medicine and Rehabilitation*, vol. 87, no. 7, pp. 962–966, 2006.

[21] G. Uswatte, E. Taub, D. Morris, M. Vignolo, and K. McCulloch, "Reliability and validity of the upper-extremity motor activity log-14 for measuring real-world arm use," *Stroke*, vol. 36, no. 11, pp. 2493–2496, 2005.

[22] E. W. A. Cacho, R. De Oliveira, R. L. Ortolan, R. Varoto, and A. Cliquet Jr., "Upper limb assessment in tetraplegia: clinical, functional and kinematic correlations," *International Journal of Rehabilitation Research*, vol. 34, no. 1, pp. 65–72, 2011.

[23] A. Gil-Agudo, A. De los Reyes-Guzmán, I. Dimbwadyo-Terrer et al., "An inertial sensor-based motion tracking system for clinical upper limb rehabilitation," *Neural Regeneration Research*, vol. 8, no. 19, pp. 1773–1782, 2013.

[24] R. J. Marino, T. Barros, F. Biering-Sorensen et al., "International standards for neurological classification of spinal cord injury," *The Journal of Spinal Cord Medicine*, vol. 26, pp. S50–S56, 2003.

[25] A. Catz, M. Itzkovich, E. Agranov, H. Ring, and A. Tamir, "SCIM—spinal cord independence measure: a new disability scale for patients with spinal cord lesions," *Spinal Cord*, vol. 35, no. 12, pp. 850–856, 1997.

[26] C. Rudhe and H. J. A. Van Hedel, "Upper extremity function in persons with tetraplegia: relationships between strength, capacity, and the spinal cord independence measure," *Neurorehabilitation and Neural Repair*, vol. 23, no. 5, pp. 413–421, 2009.

[27] G. Demeurisse, O. Demol, and E. Robaye, "Motor evaluation in vascular hemiplegia," *European Neurology*, vol. 19, no. 6, pp. 382–389, 1980.

[28] B. B. Hamilton, J. A. Laughlin, C. V. Granger, and R. M. Kayton, "Interrater agreement of the seven level Functional Independence Measure (FIM)," *Archives of Physical Medicine and Rehabilitation*, vol. 72, p. 790, 1991.

[29] J. Zariffa, N. Kapadia, J. L. K. Kramer et al., "Relationship between clinical assessments of function and measurements from an upper-limb robotic rehabilitation device in cervical spinal cord injury," *IEEE Transactions on Neural Systems and Rehabilitation Engineering*, vol. 20, no. 3, pp. 341–350, 2012.

[30] T. Fujiwara, Y. Hara, K. Akaboshi, and N. Chino, "Relationship between shoulder muscle strength and functional independence measure (FIM) score among C6 tetraplegics," *Spinal Cord*, vol. 37, no. 1, pp. 58–61, 1999.

[31] I. Laffont, E. Briand, O. Dizien et al., "Kinematics of prehension and pointing movements in C6 quadriplegic patients," *Spinal Cord*, vol. 38, no. 6, pp. 354–362, 2000.

[32] O. Celik, M. K. O'Malley, C. Boake, H. S. Levin, N. Yozbatiran, and T. A. Reistetter, "Normalized movement quality measures for therapeutic robots strongly correlate with clinical motor impairment measures," *IEEE Transactions on Neural Systems and Rehabilitation Engineering*, vol. 18, no. 4, pp. 433–444, 2010.

Hindawi Publishing Corporation
BioMed Research International
Volume 2014, Article ID 646347, 7 pages
http://dx.doi.org/10.1155/2014/646347

Research Article

Ghostman: Augmented Reality Application for Telerehabilitation and Remote Instruction of a Novel Motor Skill

Winyu Chinthammit,[1] Troy Merritt,[1] Scott Pedersen,[2] Andrew Williams,[3] Denis Visentin,[3] Robert Rowe,[1] and Thomas Furness[4]

[1] *Human Interface Technology Laboratory Australia (HIT Lab AU), School of Engineering and ICT, University of Tasmania, Launceston, Tas 7250, Australia*
[2] *Active Work Laboratory, Faculty of Education, University of Tasmania, Launceston, Tas 7250, Australia*
[3] *School of Health Sciences, University of Tasmania, Launceston, Tas 7250, Australia*
[4] *Human Interface Technology Laboratory (HIT Lab), University of Washington, Seattle, WA 98195, USA*

Correspondence should be addressed to Winyu Chinthammit; winyu.chinthammit@utas.edu.au

Received 28 January 2014; Revised 12 March 2014; Accepted 13 March 2014; Published 15 April 2014

Academic Editor: Alessandro De Mauro

This paper describes a pilot study using a prototype telerehabilitation system (Ghostman). Ghostman is a visual augmentation system designed to allow a physical therapist and patient to inhabit each other's viewpoint in an augmented real-world environment. This allows the therapist to deliver instruction remotely and observe performance of a motor skill through the patient's point of view. In a pilot study, we investigated the efficacy of Ghostman by using it to teach participants to use chopsticks. Participants were randomized to a single training session, receiving either Ghostman or face-to-face instructions by the same skilled instructor. Learning was assessed by measuring retention of skills at 24-hour and 7-day post instruction. As hypothesised, there were no differences in reduction of error or time to completion between participants using Ghostman compared to those receiving face-to-face instruction. These initial results in a healthy population are promising and demonstrate the potential application of this technology to patients requiring learning or relearning of motor skills as may be required following a stroke or brain injury.

1. Introduction

To minimise ongoing disability and its associated costs, rehabilitation following surgery, stroke, or a musculoskeletal injury typically requires a course of frequent consultations with allied health professionals to determine and direct a treatment during the rehabilitation period [1]. Ageing is associated with increased disability. As the population ages the need for rehabilitation services will increase, placing additional stress on health services staff and budgets [2]. In addition, costs associated with transporting patients long distances and associated decreases in productivity, particularly for patients from rural areas, will add to the community burden of delivering appropriate services. This will place increasing stress on health services and consequently therapeutic solutions need to become more flexible in delivery.

Best practice face-to-face instruction involves the therapist describing the movement with focus on key areas, performing the movement observed by the trainee and then the trainee practising the movement while the trainer provides verbal feedback on performance, and in some cases manually assisting the target movement. In this situation it has been demonstrated that facilitation of the patient's movement or motor performance is a critical part of the prescribed exercise [3]. In contrast, the lower end of the therapeutic scale may involve patients only receiving brief instruction in the therapist's office and then being sent home to practice the new skills by themselves with only a printed sheet of verbal instructions provided by the therapist to consult (sometimes with model drawings). Alarmingly, the latter example is the most common and is usually attributed to high patient

caseloads and limited availability of specialists concentrated within geographical locations outside of metropolitan areas.

Telerehabilitation combines telecommunication, sensing and display technologies, and computing technologies to enable rehabilitation to be conducted at a distance [4]. A telerehabilitation system can increase the reach of a therapist, by enabling them to deliver instruction and assess patient performance remotely. To facilitate this increase in reach and reduction in cost, a system must allow the therapist to perform these services remotely. That is, by reducing the need for patient travel, the cost of accessing rehabilitation services is reduced. There is also a lower chance of further injury and less discomfort for the patient, which may also reduce the impact on the patient's caregiver. By using technology to measure and assess the patient's performance, less time is needed for assessment and, consequently, the efficiency of the therapist may also be improved. By improving the intensity of therapy sessions, greater functional gains can occur [5].

Video-based approaches allow for the remote delivery of instruction and the monitoring of patient performance [6, 7]. Another approach is to capture patient performance and display it in a virtual environment. Performance capture can be achieved via sensor-based approaches, such as data gloves [8, 9] and electromagnetic trackers [8, 10–12], or vision-based approaches such as a webcam [13] or marker tracking [14–16]. This performance information can be displayed in a completely virtual environment [10] or augmented into the real world [14].

Virtual reality (VR) and augmented reality (AR) are potential methods of delivering rehabilitative health services remotely. Both have been effective in the delivery of finger and hand rehabilitation after stroke [17, 18] while VR has also been shown to result in significant improvements in motor function and laterality index score in chronic stroke patients [19]. VR systems have been effectively implemented in telerehabilitation [20] and for remote training [21]. AR systems have been shown to be capable of measuring task-completion time, compactness of task, and speed of hand movement by capturing the patients' hand movements whilst moving a tangible object [14] or with marker-based tracking [15]. Khademi et al. [16] used haptic feedback in conjunction with AR to measure stiffness in a user's arm.

There is evidence that training outcomes are positive when users utilised a first-person viewpoint [7, 22]. Yang et al. used a VR approach with "ghost" metaphor and a first-person viewpoint. The motions of trainer/trainee were captured and recreated entirely in the virtual environment in which the trainer operated. However, the use of the VR approach prevents the trainer to view the real environment, which raises concerns in safety issues and a lack of ability to view other subtle visual cues in the environment such as other parts of the limbs not being tracked/targeted. Kumagai et al. [7] used an AR approach. While it is rendered with a first-person viewpoint, the trainer/trainee was viewing the scene via external computer monitors, as a result, causing a viewpoint displacement between the physical limbs and displayed limbs. The displacement requires users to perform an additional cognitive step, a hand-eye coordination operation (similar to using a computer mouse to move a cursor on the display screen). Nevertheless, the benefit of the first-person view is still evident and likely due to the fact that there is a more direct and correct transfer of proprioceptive information [22], which leads to the core of our proposed Ghostman Design.

2. Ghostman Design

This paper discusses proof of concept of our proposed telerehabilitation system, called "Ghostman." Ghostman is a wearable visual augmentation system in egocentric view through which users can observe their own movement being overlaid with a "ghost" image of the instructor's body in real time. Unlike Yang and Kim [22], the Ghostman uses an AR approach, in which the viewing of the real-world environment is preserved. This allows the users to "inhabit" the other's viewpoint, in a technique we call *inhabiting visual augmentation*, illustrated in Figure 2. The use of AR technology enables Ghostman to closely match sensory modalities of the user such as correct and natural visual cues. The Ghostman makes use of a wearable display, a head mounted display (HMD), which helps minimize the viewpoint displacement between the rendered limbs and the actual limbs. By wearing an HMD, trainees can intuitively mimic the movements of the trainer by observing both their own and the trainer's movements simultaneously through the use of colocated overlaying AR images. An HMD with a pair of inbuilt stereoscopic cameras is connected to a desktop computer, which processes and renders the video, as well as providing network communication.

Ghostman consists of two subsystems: one is operated by a trainee (patient) and the other by a trainer (therapist), as illustrated in Figure 1. The two subsystems communicate over the internet network, which enables Ghostman to be applied remotely in telepresence applications. Each of the Ghostman subsystems consists of an AR HMD (Vuzix 920AR) that contains a pair of 640 × 480 liquid crystal displays (LCD), a pair of 640 × 480 video cameras, and 3 degrees-of-freedom (DoF) orientation sensors (pitch, yaw, and roll). Each camera is located directly in front of the LCD for each eye minimizing the eye displacement between the display viewpoint and the camera viewpoint, allowing the user to effectively "see through" the HMD with a video see-through AR view. A key design for Ghostman is its ability to visually align the viewpoints of the two HMDs. In order to achieve this posture alignment, one would have to capture the complete movement (6 DoF: 3 orientations and 3 translations) of the heads and hands of both trainer and trainee. However, in this initial study, our aim was to study the performance of a given task with a focus on using the inhabiting visual augmentation technique. Therefore, we decided to limit our task with only orientation head movement to simplify our setup; as a result, our Ghostman proof-of-concept system used only the HMD inbuilt orientation sensor to generate a navigation cue (shown at the top right-handed corner in Figure 2) within the HMD display to allow the trainer to align his head orientation with the trainee's prior to the instructions being given. Furthermore, in order to properly visually align the body parts of the trainer and the trainee, we would have to rescale

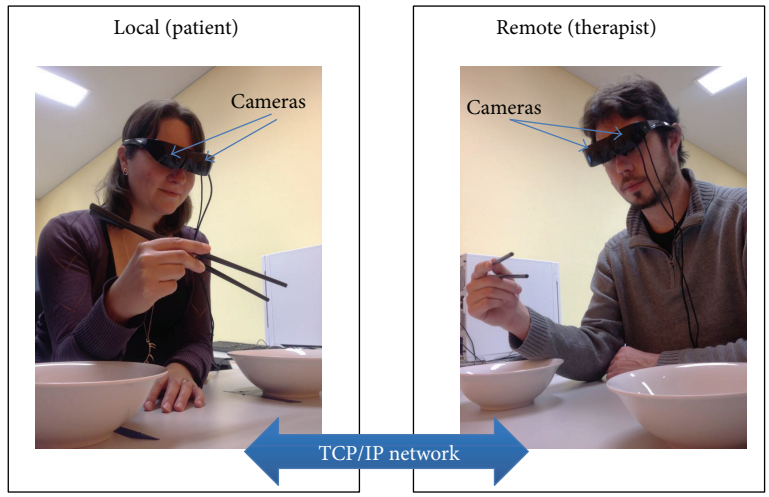

Figure 1: Ghostman setup.

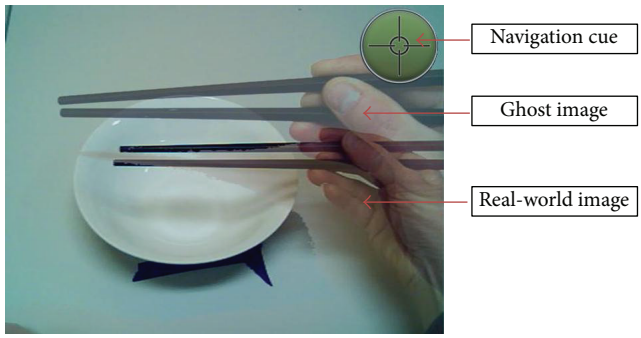

Figure 2: Inhabiting visual augmentation.

the overlaid remote limb (depending upon if it is a trainer or trainee) to match the scale of the local limb (undistorted) prior to the overlaying process. The rescaling process is a complicated process, which requires the system to estimate the size of the limbs (e.g., the length of forearm, fingers, and position of elbow) of both trainer/trainee and then rescale the remote limb to match the local limb in real time. However, the focus of this initial study is on the effectiveness of using an inhabiting visual augmentation technique; consequentially, we simplified the setup by assuming the size of the limb (i.e., hand) is the same across all users and therefore there is no rescaling required. It is worth noting that this limb size assumption is not detrimental to this pilot study, as the only visible limb is the hand and lower part of the forearm; thus the effect of rescaling is very small.

Learning by imitation is a key motor learning strategy that has been used previously to evaluate telerehabilitation systems [23]. With Ghostman, the trainee can learn the movements of the trainer by *simultaneously* observing both his/her own and the trainer's movements through the use of real-time overlaying images. Furthermore, Ghostman works in reciprocal fashion allowing the trainer to provide corrective movement feedback in real time.

Ghostman provides a unique environment in delivering movement instructions in egocentric view with a method of integrating description (audio), performance/practice (visual), and assistance/correction (evaluation). With its real-time capability, Ghostman also has the advantage of having the timing of movements as a natural feature of the system, overcoming one of the obstacles when learning a new skill. Therefore, Ghostman might provide an alternative solution in providing therapeutic instructions where more traditional face-to-face methods are difficult to negotiate.

For the cost analysis, each Ghostman system costs approximately $3,000 (AUD) to implement with current hardware. The current cost may not really be suitable for large-scale deployment to patients' home but could be more practical to a remote healthcare community facility where it would only require patients to travel for a short distance.

3. Pilot Study

To prove the concept of system a pilot study was conducted to determine the effectiveness of Ghostman in comparison to a best practice method used by physio- and occupational therapists to deliver a complex motor learning sequence to patients. A key component of rehabilitation is the teaching of simple motor skills. The teaching of these skills requires time and expertise of a therapist. The availability and cost of these demands are leading to the use of a telerehabilitation model to reach a wider population of potential clients. The results of this study might provide valuable information regarding the effectiveness of this innovation for motor skill learning, with important implications for the delivery of therapy in an e-health environment.

The aim of this study was to determine the effectiveness of using Ghostman in assisting individuals to learn to perform a novel motor skill using their dominant hand (manipulating chopsticks). The use of chopsticks is a task that can be described as a novel skill that can be learnt within a few minutes and can lead to various levels of expertise. Due to

the limitations of the field of view of the Ghostman HMD's cameras, this task was deemed suitable for instructional purposes.

We hypothesise that novice individuals, who use Ghostman to shadow a skilled performer in real time, will be as effective in learning chopstick manipulation technique as individuals who will be similarly trained using a traditional therapeutic method of observing and receiving feedback from a skilled performer in a face-to-face clinical environment. Thus, we tested the null hypothesis with the aim to accept this hypothesis demonstrating that the two types of service delivery are not significantly different in terms of motor learning a novel skill. Due to the limited availability of rehabilitation patients we chose to conduct this pilot study on a healthy population using a convenient sample to provide data for proof of concept of this telerehabilitation.

4. Experiment Design

A randomised controlled pilot study was conducted to evaluate the efficacy of the Ghostman prototype as a tool for remote teaching of a novel motor skill using chopsticks. Participants were randomised to receive one teaching session with a skilled instructor delivering the lesson via traditional face-to-face interaction or delivering the lesson via an inhabiting visual augmentation system (Ghostman).

4.1. Inclusion Criteria. Adult participants were self-identified as right-handed, as the skilled instructor was right-handed. All participants, who were unfamiliar with using chopsticks (≤ once per year), were recruited through the use of flyers advertising the study.

4.2. Exclusion Criteria. Individuals with previously diagnosed dementia or who were unable to comprehend English, individuals with neurological disorders that may affect their ability to learn motor skills, and individuals who had any other conditions preventing use of their right hand were excluded from the study.

4.3. Protocol. Degree of handedness was assessed using a widely used and validated inventory [24]. The testing protocol was designed to follow standard motor learning experiment principles that separate actual skill learning from performance improvements through the use of retention tests [25]. The protocol involved a 7-minute training session and four identical performance tests that were performed at four different sequential times: prior to training (pretest), 5 minutes after training (posttest), 24 hours after training (retention 1), and 7 days after training (retention 2). In each of the tests, participants were seated in front of two identical shallow bowls at a distance of 30 cm from the edge of the table where the participant seated (Figure 3—experiment setup). The source bowl was placed 15 cm to the left side of the participant's midline (xiphoid process) and contained 20 small plastic blocks, all of similar size. The target bowl, which was placed 15 cm to the right side of the participant's midline, was initially empty. Participants were presented with

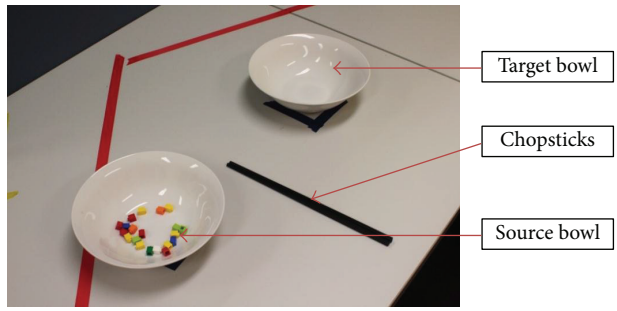

Figure 3: Experiment setup.

a pair of chopsticks and instructed to transfer all the blocks one at a time to the target bowl. The instructor replaced all dropped pieces back into the source bowl. Total skill errors, the primary dependent variable, were defined as any drops (either within the source bowl or in transit between the two bowls) or gripping errors within the source bowl. The number of skill errors made during each test session was recorded. When blocks were dropped in transit, the instructor collected the errant piece and placed it in the source bowl by hand while the participant continued with the task by attempting to move the next piece. Task completion time, the secondary dependent variable, was measured using a stopwatch to record the time taken to successfully transfer 20 blocks from the source bowl to the target bowl.

Both groups received standardised training from the same expert instructor. The only difference was the method of delivery: Ghostman or face-to-face. The training sessions commenced with instruction on how to hold chopsticks, followed by how to pick up objects with chopsticks. Participants then proceeded to perform a series of practice exercises using blocks of various sizes and received ongoing feedback about their performance from the instructor continuously throughout the seven-minute training session. No feedback was provided during the testing sessions. Ghostman participants were located within the same room as the instructor who was concealed behind a screen, whereas the face-to-face participants had the instructor sitting next to the participant for the duration of the training session. Video recordings of the hand movement and a top view of the test area (i.e., table, bowls) were made of each testing and training session for later analysis.

A user experience questionnaire was provided to assess user perceptions of the instruction methods. Participants were provided a questionnaire to rate their perceptions of the training methods. The five following statements were presented and answered using a 5-point Likert scale, with anchors of 5 corresponding to strong agreement with the statement and 1 indicating strong disagreement with the statement:

(1) the instructions I was given were easy to follow,

(2) the instructions helped me learn how to use chopsticks,

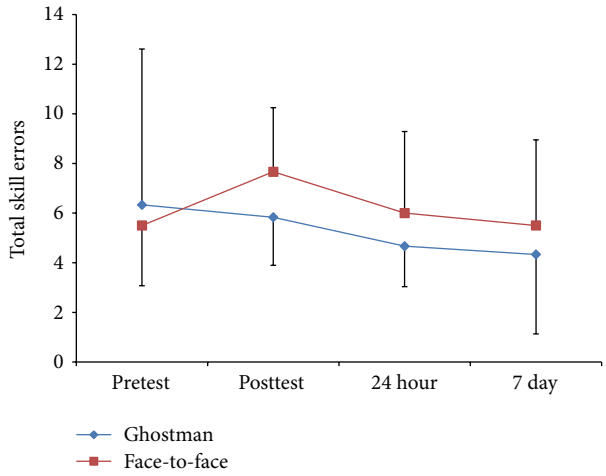

Figure 4: Group by test descriptive statistics (mean ± standard deviation) for total skills errors (frequency count).

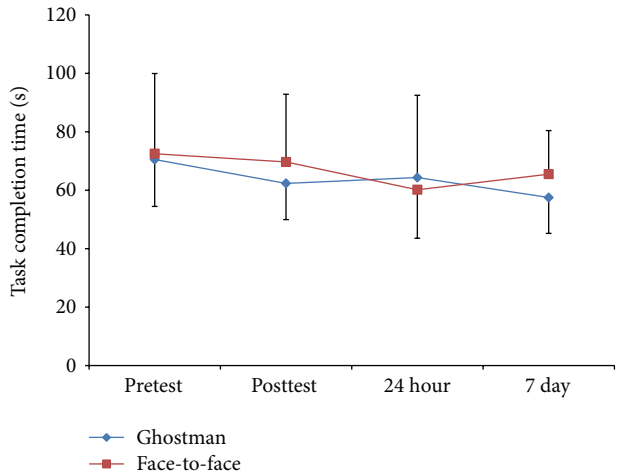

Figure 5: Group by test descriptive statistics (mean ± standard deviation) for task completion time (seconds).

(3) the instructor clearly showed me how to hold the chopsticks,

(4) the training programme helped me to learn how to use chopsticks,

(5) I feel I am better able to use chopsticks than before the study.

4.4. Data Analysis. Demographic data were compared at baseline using independent samples t-tests. Questionnaire data were analysed using independent samples t-tests to determine any group differences. A 2 (group) X 4 (test) mixed design ANOVA with repeated measures on the last factor was used to test for significant differences for the two dependent variables (total skill error and task completion time) separately, with an alpha level set at 0.05. All statistics were analyzed using IBM SPSS Statistics package version 22. Descriptive statistics were reported as means and standard deviations.

5. Results

Preliminary data were collected from 12 participants (6 Ghostman/6 face-to-face), except for the questionnaire data where data were obtained for only five Ghostman participants. There were no differences between the two groups for any variable at baseline (Table 1).

Regarding the primary dependent variable, there was no significant interaction ($F(3, 30) = 0.55$, $P = 0.65$) or main effects for group ($F(1, 10) = 0.40$, $P = 0.54$) or test ($F(3, 30) = 1.00$, $P = 0.40$) for total skill errors (Figure 4).

As illustrated in Figure 4, the Ghostman group improved their total skill errors throughout the study as can be interpreted in the mean values from pretest ($M = 6.33 \pm 6.28$) to posttest ($M = 5.83 \pm 1.94$) to 24-hour retention ($M = 4.67 \pm 1.63$) to seven-day retention ($M = 4.33 \pm 3.20$), whereas the face group got worse from pretest ($M = 5.50 \pm 2.43$) to posttest ($M = 7.67 \pm 2.58$), showed slight improvements after 24 hours ($M = 6.00 \pm 3.29$), and finally returned to baseline performance after seven days ($M = 5.50 \pm 3.45$) although none of these differences were significant.

Table 1: Comparison of demographic data between the treatment groups (mean ± standard deviation).

Variable	Ghostman	Face-to-face	Significance (P)
Gender (M/F)	4/2	4/2	
Age (years)	36.7 ± 11.8	42.2 ± 14.7	0.49
Experience (previous uses)	0.2 ± 0.4	1.0 ± 1.5	0.23
Right handedness (%)	74.1 ± 23.6	93.6 ± 9.9	0.09

Similarly, for the task completion time dependent variable there was no significant interaction ($F(3, 30) = 0.85$, $P = 0.48$) or main effects for group ($F(1, 10) = 0.11$, $P = 0.75$) or test ($F(3, 30) = 2.23$, $P = 0.10$) (Figure 5). The detail data of Figure 5 are as follows: pretest (Ghostman: $M = 70.50 \pm 16.05$, face-to-face: $M = 72.50 \pm 27.42$), posttest (Ghostman: $M = 62.33 \pm 12.37$, face-to-face: $M = 69.67 \pm 23.19$), 24-hour retention (Ghostman: $M = 64.33 \pm 28.12$, face-to-face: $M = 60.17 \pm 16.57$), and 7-day retention (Ghostman: $M = 57.50 \pm 12.29$, face-to-face: $M = 65.50 \pm 14.90$)

Finally, there were no differences between groups for any of the Likert scale statements regarding user perceptions of the training methods (Table 2).

6. Discussion

The primary outcome of this study (Figures 4 and 5) demonstrated that Ghostman is as effective, in terms of reduction in skill errors and improvements in task completion time, as current best practice face-to-face instruction for learning a novel skill (null hypothesis). Moreover, from the user experience questionnaires (Table 2), participants also felt Ghostman training was as effective as face-to-face training.

Table 2: Group by statement descriptive statistics (mean ± standard deviation) for questionnaire data (5-point Likert scale).

	Ghostman ($n = 5$)	Face-to-face ($n = 6$)	Significance (P)
Statement 1	4.60 ± 0.55	4.67 ± 0.52	0.84
Statement 2	4.20 ± 0.84	4.50 ± 0.55	0.51
Statement 3	4.80 ± 0.45	4.83 ± 0.41	0.90
Statement 4	4.40 ± 0.55	4.17 ± 0.75	0.57
Statement 5	4.60 ± 0.55	4.17 ± 0.98	0.38

This provided early evidence that the inhabiting visual augmentation (Ghostman) could be an effective technique for motor learning in a telerehabilitation context. As this is the first study of its kind using telerehabilitation to test the learning of novel skills and there is no previous data for comparison, this pilot study provides promising results for future studies.

Previously, home-based rehabilitation has been demonstrated to be more cost effective than hospital-based rehabilitation [26]. Traditionally, both forms of rehabilitation involve colocation of a therapist and a patient in the same setting, which involves costs associated with transport of the patient/therapist to the setting. The results of the current study indicate that Ghostman is an effective learning tool, which provides further support for the efficacy of a telerehabilitation approach. In addition, telerehabilitation has real potential to reduce cost of rehabilitation delivery by reducing time and travel-related expenses for practitioners and patients alike. However, the cost effectiveness of telerehabilitation delivery has yet to be established [27]. Moreover, the Ghostman telerehabilitation system requires further, larger-scale investigations into the efficacy of this system with clinical populations requiring physical rehabilitation, such as stroke patients or those suffering Parkinson's disease.

6.1. Limitations. Caution in interpreting these data is warranted due to the small, convenient sample size used in this study ($n = 12$). As a result, it might be suggested that the lack of statistically significant difference in outcomes between the two training methods might be due to the study being underpowered and thereby making Ghostman appear to be as effective a learning tool as traditional methods. To test the theory that the study was underpowered thereby making Ghostman appear more effective than it is, we conducted post hoc power calculations on the data obtained in this study. These analyses demonstrated that, on the basis of existing data, a total of 508 participants would be required to yield a statistically significant difference in changes in error rate, while 840 participants would be required to produce a statistically significant difference in changes in time to complete the task. In addition, there were greater mean improvements in learning (24-hour and 7-day retention tests) as identified by reductions in skill errors and task completion time when using Ghostman indicating that obtaining a sample size of that projected magnitude would be likely to demonstrate Ghostman to be a more effective learning tool than face-to-face instruction. Another limitation of the study was the training period. Training consisted of a single 7-minute session, regardless of the group. This may not have been a long enough exposure to produce significant improvements in participants. However, this brief amount of training time is consistent with the instruction time typically utilized by therapists when first meeting with new patients. Finally, participants that have been used in this research have been drawn from a healthy population. As such, it is difficult to claim that the technique is valid without examining its efficacy with participants that are currently completing a course of rehabilitation.

7. Conclusions

This paper describes our proposed telerehabilitation system (Ghostman) and a pilot study using Ghostman for remotely teaching a novel motor skill. Findings from the pilot study indicated that Ghostman is as effective for motor learning, in terms of reduction in skill errors and improvements in task completion time, as the current best practice face-to-face training. This suggests that Ghostman could be an effective technique for telerehabilitation and for remote instruction of novel motor skill learning applications by physio- and occupational therapists. Given the difficulties that rural and remote communities experience in gaining face-to-face access to health professionals, this outcome holds promise for future development of this technology.

While the early results are encouraging, further development of the Ghostman system and larger-scale studies are required to determine its efficacy in telerehabilitation context. The future development on the current Ghostman system will address the following three main areas: (1) the limited field of view of the camera and of the display (HMD), (2) the rescaling of the remote user's limb (to match with the (undistorted) local limb), and (3) the reduction of the unit cost for large-scale deployment. With these technical improvements, the Ghostman system can then be tested in a large group of participants with more comprehensive case studies that includes expanding ranges of the user movement and working with full-bodied tasks. Ultimately, this would provide valid evidence that the system is ready for real patient trials.

Conflict of Interests

The authors declare that there is no conflict of interests regarding the publication of this paper.

Acknowledgments

The authors would like to thank the University of Tasmania, the Deputy Vice Chancellor (Research) Professor Patrick Nixon, and Pro-Vice Chancellor (Regional Development) Professor Janelle Allison for their support to the project. Also, the authors would like to thank Bruce Andrews, Jonathan O'Duffy, Peter Seaton, Shannon Woolley, Shaun Walker, and Yuzhe Yang for their contribution to the project.

References

[1] S. Levin, "Early mobilization speeds recovery," *Physician and Sportsmedicine*, vol. 21, no. 8, pp. 70–74, 1993.

[2] D. N. Mendelson and W. B. Schwartz, "The effects of aging and population growth on health care costs," *Health Affairs*, vol. 12, no. 1, pp. 119–125, 1993.

[3] G. M. Jensen, J. Gwyer, K. F. Shepard, and L. M. Hack, "Expert practice in physical therapy," *Physical Therapy*, vol. 80, no. 1, pp. 28–52, 2000.

[4] R. A. Cooper, S. G. Fitzgerald, M. L. Boninger et al., "Telerehabilitation: expanding access to rehabilitation expertise," *Proceedings of the IEEE*, vol. 89, no. 8, pp. 1174–1193, 2001.

[5] R. K. Bode, A. W. Heinemann, P. Semik, and T. Mallinson, "Relative importance of rehabilitation therapy characteristics on functional outcomes for persons with stroke," *Stroke*, vol. 35, no. 11, pp. 2537–2542, 2004.

[6] W. K. Durfee, L. Savard, and S. Weinstein, "Technical feasibility of teleassessments for rehabilitation," *IEEE Transactions on Neural Systems and Rehabilitation Engineering*, vol. 15, no. 1, pp. 23–29, 2007.

[7] T. Kumagai, J. Yamashita, O. Morikawa et al., "Distance education system for teaching manual skills in endoscopic paranasal sinus surgery using "HyperMirror" telecommunication interface," in *Proceedings of the IEEE Virtual Reality (VR '08)*, pp. 233–236, March 2008.

[8] M. McNeill, L. Pokluda, S. McDonough, and J. Crosbie, "Immersive virtual reality for upper limb rehabilitation following stroke," in *Proceedings of the IEEE International Conference on Systems, Man and Cybernetics (SMC '04)*, pp. 2783–2789, October 2004.

[9] S. Subramanian, L. A. Knaut, C. Beaudoin, B. J. McFadyen, A. G. Feldman, and M. F. Levin, "Virtual reality environments for post-stroke arm rehabilitation," *Journal of NeuroEngineering and Rehabilitation*, vol. 4, article 20, 2007.

[10] G. Burdea, V. Popescu, V. Hentz, and K. Colbert, "Virtual reality-based orthopedic telerehabilitation," *IEEE Transactions on Rehabilitation Engineering*, vol. 8, no. 3, pp. 430–432, 2000.

[11] M. K. Holden and E. Todorov, "Use of virtual environments in motor learning and rehabilitation," in *Handbook of Virtual Environments: Design, Implementation, and Applications*, vol. 44, pp. 1–35, 2002.

[12] L. Piron, P. Tonin, F. Cortese et al., "Post-stroke arm motor telerehabilitation web-based," in *Proceedings of the 5th International Workshop on Virtual Rehabilitation (IWVR '06)*, pp. 145–148, August 2006.

[13] R. Kizony, P. L. Weiss, M. Shahar, and D. Rand, "TheraGame: a home based virtual reality rehabilitation system," *International Journal on Disability and Human Development*, vol. 5, no. 3, pp. 265–270, 2006.

[14] A. Alamri, J. Cha, M. Eid, and A. E. Saddik, "Evaluating the post-stroke patients progress using an augmented reality rehabilitation system," in *Proceedings of the IEEE International Workshop on Medical Measurements and Applications (MeMeA '09)*, pp. 89–94, May 2009.

[15] H. M. Hondori, M. Khademi, L. Dodakian, S. C. Cramer, and C. V. Lopes, "A spatial augmented reality rehab system for post-stroke hand rehabilitation," *Studies in Health Technology and Informatics*, vol. 184, pp. 279–285, 2013.

[16] M. Khademi, H. Mousavi Hondori, C. V. Lopes, L. Dodakian, and S. C. Cramer, "Haptic augmented reality to monitor human arm's stiffness in rehabilitation," in *Proceedings of the IEEE Conference on Biomedical Engineering and Sciences (IECBES '12)*, pp. 892–895, 2012.

[17] S. V. Adamovich, A. S. Merians, R. Boian et al., "A virtual reality based exercise system for hand rehabilitation post-stroke: transfer to function," in *Proceedings of the 26th Annual International Conference of the IEEE Engineering in Medicine and Biology Society (EMBC '04)*, pp. 4936–4939, September 2004.

[18] X. Luo, T. Kline, H. C. Fischer, K. A. Stubblefield, R. V. Kenyon, and D. G. Kamper, "Integration of augmented reality and assistive devices for post-stroke hand opening rehabilitation," in *Proceedings of the 27th Annual International Conference of the Engineering in Medicine and Biology Society (IEEE-EMBS '05)*, vol. 7, pp. 6855–6858, September 2005.

[19] S. H. You, S. H. Jang, Y.-H. Kim et al., "Virtual reality-induced cortical reorganization and associated locomotor recovery in chronic stroke: an experimenter-blind randomized study," *Stroke*, vol. 36, no. 6, pp. 1166–1171, 2005.

[20] M. J. Rosen, "Telerehabilitation," *NeuroRehabilitation*, vol. 12, no. 1, pp. 11–26, 1999.

[21] G. Kurillo, R. Bajcsy, K. Nahrsted, and O. Kreylos, "Immersive 3D environment for remote collaboration and training of physical activities," in *Proceedings of the IEEE Virtual Reality (VR '08)*, pp. 269–270, March 2008.

[22] U. Yang and G. J. Kim, "Implementation and evaluation of "just follow me": an immersive, VR-based, motion-training system," *Presence: Teleoperators and Virtual Environments*, vol. 11, no. 3, pp. 304–323, 2002.

[23] M. K. Holden, "Neurorehabilitation using "learning by imitation" in virtual environments," in *Usability Evaluation and Interface Design: Cognitive Engineering, Intelligent Agents and Virtual Reality*, pp. 624–628, Lawrence Erlbaum, London, UK, 2001.

[24] M. P. Bryden, "Measuring handedness with questionnaires," *Neuropsychologia*, vol. 15, no. 4-5, pp. 617–624, 1977.

[25] J. B. Shea and R. L. Morgan, "Contextual interference effects on the acquisition, retention, and transfer of a motor skill," *Journal of Experimental Psychology: Human Learning and Memory*, vol. 5, no. 2, pp. 179–187, 1979.

[26] C. Anderson, C. N. Mhurchu, S. Rubenach, M. Clark, C. Spencer, and A. Winsor, "Home or hospital for stroke rehabilitation? Results of a randomized controlled trial. II: cost minimization analysis at 6 months," *Stroke*, vol. 31, no. 5, pp. 1032–1037, 2000.

[27] K. E. Laver, D. Schoene, M. Crotty, S. George, N. A. Lannin, and C. Sherrington, *Telerehabilitation Services for Stroke*, The Cochrane Library, 2012.